Award Number: W81XWH-10-1-0504

TITLE: A New Therapeutic Strategy for Autosomal Dominant Polycystic Kidney Disease: Activation of AMP Kinase by Metformin

PRINCIPAL INVESTIGATOR: Michael Caplan

CONTRACTING ORGANIZATION: Yale University
 New Haven, CT 06511

REPORT DATE: July 2014

TYPE OF REPORT: Addendum to Final

PREPARED FOR: U.S. Army Medical Research and Materiel Command
                        Fort Detrick, Maryland 21702-5012

DISTRIBUTION STATEMENT: Approved for Public Release;
                        Distribution Unlimited

The views, opinions and/or findings contained in this report are those of the author(s) and should not be construed as an official Department of the Army position, policy or decision unless so designated by other documentation.

REPORT DOCUMENTATION PAGE

Form Approved
OMB No. 0704-0188

Public reporting burden for this collection of information is estimated to average 1 hour per response, including the time for reviewing instructions, searching existing data sources, gathering and maintaining the data needed, and completing and reviewing this collection of information. Send comments regarding this burden estimate or any other aspect of this collection of information, including suggestions for reducing this burden to Department of Defense, Washington Headquarters Services, Directorate for Information Operations and Reports (0704-0188), 1215 Jefferson Davis Highway, Suite 1204, Arlington, VA 22202-4302. Respondents should be aware that notwithstanding any other provision of law, no person shall be subject to any penalty for failing to comply with a collection of information if it does not display a currently valid OMB control number. **PLEASE DO NOT RETURN YOUR FORM TO THE ABOVE ADDRESS.**

1. REPORT DATE *JULY 2014*	2. REPORT TYPE **Addendum to Final**	3. DATES COVERED 1Jul2013 - 30Jun2014

4. TITLE AND SUBTITLE

A New Therapeutic Strategy for Autosomal Dominant Polycystic Kidney Disease: Activation of AMP Kinase by Metformin

5a. CONTRACT NUMBER
W81XWH-10-1-0504

5b. GRANT NUMBER

5c. PROGRAM ELEMENT NUMBER

6. AUTHOR(S)

Michael J. Caplan
email: michael.caplan@yale.edu

5d. PROJECT NUMBER

5e. TASK NUMBER

5f. WORK UNIT NUMBER

7. PERFORMING ORGANIZATION NAME(S) AND ADDRESS(ES)

Yale University
Cellular & Molecular Physiology
333 Cedar St., P.O. Box 208026
New Haven, CT 06520-8026

8. PERFORMING ORGANIZATION REPORT NUMBER

9. SPONSORING / MONITORING AGENCY NAME(S) AND ADDRESS(ES)
U.S. Army Medical Research And Materiel Command
Fort Detrick, Maryland 21702-5012

10. SPONSOR/MONITOR'S ACRONYM(S)

11. SPONSOR/MONITOR'S REPORT NUMBER(S)

12. DISTRIBUTION / AVAILABILITY STATEMENT
Approved for public release; distribution unlimited

13. SUPPLEMENTARY NOTES

14. ABSTRACT

Autosomal dominant polycystic kidney disease is a common inherited disorder. Patients are born with normal kidneys but, over the course of decades, they develop large fluid filled cysts that damage the normal kidney tissue. The damage caused by these cysts can lead ultimately to kidney failure, necessitating kidney transplantation or dialysis. There are currently no approved medications for this condition. Recent research reveals that cyst formation is due in part both to inappropriate cell growth and fluid secretion. The enzyme AMPK controls a number of cellular pathways, including those involved in cell growth and fluid secretion. Drugs that activate AMPK, therefore, may constitute an effective therapeutic option for slowing or preventing cyst growth. This research project is aimed at examining the potential of an approved, widely used, inexpensive and low-toxicity drug that can activate AMPK as a potential therapy for the treatment of polycystic kidney disease.

15. SUBJECT TERMS
Autosomal Dominant Polycystic Kidney Disease; Metformin

16. SECURITY CLASSIFICATION OF:			17. LIMITATION OF ABSTRACT	18. NUMBER OF PAGES	19a. NAME OF RESPONSIBLE PERSON USAMRC
a. REPORT U	**b. ABSTRACT** U	**c. THIS PAGE** U	UU	48	19b. TELEPHONE NUMBER *(include area code)*

Standard Form 298 (Rev. 8-98)
Prescribed by ANSI Std. Z39.18

Table of Contents

Introduction

Autosomal dominant polycystic kidney disease (ADPKD) is characterized by slow and continuous development of cysts derived from renal tubular epithelial cells. The cysts profoundly alter renal architecture, compressing normal parenchyma and compromising renal function. Nearly half of ADPKD patients ultimately require renal replacement therapy. ADPKD is a common genetic disorder, affecting at least 1 in 1,000 individuals (1). There are currently no effective specific clinical therapies for ADPKD. Cystic growth and expansion in ADPKD are thought to result from both fluid secretion into cyst lumens and abnormal proliferation of the cyst-lining epithelium. The rate of fluid secretion into the cyst lumen is directly proportional to the amount of the Cystic Fibrosis Transmembrane Regulator (CFTR) chloride channel in the apical membranes of cyst-lining epithelial cells (2). The cells surrounding the cysts manifest increased proliferation (3, 4). Mammalian Target of Rapamycin (mTOR) activity is elevated in models of PKD and is likely to be responsible, at least in part, for this hyperproliferative phenotype (3). mTOR is a serine/threonine kinase that regulates cell growth and proliferation, as well as transcription and protein synthesis. Interestingly, both the CFTR chloride channel and the mTOR signaling pathway are negatively regulated by the "energy sensing" molecule, Adenosine Monophosphate-activated Protein Kinase (AMPK). AMPK phosphorylates and directly inhibits CFTR, and indirectly antagonizes mTOR through phosphorylation of TSC2 and Raptor (5-8). Both of these actions are consistent with the role of AMPK as a regulator that decreases energy-consuming processes such as transport, secretion, and growth when cellular ATP levels are low (9). Thus, a drug that activates AMPK might inhibit both the secretory and the proliferative components of cyst expansion. Metformin, a drug in wide clinical use for both non-insulin dependent diabetes mellitus and Polycystic Ovary Syndrome, stimulates AMPK (10, 11). We therefore wish to examine whether metformin-induced activation of AMPK can slow cystogenesis through inhibition of mTOR-mediated cellular proliferation and inhibition of CFTR-mediated fluid secretion.

<u>**Body**</u>

Research Accomplishments Associated with Each Task Outlined in the Approved Statement of Work

Task 1. Characterize the effects of AMPK stimulation on its downstream targets in renal epithelia *in vivo* (months 1-20). The studies encompassed in this task group are designed to determine whether and how AMPK stimulation impacts upon the cellular pathways that are involved in cyst development and expansion. These experiments will make use of cultured MDCK cells and in vitro assays of both AMPK activation and the functional status of AMPK's downstream targets.

Task 1a. **Establish AMPK stimulation by its pharmacologic activator, metformin in renal epithelial cells *in vitro*.** By immunoblotting for the downstream targets of AMPK, we will confirm that AMPK stimulation has the same effects on its downstream targets in renal epithelia as has been reported in other tissues **(months 1-8)**.

Research Accomplishments: Metformin stimulates AMPK and pACC.

We first treated Madin Darby Canine Kidney (MDCK) renal epithelial cells with metformin to evaluate AMPK activation. Activated AMPK is phosphorylated at residue Thr172 of its α subunit. We performed Western blotting using a phosphospecific antibody to measure the level of the phosphorylated AMPK, pAMPK (Fig. 1a). We found that incubation with metformin for as little as 2 hours significantly increases pAMPK levels (Fig. 1b). To determine whether this effect was correlated with increased phosphorylation of an AMPK target, we evaluated metformin's effect on the AMPK-mediated inhibitory
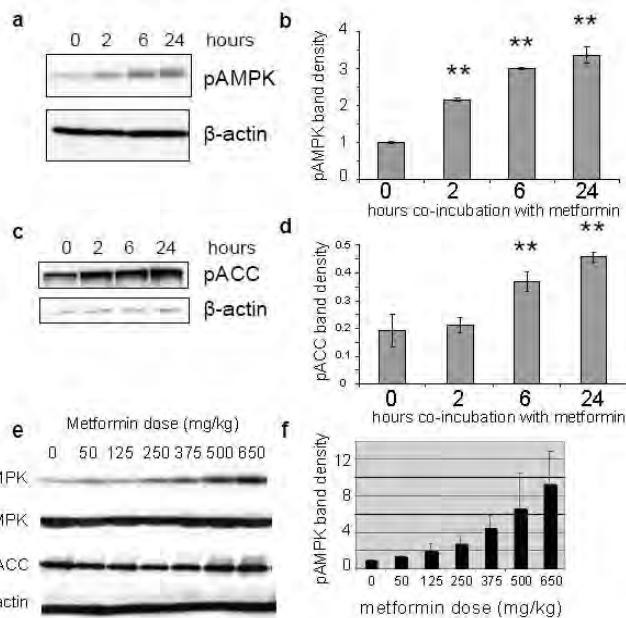

Figure 1: Metformin activates AMPK in vitro and in vivo. (a) MDCK cells were incubated with 1.0 mM metformin for the number of hours stated. Cells lysates blotted for pAMPK, the activated form of AMPK. (b) Quantitation of pAMPK band density normalized to β-actin. Comparisons of the mean (± SEM) are shown for each timepoint. (c) MDCK cells treated as above, blotted with pACC, a downstream target of pAMPK. (d) Comparisons of the mean band density relative to β-actin (± SEM) are shown for each timepoint. (e) 8-week-old C57BL/6 mice were treated with intraperitoneal metformin or with vehicle for three. Western blot analysis of kidney homogenates using anti-pAMPK demonstrates increasing activation of AMPK with increasing metformin dosing. (f) Quantitation of Western blot of in vivo pAMPK levels by normalized band density to β-actin.

2

phosphorylation of Acetyl-CoA Carboxylase (ACC) (Fig. 1c). Incubation of MDCK cells with metformin produced a significant increase in pACC levels in six hours (Fig. 1d). In AMPK α1 knockdown cells, metformin's effects on pAMPK and pACC levels are substantially blunted. Treatment of mice with increasing doses of metformin, administered daily for three days, results in increasing levels of pAMPK throughout the nephron (Fig. 1e and 1f).

Task 1b. **Characterize the physiological consequences of inhibition of AMPK downstream target CFTR.** This will be accomplished via short circuit current measurements performed on MDCK cells transfected to express CFTR and grown on permeable filter supports **(months 6-16)**.

Research Accomplishments: Inhibition of CFTR-dependent Isc by Metformin in MDCK Cells is AMPK-dependent.

We next examined the effect of metformin treatment on the CFTR chloride channel, which is inhibited by AMPK phosphorylation (12-14). Since CFTR drives, at least part of the fluid secretion
in PKD cystogenesis, we hypothesized that metformin-stimulated AMPK activity would inhibit CFTR channels in renal epithelial cells and slow the rate of cyst growth (15, 16). To test whether metformin inhibits CFTR via AMPK in a kidney-derived epithelial cell line, CFTR was expressed by adenoviral transduction in three different polarized MDCK type II cell lines stably transfected with either an empty vector, or shRNA plasmids directed against two isoforms of the catalytic α subunit of AMPK. MDCK cells endogenously express high concentrations of the α1 isoform of the AMPK catalytic α subunit and very low concentrations of the α2 isoform. Expression of the α1 shRNA construct reduced this protein's expression by ~90%, whereas the α2 shRNA had no effect on α1 protein expression. Knockdown of α1 also reduced the level of total phospho-AMPK
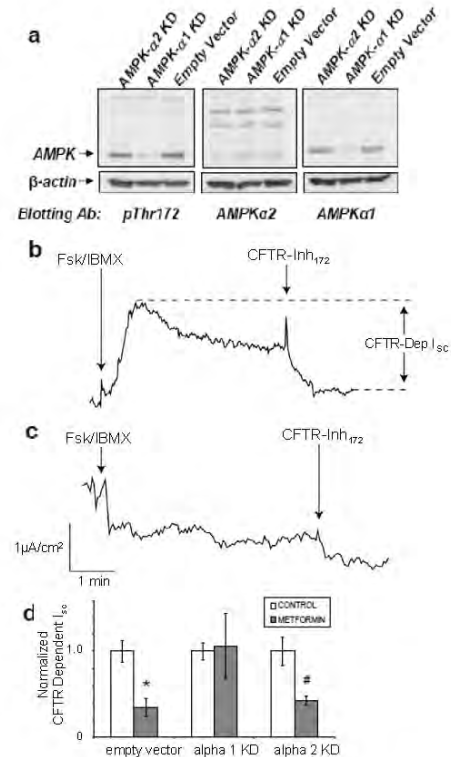

Figure 2: Metformin inhibits Isc in an AMPK-dependent manner. (a) MDCK cells stably expressing either empty vector or shRNA plasmids directed against either the catalytic α1 or α2 subunits of AMPK (AMPK-α1 KD and AMPK-α2 KD cells, respectively) were blotted with antibodies against either pThr172, AMPKα2, or AMPKα1 to measure the level of AMPK expression. (b) A representative Isc trace of cells with or without 1 mM metformin pre-treatment. Mock-transduced or NH2-terminally GFP-tagged-CFTR-transduced MDCK "empty vector" control cells, AMPK-α1 KD or AMPK-α2 KD cells were treated with 1 mM metformin or vehicle for 2-4 h prior to Ussing chamber measurements of Isc. A representative Isc trace of vehicle pre-treated CFTR-expressing "empty vector" control MDCK cells treated with IBMX and forskolin and then CFTR-Inh172 at the indicated times is shown. (c) A similar representative trace of mock-transduced "empty vector" control cells shows no response to these cAMP agonists or to CFTR-Inh172. There was also no significant change in Isc following addition of 10 μM amiloride, indicating that the epithelial Na+ channel does not significantly contribute to Isc in these MDCK cells. (d) Comparisons of the normalized mean (± SEM) CFTR-dependent Isc in "empty vector" control, AMPK-α1 KD, and AMPK-α2 KD cells with (dark gray bars) or without (white bars) metformin pre-treatment.

3

(pAMPK) by ~90% (Fig. 2a). CFTR-dependent Isc was measured for cells grown on filters mounted in Ussing chambers for four days following adenoviral transduction, with or without exposure to 1 mM metformin for 2-4 hours prior to measurement. To initiate CFTR-mediated secretion, CFTR-expressing and mock-transduced MDCK cells were treated with the cAMP agonists IBMX and forskolin, and the experiment was concluded through application of the specific CFTR inhibitor CFTR-Inh172 (17). Typical traces of Isc changes are shown in Fig. 2b and Fig. 2c. In CFTR-expressing cells there was generally an early peak in Isc within 1-2 min following forskolin/IBMX treatment, followed by a lower plateau current within ~5 min. This remaining current was sensitive to inhibition by CFTR-Inh172. Metformin (1 mM) pretreatment of empty vector-transfected and AMPK-α2 knockdown MDCK cells significantly reduced CFTR-dependent Isc by 60-70% relative to cells pretreated with vehicle (Fig. 2d). However, there was no metformin-dependent inhibition of CFTR current in AMPK-α1 knockdown MDCK cells, suggesting that the metformin-induced inhibition of CFTR occurs specifically via an AMPK-α1-dependent mechanism.
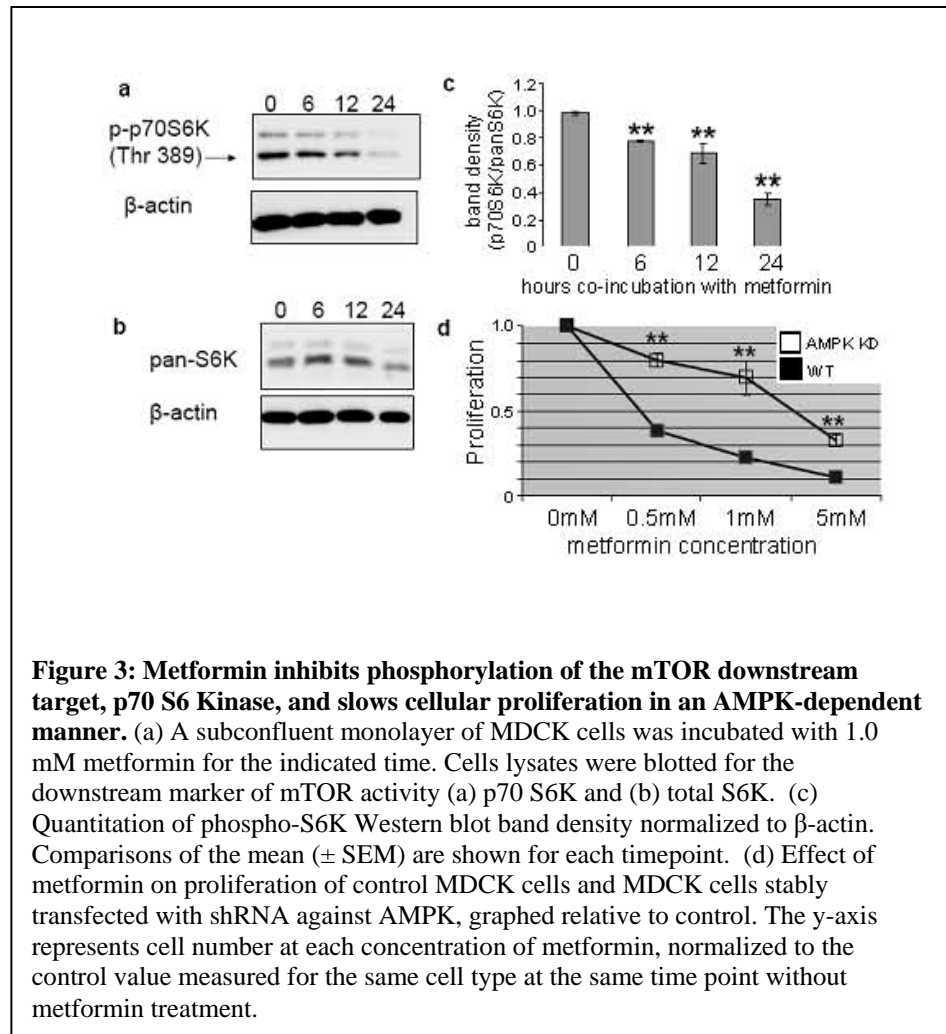
Task 1c. **Assess AMPK-mediated mTOR inhibition.** This will be accomplished both by direct assay of the phosphorylation status of downstream mTOR targets and by determining the physiological implications of this inhibition through measurements of cell proliferation **(months 10-20)**.

Research Accomplishments: Inhibition of mTOR by Metformin in MDCK Cells is AMPK-dependent.

To determine whether metformin induces AMPK-mediated inhibition of mTOR activity, we tested whether mTOR activity is diminished in MDCK cells cultured in the presence of metformin by blotting for the phosphorylated form of the mTOR downstream target ribosomal S6K p70 subunit (p70 S6K) (Fig. 3a) relative to pan-S6K (Fig. 3b). This inhibition is time-dependent, with increasing exposure to metformin resulting in greater suppression of this pathway. Total S6K

Figure 3: Metformin inhibits phosphorylation of the mTOR downstream target, p70 S6 Kinase, and slows cellular proliferation in an AMPK-dependent manner. (a) A subconfluent monolayer of MDCK cells was incubated with 1.0 mM metformin for the indicated time. Cells lysates were blotted for the downstream marker of mTOR activity (a) p70 S6K and (b) total S6K. (c) Quantitation of phospho-S6K Western blot band density normalized to β-actin. Comparisons of the mean (± SEM) are shown for each timepoint. (d) Effect of metformin on proliferation of control MDCK cells and MDCK cells stably transfected with shRNA against AMPK, graphed relative to control. The y-axis represents cell number at each concentration of metformin, normalized to the control value measured for the same cell type at the same time point without metformin treatment.

levels remain constant. The inhibition takes longer to achieve than inhibition of CFTR or ACC,

consistent with the fact that AMPK indirectly inhibits mTOR via TSC2/1 and Rheb (Fig. 3c). This effect is markedly less pronounced in AMPK-α1 KD cells. To evaluate whether these changes in phospho-protein levels translated into changes in proliferation, an Alamar Blue assay was used to quantitate proliferation in wild-type and AMPK-α1 knockdown MDCK cells. The y-axis depicts cell number measured at each given concentration of metformin and normalized to the control value, which was obtained for the same cell type at the same time point without metformin treatment. Wild-type MDCK cells exhibited a metformin dose-dependent decrease in proliferation, while this response was significantly diminished in the AMPK-α1 knockdown MDCK cells. (Fig. 3d) It should be noted that at the highest concentration of metformin tested (5 mM) substantial growth suppression was detected in AMPK knockdown cells. This may be due to the low level of residual AMPK that is expressed in these knockdown cells (see Fig. 2a) or to effects of high doses of metformin on yet to be identified AMPK-independent pathways. A similar suppressive effect of metformin treatment on proliferation is observed in vivo. We performed immunofluorescence analyses on kidneys from metformin treated and vehicle treated cystic Pkd1flox/-;Ksp-Cre mice using an antibody directed against Ki67, a marker of actively proliferating cells. In kidneys from vehicle-treated mice 19.7±3.8% s.e.m. of the cells exhibited Ki67 positivity (450 cells counted from each of n=6 mice) in comparison to 10.6±3.6% s.e.m. (450 cells counted from each of n=4 mice) in metformin-treated mice (p<0.0074). To assess whether the effects of metformin treatment on proliferation correlate with the level of mTOR activity in the cystic kidneys before and after metformin treatment, we performed immunohistochemistry using an antibody directed against the activated form of an mTOR target. We stained tissue from control and metformin treated cystic mice with an antibody that detects the phosphorylated form of 4E-BP1 (), an mTOR target whose level of phosphorylation is commonly used to report on levels of mTOR activity (18). We find that the level of p4E-BP1 is generally higher in the cyst lining epithelial cells in control animals as compared to those observed in metformin treated animals, consistent with the interpretation that metformin treatment reduced the level of mTOR activation.

Additional Progress on Task 1 Studies:

I. Identification of Dosing Regimens that Produce AMPK Activation in Wild Type Mice

We measured the effects of varying doses of metformin on AMPK activity in mice *in vivo*. This analysis was performed by immunocytochemistry and by western blotting. In both cases, ischemic injury was used as a positive control to produce maximal AMPK activation. AMPK is activated in response to energy deprivation, which
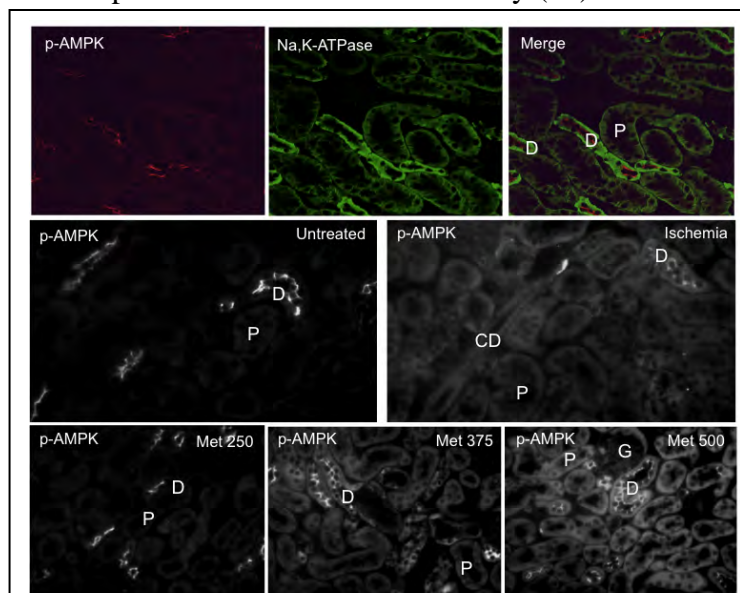

Figure 4: Immunocytochemical assessment of AMPK activation in mouse kidneys in situ. AMPK activation levels were assessed by staining sections with an antibody directed against p-AMPK. We find that treatment with 375 mg/kg produces levels of AMPK activation that are comparable to those produced by renal ischemia.

results in the accumulation of high cytosolic levels of the enzyme's allosteric activator AMP. Renal ischemia produces energy deprivation in renal tubules and is a powerful stimulus leading to the activation of AMPK in the kidney. The localization of activated, phosphorylated form of AMPK (p-AMPK) at baseline and after acute kidney ischemia has been characterized in the rat (19, 20). In murine kidneys, we demonstrate similar localization of p-AMPK under these conditions. Upon immunofluorescence staining using a p-AMPK-specific antibody, p-AMPK was detected in the apical membranes of distal tubules of mice at baseline. Following ischemia, there was a diffuse increase in p-AMPK fluorescence globally, including within proximal tubules and glomeruli (Fig. 4). Metformin has been demonstrated to activate AMPK in the heart, vascular tissue, and kidney homogenates (21-23). We observed that treatment with metformin delivered by IP injection results in increased fluorescence of p-AMPK in all cortical tubule segments (Fig. 4). Furthermore, this activation appears to be dose-dependent, as assessed by immunofluoresence microscopy. Western blot analysis to measure p-AMPK levels was also performed on renal tissue that was snap-frozen in situ using a specially designed forceps that had been pre-cooled in liquid nitrogen. This method also confirmed that AMPK activation occurs in response to increasing metformin doses (Figure 5). The data suggest that the metformin dose that has been used in our in vivo studies (24) produces reproducible AMPK activation in situ (Figure 6). Our efforts to assess the isoform specificity of AMPK activation *in vivo* will continue, as will our efforts to determine the effects of AMPK activation on CFTR distribution and mTOR activity in kidneys *in vivo*.
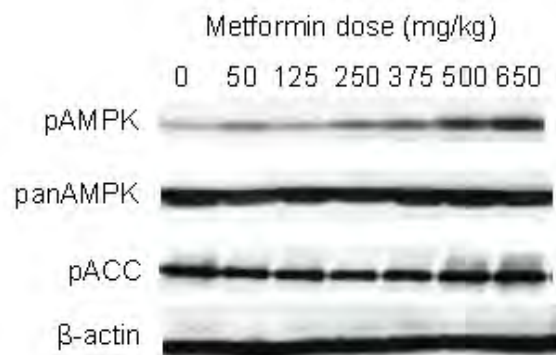

Figure 5: Western blot analysis of tissue prepared from snap-frozen kidneys from metformin-treated mice. AMPK activation was assessed by blotting for p-AMPK. Treatment with metformin produces dose-dependent activation of AMPK.
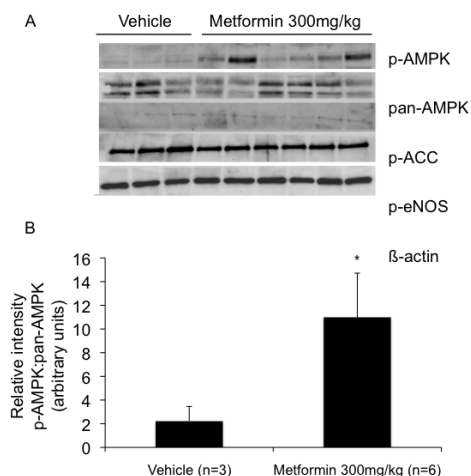

Figure 6: Western blot analysis of tissue prepared from snap-frozen kidneys from metformin-treated mice. Treatment *in vivo* results in reproducible activation of renal AMPK.

II. Further investigation of metformin's mode of action.

Very recent published data suggests that the mechanism of action of metformin *in vivo* may involve pathways other than those related to AMPK (25). It is critically important to determine whether the potential therapeutic effects of metformin that we have identified in the context of Autosomal Dominant Polycystic Kidney Disease are due to its capacity to activate AMPK or are

instead due to its effects on other targets. Recent research indicates that metformin can decrease cellular levels of cAMP (25). This is especially relevant in the setting of Autosomal Dominant Polycystic Kidney Disease because a substantial body of research has demonstrated that elevation of cAMP promotes cyst growth *in vitro* and *in vivo* (26, 27). Furthermore, drug therapies that reduce cAMP slow cyst growth both in mouse models of Autosomal Dominant Polycystic Kidney Disease (28) as well as in human Autosomal Dominant Polycystic Kidney Disease patients (29). To begin to explore this possibility, we have undertaken to assess the effects of other AMPK activators. These include AICAR, the A-769662 compound from Abbott Laboratories, and two new AMPK activating

Figure 7: Dose response analysis of AMPK activation by A-769662 in cultured MDCK renal epithelial cells.

compounds provided to us by Glaxo Smith Kline on an investigational basis. We have begun to assess whether these compounds modulate cystic growth of renal epithelial cells maintained in three dimensional culture conditions. If this proves to be the case we will conclude that AMPK is indeed a pharmacological target of value in Autosomal Dominant Polycystic Kidney Disease and that the therapeutic potentials of novel compounds that activate AMPK should be explored in relevant tissue culture and animal models. We have demonstrated that these compounds activate AMPK in cells in culture. We have now undertaken dose response analyses to determine the optimal concentrations and time courses for activating AMPK in renal epithelial cells in culture (see Figure 7). Once identified, these conditions will be applied in experiments designed to assess the effects of these compounds on the cystic growth of renal epithelial cells maintained in three dimensional culture.
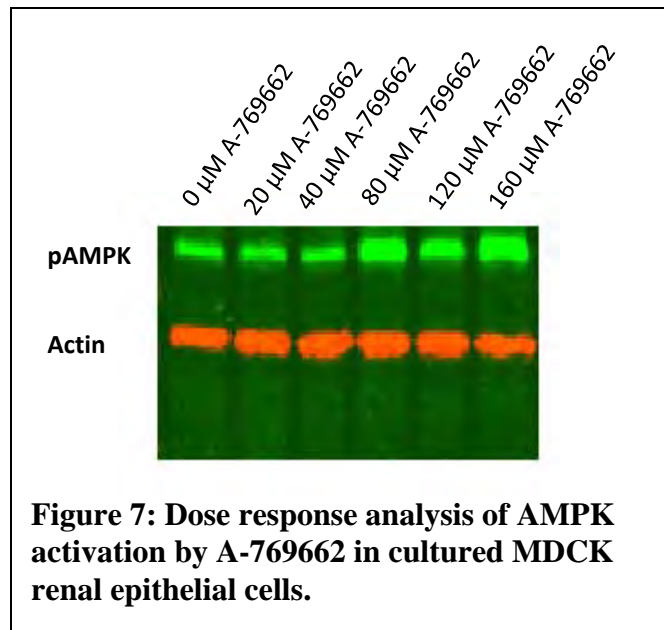
III. Exploration of a novel mechanism that may connect AMPK inhibition to the development of Autosomal Dominant Polycystic Kidney Disease.

A recent paper from the laboratory of Dr. Alessandra Boletta reported that cells homozygous for ADPKD-causing mutations manifest substantial perturbations in energy production (30). These cells exhibit very high levels of glycolysis and low levels of oxidative metabolism, reminiscent of the Warburg effect that is seen in tumor cells. As a result of the very high levels of glycolysis the cytoplasmic levels of ATP are very high and levels of active AMPK are consequently very low. These data lend further support to the idea that small molecule AMPK-activators may have therapeutic benefit in ADPKD. Very recently, we have explored the mechanisms responsible for the "Warburg-like" excessive glycolytic activity that is observed in ADPKD cells. We have identified a key enzyme that is involved in regulating energy synthesis to be another potential drug target in ADPKD.

To clarify the mechanisms underlying the metabolic perturbations observed in the absence of functional polycystin-1, we took advantage of previously characterized Pkd1^{-/-} and Pkd1[flox/-] mouse renal proximal tubule cell lines(31). These cells completely lack or are heterozygous for polycystin-1 expression, respectively. To test whether mitochondrial function was altered in the absence of Pkd1 expression, we measured oxygen consumption rate (OCR) using a Seahorse Biosciences Flux Analyzer. We found that Pkd1^{-/-} cells manifest a reduced OCR compared to Pkd1[flox/-] cells (Fig. 8a), consistent with a reduction in the quantity of OXPHOS performed by these cells.

Pyruvate dehydrogenase (PDH) is a key regulator of aerobic metabolism, transforming pyruvate into acetyl-CoA, which can enter the tricarboxylic acid cycle(32). PDH is subject to inhibitory phosphorylation by PDH kinase, and this modification is reversed by a calcium-activated PDH phosphatase(33). Calcium release from the endoplasmic reticulum alters intramtiochondrial calcium levels and stimulates aerobic metabolism by activating PDH phosphatase and thus PDH(34). Polycystin-2 is a calcium-permeable nonselective cation channel and is a member of the
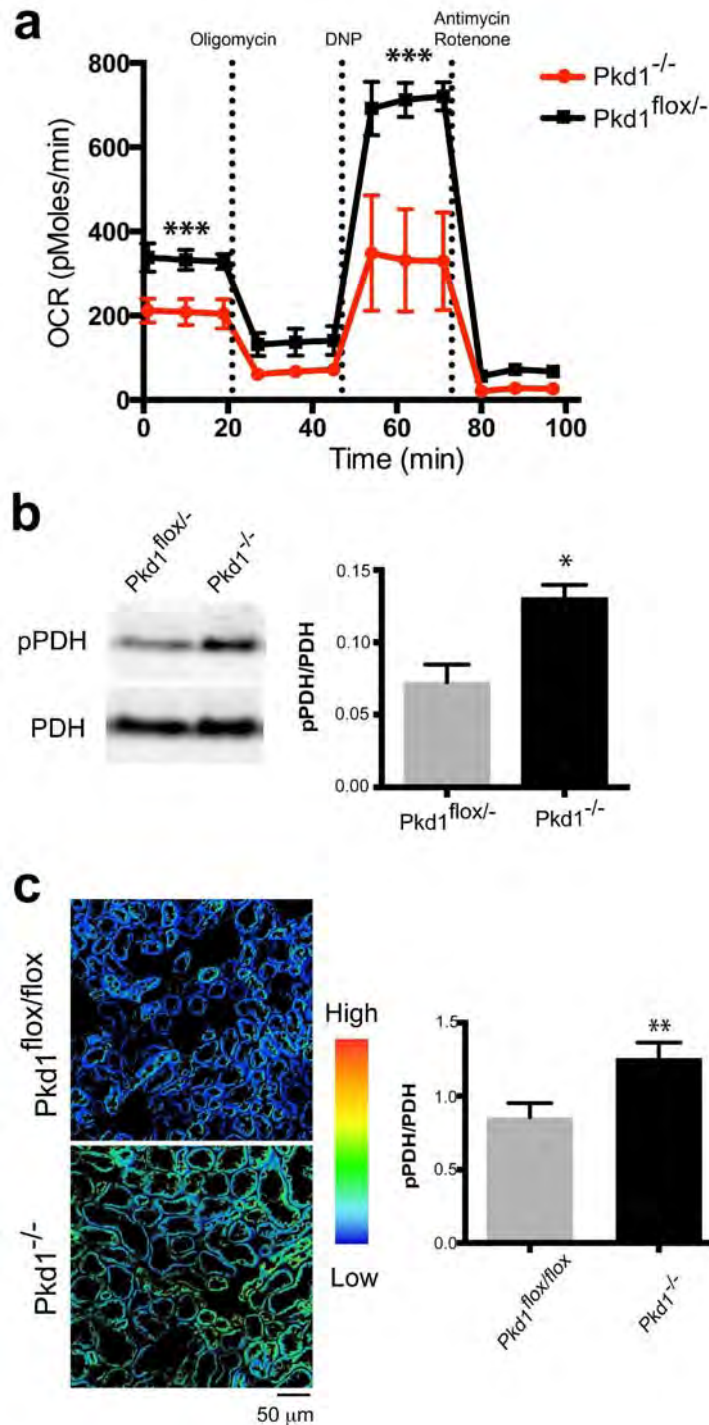

Fig. 8: The absence of polycystin-1 reduces O₂ consumption (a) and leads to increased levels of the inactive phosphorylated (b) form of PDH (b and c)

transient receptor potential (TRP) channel family(35). Polycystins localize in part to intracellular

compartments and modulate calcium release from the ER(36), suggesting that the channel activity of the polycystin complex could play a direct role in governing mitochondrial energy production through regulation of PDH. To test this hypothesis, we assessed PDH activity by measuring the ratio between pPDH (phosphorylated inactive form) and total PDH. We found that Pkd1$^{-/-}$ cells have decreased PDH activity as revealed by their increased pPDH/PDH ratio as compared to Pkd1$^{flox/-}$ cells (Fig. 8b). We also examined kidney sections from a biallelic conditional kidney-selective whole-nephron knockout mouse model of ADPKD(37, 38). Kidneys from doxycycline-inducible *Pax8rtTA*; *TetO-cre* mice were labeled with antibodies directed against total PDH and pPDH to assess the level of PDH activity. Mice were induced with oral doxycycline at P28 and maintained until P42, at which point Pkd1 expression is abolished12 but the Pkd1-/- kidneys are not yet cystic . Sections from non-induced Pkd1flox/flox and induced pre-cystic Pkd1-/- kidneys were processed for immunofluorescence analysis and the pPDH/PDH ratio was calculated using the imageJ plugin RatioPlus. Interestingly, pre-cystic kidneys lacking Pkd1 expression showed decreased PDH activity (Fig. 8c), suggesting that loss of polycystin-1 leads to reduced OXPHOS activity and that this occurs early in the process of cyst formation.

As noted above, polycystin-2 can function as an ER calcium release channel (36), and calcium release from the ER stimulates aerobic metabolism by activating PDH
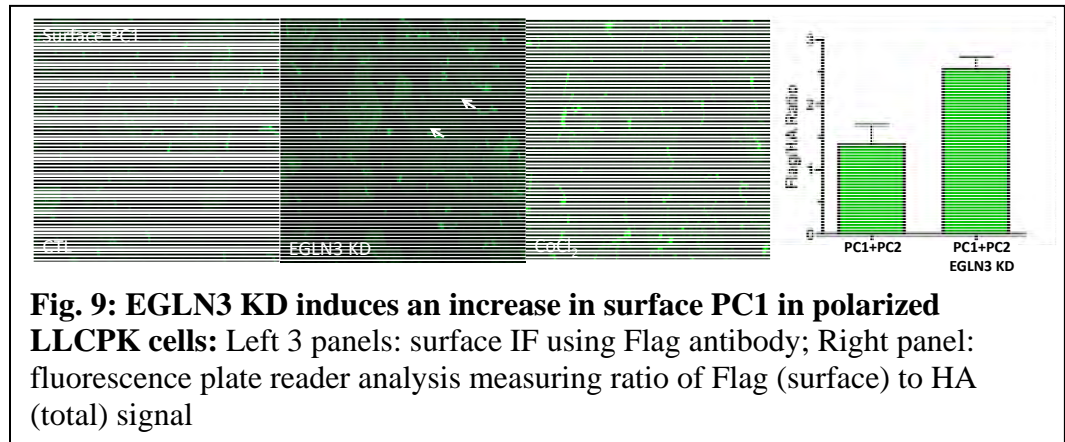

Fig. 9: EGLN3 KD induces an increase in surface PC1 in polarized LLCPK cells: Left 3 panels: surface IF using Flag antibody; Right panel: fluorescence plate reader analysis measuring ratio of Flag (surface) to HA (total) signal

phosphatase and thus PDH (34). The channel activity of TRPA1, which like polycystin-2 is a member of the TRP family, is directly regulated by oxygen through the oxidation and hydroxylation of specific cysteine and proline residues, respectively (39). This prolyl hydroxylation is mediated by prolyl hydroxylase domain containing (PHD) enzymes, which are critical sensors of changes in oxygen levels (40, 41). We have found through biochemical analysis that polycystin-1 is modified by prolyl hydroxylation. Furthermore, we have found that the polycystin 1/2 complex associates with a PHD enzyme called EGLN3, and that reducing the expression or activity of EGLN3 substantially alters polycystin 1/2 behavior.

We find that shRNA-mediated knockdown of EGLN3, which is also known as prolyl hydroxylase domain containing protein 3 (PHD3), leads to

Fig. 10 EGLN3 Co-IPs with HA-tagged PC1, and this Co-IP is blocked by EGLN3 inhibitor DMOG

increased surface expression of PC1 (Figure 8). As noted above, the PHD proteins are cellular O_2

sensors and regulate the cell's hypoxia response pathway. In the presence of O_2, PHD proteins hydroxylate proline residues on the hypoxia induced factor HIF1α and this modification targets HIF1α for degradation (40). PHD modification of TRPA1 contributes to the O_2-sensitivity of TRPA1 channel gating and also modulates its cell surface expression (39). The O_2-sensitivity of TRPA1 gating also involves direct non-enzymatic oxidation of TRPA1 cysteine residues. We find that knockdown of EGLN3 expression or inhibition of EGLN3 activity (using CoCl2) in LLC-PK1 cells stably expressing polycystin-1 and polycystin-2 led to a substantial increase in the quantity of polycystin-1 present in the apical plasma membrane (Fig. 9). Mass spectrometric analysis of polycystin-1 and polycystin-2 purified from transfected cells by immunoprecipitation reveals the presence of several hydroxylated proline residues and oxidized cysteine residues. The oxidized cysteines reside in close proximity to the hydroxylated prolines, and several of these residues are found in sequence motifs that resemble the PHD target site in TRPA1. EGLN3 co-immunoprecipitates with PC1, and this association is prevented by inhibiting EGLN3 with DMOG (Figure 10). Taken together, these data support the exciting hypothesis that the trafficking and channel activity of the polycystin-1/2 complex is modulated by PHD proteins in response to changes in cellular O_2 levels. These findings further suggest a novel hypothesis that accounts for the metabolic perturbations that accompany the loss of polycystin 1 expression and the potential therapeutic utility of metformin. We propose that oxygen levels regulate the calcium channel activity of the polycystin 1/2 complex, which in turn regulates oxidative metabolism by mediating the release of calcium from the ER, leading to activation of PDH-phosphatase and hence of PDH.

Task 2. Evaluate the *in vitro* and *in vivo* effects of metformin-induced AMPK inhibition of mTOR and CFTR in the context of *in vitro* and *in vivo* models of cystic kidney disease
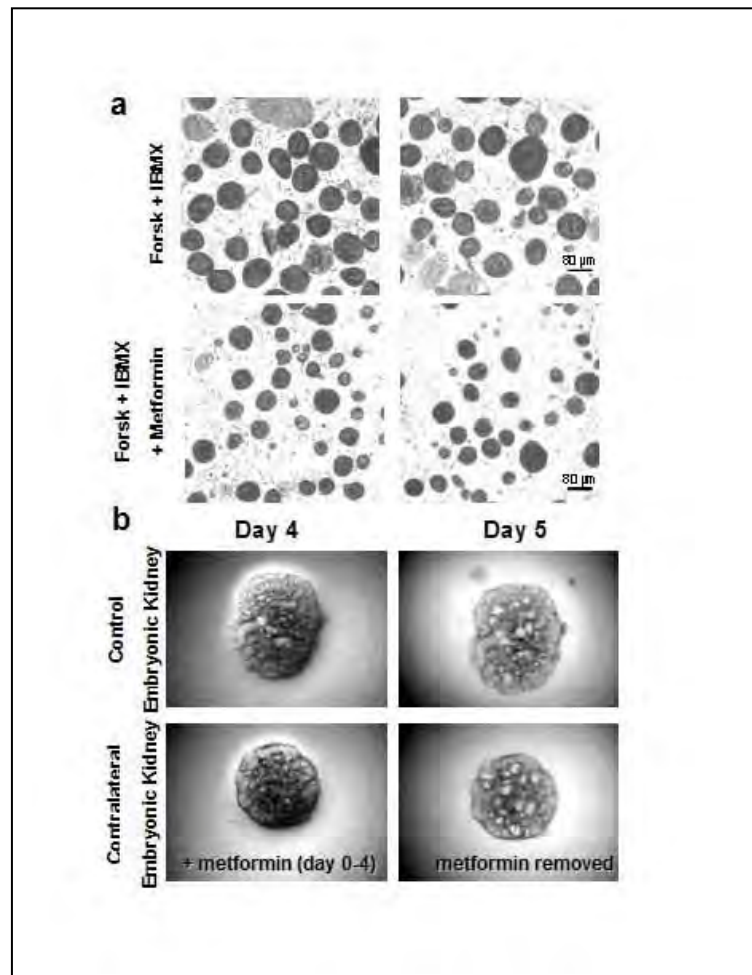

Figure 11: Metformin reduces cyst size *in vitro* and *ex vivo*. (a) Representative light micrographs of MDCK cell cysts grown in collagen gels. Cysts were treated with forksolin and IBMX, to enhance apical fluid secretion, with (bottom) or without (top) 1.0 mM metformin for 20 days. Gels were melted and the cysts were allowed to precipitate to the bottom for imaging. (b) Metformin treatment reduces cyst size in an *ex vivo* model of renal cystogenesis. Embryonic kidneys were placed in culture at E12 and maintained for 5 days in the continued presence of 100 µM 8-Br-cAMP. Representative light microscopic images are shown from one mouse. Each row shows the same kidney. The contralateral kidney (bottom row) was treated with metformin for 4 days, and then switched to normal media, illustrating that the embryonic kidney remains viable and capable of cystogenesis.

(months 12-36).

Task 2a. **Determine the effect of metformin treatment on average cyst size and cyst number using *in vitro* models of cystogenesis.** These experiments will be performed with renal epithelial cells that spontaneously form cysts when suspended in a collagen matrix. Cyst size and number will be determined by quantitative fluorescence microscopy techniques **(months 12-24)**.

Research Accomplishments: Metformin treatment slows cystogenesis *ex vivo*. Two-dimensional culture models do not accurately depict cell growth in the three-dimensional environment in which cysts develop. To evaluate metformin's effects in the context of cystogenesis, we suspended MDCK cells in a three-dimensional collagen matrix and allowed them to form cysts spontaneously in the presence of forskolin and IBMX (42). Cultures co-incubated with metformin for the duration of cyst growth produced significantly smaller cysts than those similarly treated with forskolin and IBMX alone (p=0.003, unpaired t-test, n=3 gels for each experimental condition) (Fig 11a).

We next tested the effect of metformin on ex vivo cystogenesis. Embryonic kidneys (E12.5) were removed from C57/B6 mice. One embryonic kidney was cultured in the presence of membrane permeable 8-Br-cAMP to stimulate fluid secretion, while the contralateral kidney was co-incubated with 8-Br-cAMP and metformin for 4 days. Culture in the presence of 8-Br-cAMP induces cyst formation in embryonic mouse kidneys (43). Metformin treatment significantly decreased fractional cyst area (p=0.04, unpaired t-test with n=4 for each experimental condition). On day 5, metformin was removed from the treated embryonic kidney and cyst growth recommenced
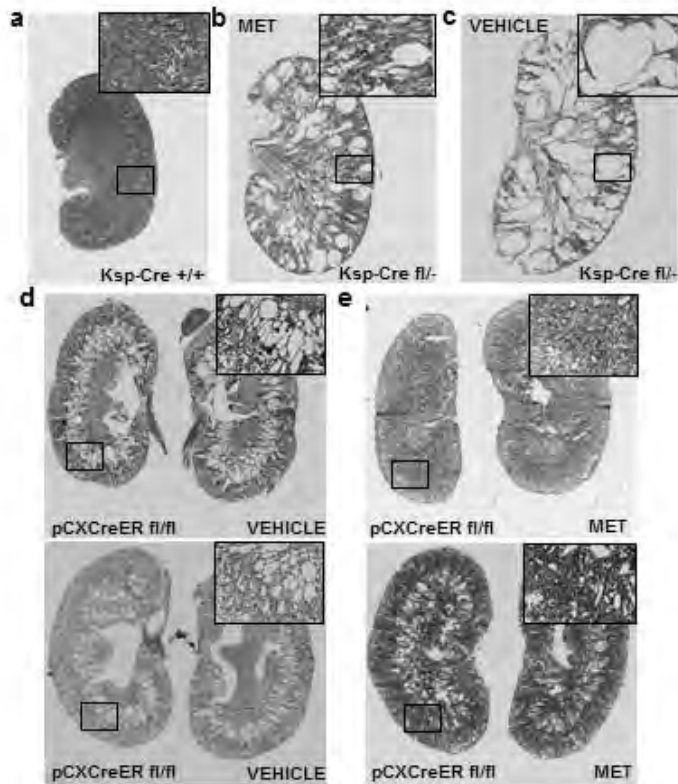

Figure 12: Metformin treatment reduces cystic index in two mouse models of ADPKD. Representative mid-sagittal sections from the kidneys of a (a) *PKD1$^{+/+}$;Ksp-Cre* mouse, (b) metformin-treated *PKD1$^{flox/-}$;Ksp-Cre* mouse, and (c) vehicle-treated P*KD1$^{flox/-}$;Ksp-Cr*e mouse at P7. The metformin and vehicle treated mice were given daily weight-adjusted intraperitoneal injections from P4 until P6. Representative images from *PKD$^{flox/-}$;pCX-CreER* mice treated with vehicle (d) or metformin (e) from P7-P17, with Cre induction at P9-10.

in the treated kidney, demonstrating that metformin treatment slowed cyst growth without affecting the viability of the tissue (Fig. 11b).

Task 2b. **Perform an *in vivo* trial of metformin treatment on Ksp-Cre, Pkd1$^{flox/-}$ mice.** This mouse model represents a very severe model of ADPKD. These experiments will permit the potential for metformin therapy to slow disease progression to be evaluated in mice that have developed cystic disease prior to the initiation of treatment **(months 12-28)**. These experiments will utilize 75 mice, 25 of which will be used in months 1-12 for breeding purposes, to generate a stable colony of 50 mice with the required genotypes that will be used in the experiments associated with this task.

Research Accomplishments: Metformin treatment slows cystogenesis in an aggressive constitutive *in vivo* model of PKD.

    We next tested whether metformin slows cyst growth in a murine model of PKD. Initially, we used the most aggressive viable murine model of PKD (Pkd1flox/-;Ksp-Cre) in which there is progression of renal cystic disease within the first week of life and death between two and three weeks of life (4). We treated these mice with daily intraperitoneal injections of metformin (300 mg/kg/day) dissolved in a 5% dextrose solution from P4 until P6. This is a dose known to activate AMPK (23). Mice were then sacrificed and kidneys harvested at P7.   The vehicle treated Pkd1flox/;Ksp-Cre kidneys (Fig. 12c) were profoundly cystic and greatly enlarged compared to the Pkd1+/+;Ksp-Cre kidneys (Fig. 12a). In contrast cyst, burden is significantly reduced in the kidneys from the metformin-treated Pkd1flox/-;Ksp-Cre mice (Fig. 12b). Because metformin can affect body weight, kidney weight: body weight ratio was not used as an endpoint (44). Instead, the effect of metformin on renal morphology was quantitated by evaluating cystic index, which determines the fraction of a given section that corresponds to luminal area (including both tubule and cyst lumens). Untreated Pkd1flox/-;Ksp-Cre kidneys had a cystic index of 71.4±4.0% s.e.m., whereas that of metformin treated Pkd1flox/-;Ksp-Cre kidneys was 51.8±5.2% s.e.m. (p=0.029; unpaired t-test with n=4 control and n=8 metformin treated mice). In wild type kidneys, this evaluation calculates a cystic index of 10% due to tubular lumens. Notably, while the metformin-treated kidney is still cystic, it displays significantly more parenchyma than the vector-treated control. While metformin might prevent further cyst growth, it is unlikely that treatment reduces the size of pre-existing cysts.

Task 2c. **Evaluate the effect of metformin in a mouse model of inducible PKD.** We will use an inducible mouse model of PKD (pCAGGS-cre, tamoxifen-activatable Pkd1$^{flox/-}$ mice), which will allow mice to be pre-treated with metformin prior to disease induction. This will allow us to gauge the therapeutic benefit of metformin under conditions that may more accurately mimic at least certain aspects of the progression of the human disease **(months 20-36)**. These experiments will utilize 75 mice, 25 of which will be used in months 1-12 for breeding purposes, to generate a stable colony of 50 mice with the required genotypes that will be used in the experiments associated with this task.

Research Accomplishments: Metformin treatment slows cystogenesis in an inducible *in vivo* model of PKD.

    We established an inducible model for Pkd1 inactivation using a conditional Pkd1flox allele in combination with a tamoxifen inducible Cre recombinase (pCX-CreERTM) (4, 45, 46). Induction of Cre expression prior to P13 leads to rapidly progressive cystic disease in Pkd1flox/flox animals (47). In this system, it is possible to initiate metformin treatment prior to or during cyst development.

12

Thus, this model might more accurately replicate the clinical scenario, in which metformin therapy could commence early in the disease process and act to prevent or slow subsequent cyst development. We initiated metformin treatment (300 mg/kg/day) at day P7 and then injected intraperitoneal tamoxifen at day P9 and P10 to initiate disease induction. We continued daily metformin injections until P18, when the animal was sacrificed and kidneys harvested for histology and cystic index evaluation. Once again, metformin treatment resulted in a smaller fractional cyst burden than vehicle-treated controls. The kidneys from vehicle-treated mice had a cystic index of 43%, whereas that of metformin treated mice was 31% (p=0.041, unpaired t-test with n=6 for vehicle treated and n=7 for metformin treated mice), a decrease of nearly one-third in the cyst burden (Fig. 11d,e).

Additional Task 2-related Research Accomplishments

I. **Identification of a novel small molecule approach to correcting the perturbation in energy metabolism that is associated with Autosomal Dominant Polycystic Kidney Disease**

As noted above, we hypothesize that AMPK activity may be reduced in the context of Autosomal Dominant Polycystic Kidney Disease due to the inappropriate acceleration of glycolytic activity, resulting in high levels of ATP and
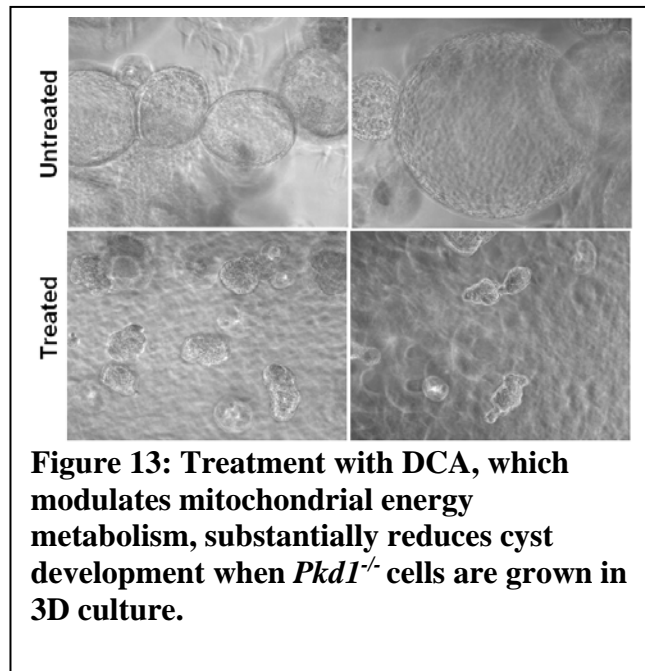

Figure 13: Treatment with DCA, which modulates mitochondrial energy metabolism, substantially reduces cyst development when *Pkd1⁻ᐟ⁻* cells are grown in 3D culture.
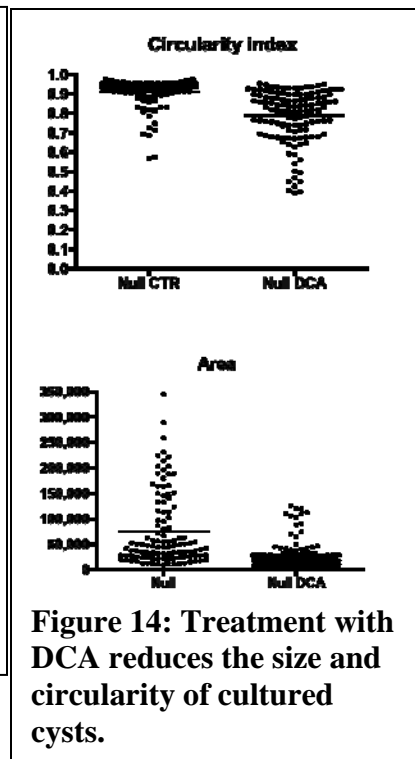

Figure 14: Treatment with DCA reduces the size and circularity of cultured cysts.

reduced levels of AMP. The reduced AMPK activity could contribute to the pathogenesis of Autosomal Dominant Polycystic Kidney Disease by de-repressing mTOR and CFTR activities. Thus, correcting the perturbation in energy metabolism could potentially help to correct the reduction in AMPK activity and with it the Autosomal Dominant Polycystic Kidney Disease pathological phenotype. Pyruvate dehydrogenase is inhibited via a phosphorylation event that is mediated by pyruvate dehydrogenase kinase. Dichloroacetic acid (DCA) is a very well characterized inhibitor of pyruvate dehydrogenase kinase (48). Administration of DCA stimulates the tricarboxylic acid cycle and aerobic metabolism. Furthermore, DCA has been used in human clinical trials designed to test its therapeutic potential in the setting of congenital lactic acidosis and also in the setting of cancer. Taking advantage of a 3-dimensional culture in vitro cyst growth assay that we have used extensively in our laboratory, we find that treatment with DCA dramatically

inhibits cyst formation by ADPKD cells, and instead induces them to grow into tubule-like structures (Figure 14). The size and circularity of the DCA-treated versus control cysts are quantitated in Figure 13. Thus, we believe that the enzyme that we have identified constitutes another extremely interesting target for ADPKD drug development.

II. Treatment with DCA and metformin attenuates cyst development in vivo.

To assess the potential therapeutic efficacy of DCA in the setting of polycystic kidney disease, we assessed its affects using the *PKD$^{flox/-}$;pCX-CreER* mouse model that was employed in Figure 12. DCA was delivered through the drinking water, either alone or in combination with metformin. At the end of the treatment period, mice were sacrificed and cyst development was assessed by measuring the ratio of kidney weight to body weight. As can be seen if Figure 15, treatment with DCA alone produces a trend towards reduced kidney weight:body weight, although this effect did not reach statistical significance in the present study. Combination therapy with DCA and metformin produced a statistically significant reduction in kidney weight:body weight. These data suggest the very exciting possibility that these two drugs produce synergistic effects, and that combination therapy employing both of them might constitute a novel and effective approach to the treatment of polycystic kidney disease.
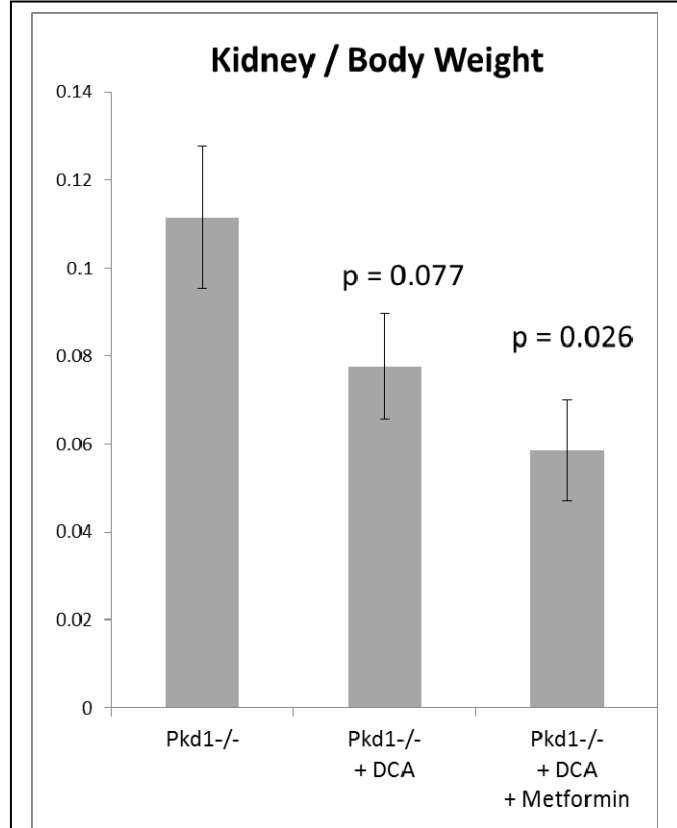

Figure 15: Treatment with DCA, alone or in association with metformin, slows cyst growth

14

Key Research Accomplishments

- Metformin stimulates AMPK and pACC.
- Inhibition of CFTR-dependent I_{sc} by Metformin in MDCK Cells is AMPK-dependent.
- Inhibition of mTOR by Metformin in MDCK Cells is AMPK-dependent.
- Metformin treatment slows cystogenesis ex vivo and in vivo.
- Metformin treatment slows cystogenesis in in vivo models of PKD.
- Polycystin 1 and 2 regulate oxidative phosphorylation by regulating the the levels of the active (non-phosphorylated form) of mitochondrial pyruvate dehydrogenase.
- The activity of the polycystin 1/polycystin 2 complex is regulated by cellular oxygen sensing machinery
- Drug treatments designed to increase oxidative metabolism slow cyst growth in vitro and in vivo.

Reportable Outcomes

- Peer reviewed primary data publication:

  Takiar, V., S. Nishio, J.D. King Jr., H. Li, L. Zhang, A. Karihaloo, K.R. Hallows, S. Somlo, M.J. Caplan. Activating AMPK slows renal cystogenesis. Proc. Nat. Acad. Sci, 108:2462-2467, 2011.

  Choi, Y.H., A. Suzuki, S. Hajarnis, Z. Ma, H.C. Chapin, M.J. Caplan, M. Pontoglio, S. Somlo and P. Igarashi. Polycystin-2 and phosphodiesterase 4C are components of a ciliary A-kinase anchoring protein complex that is disrupted in cystic kidney diseases. Proc. Nat. Acad. Sci. 108:10679-10684, 2011.

  Karihaloo, A., F. Koraishy, S.C. Huen, Y. Lee, D. Merrick, M.J. Caplan, S. Somlo and L.G. Cantley. Macrophages Promote Cyst Growth in Polycystic Kidney Disease. J. Am. Soc. Nephrol. 22: 1809–1814, 2011.

  Merrick, D.M., H.C. Chapin, Z. Yu, S. Somlo, J. Hogenesch, and M.J. Caplan The γ-secretase cleavage product of Polycystin-1 regulates Tcf and CHOP-mediated transcriptional activation through a p300-dependent mechanism. Dev. Cell, 22, 197–210, 2012.

  Pedrozo Z, A. Criollo, P.K. Battiprolu, C.R. Morales, A. Contreras, C. Fernández, N. Jiang, X. Luo, M.J. Caplan, S. Somlo, B.A. Rothermel, T.G. Gillette, S. Lavandero and J.A. Hill. Polycystin-1 is a Cardiomyocyte Mechanosensor That Governs L-type Ca2+ Channel Protein Stability. Circulation, In press, 2015

- Invited review articles:

  Takiar, V. and M.J. Caplan. Telling kidneys to cease and decyst. Nature Medicine, 16:751-752, 2010.

  Takiar, V. and M.J. Caplan. Polycystic Kidney Disease: Pathogenesis and Potential Therapies. Biochim. Biophys. ACTA, 1812: 1337–1343, 2011.

  Lal, M. and M.J. Caplan. Regulated intramembrane proteolysis: signaling pathways and biological functions. Physiology 26:34-44, 2011.

  Pluznick J.L. and M.J. Caplan. Novel sensory signaling systems in the kidney. Curr. Opin. Nephrol. Hypertens. 21:404-409, 2012.

  Somlo, S., V. Torres and M.J. Caplan. Autosomal Dominant Polycystic Kidney Disease and Inherited Cystic Diseases. In: The Kidney: Physiology and Pathophysiology (O. Moe, M.J. Caplan and R. Alpern, eds.) 5th edition, Elsevier, San Diego, CA, pp. 2645-2687, 2012.

  Bertuccio, C.A. and M.J. Caplan. Polycystin-1 C terminus cleavage and its relation with polycystin-2, two proteins involved in polycystic kidney disease. Medicina (B Aires) 73:155-162, 2013.

Pluznick, J.L. and M.J. Caplan. Chemical and Physical Sensors in the Regulation of Renal Function. Clin. J. Am. Soc. Neph. In press.

List of Personnel Supported

Garnett, Carolyn	07/04/2010-06/30/2013	Laboratory Assistant
Gilder, Allison Louise, B.S.	09/05/2012-06/30/2014	Graduate Student
Gresko, Nikolay, Ph.D.	10/19/2012-06/30-2014	Postdoctoral Associate
Hull, Michael J.	10/01/2012-06/30/2014	Research Associate
Mentone, Sue Ann	07/01/2010-06/30/2014	Research Associate
Merrick, David, B.S.	07/01/2012-05/31/2013	Graduate Student
Padovano, Valeria, Ph.D.	03/01/2011-06/30/2014	Postdoctoral Associate
Rajendran, Vanathy	09/01/2010-06/30/2014	Research Associate

Conclusion

AMPK activity can be pharmacologically targeted with metformin to reduce the growth of renal cysts. Metformin acts through AMPK to decrease both epithelial fluid secretion by directly inhibiting CFTR, and to decrease cellular proliferation by indirectly targeting mTOR. Metformin stimulates AMPK phosphorylation in cultured MDCK renal epithelial cells, and this phosphorylation correlates with increased AMPK activity, as evidenced by an increase in the level of the AMPK-mediated inhibitory phosphorylation of ACC. Metformin's inhibitory action on CFTR-mediated chloride transport is AMPK-dependent. Additionally, we have shown that metformin inhibition of mTOR translates into an AMPK-dependent inhibition of cell proliferation. Using both an in vitro model of MDCK cell cystogenesis as well as embryonic kidneys ex vivo, we have demonstrated that metformin decreases cyst size, and fractional cyst area, respectively. Finally, we illustrated the potential therapeutic utility of metformin by testing it in two murine models of ADPKD, both of which are attributable to inactivation of the gene encoding polycystin-1.

In this study, only one dose known to activate AMPK in vivo was tested. When considered on a simple mg/kg basis, this dose appears considerably higher than the current maximum dose prescribed for patients with diabetes or Polycystic Ovary Syndrome. However, human equivalent dose extrapolation is more accurately calculated based on body surface area than on weight. When this calculation is performed for a 60 kg adult, the dose used in our mouse studies extrapolates to a daily dose of approximately 1500 mg, which falls well within the range in which metformin is safely used in humans. It is likely, based on the established pharmacokinetics of metformin, that single daily dosing is suboptimal, and thus we are almost certainly not observing the maximal suppressive effects that metformin could potentially exert on the severity of cyst growth.(44) Support for this contention derives from the data presented in Figure 4c, since in the embryonic kidney model, cyst growth rapidly resumes shortly after removal of metformin from the culture media. Thus, short term intermittent metformin exposure may not be adequate to optimally suppress cyst development. It is quite possible that even lower doses administered more frequently might produce beneficial effects in the setting of polycystic kidney disease. It is important to note that our efforts to assess effects of metformin treatment on renal functional parameters such as serum concentrations of BUN and creatinine were inconclusive, due in part to a large degree of inter-individual variability. Further studies, perhaps employing more slowly progressive disease models, will be required to reduce this variance and to assess the extent to which metformin treatment can protect or improve renal function in the setting of polycystic kidney disease. In addition, subsequent development of metformin for this clinical application will require pharmacokinetic and pharmacodynamic studies designed to identify an ideal dosing regimen that achieves maximal activation of renal tubular AMPK. We are now working to optimize the metformin dosing regimen to ensure that it produces the most substantial and longest lasting activation of AMPK possible. These new dosing regimens will be tested in the relevant mouse models of Autosomal Dominant Polycystic Kidney Disease.

Finally, we have made a novel discovery that may explain the recent observation that energy metabolism is perturbed in kidney cells that lack the expression of polycystin-1. We have found that the polycystins interact with and are regulated by prolylhydroxylase domain containing proteins. Thus, the polycystins may serve as components of cellular oxygen sensors. Furthermore, the calcium channel activity of the polycystins may regulate metabolism by controlling the calcium-sensitive pyruvate dehydrogenase phosphatase, which in turn activates pyruvate dehydrogenase. In fact, stimulating pyruvate dehydrogenase activity with DCA ameliorates aspects of the cystic phenotype of renal epithelial cells grown in three dimensional culture. Thus, our data suggest a new

comprehensive mechanism that accounts for the perturbations in energy metabolism that are detected in Autsomal Dominant Polycystic Kidney Disease. Furthermore, these data explain the potential therapeutic utility of AMPK activation in this context and also suggest exciting new therapeutic modalities.

So What?

Metformin is taken by millions of Americans each year. It is currently FDA-approved for the treatment of Non-Insulin Dependent Diabetes (Type II DM) and, intriguingly, for Polycystic Ovary Syndrome, a disease that shares a name similar to that of Polycystic Kidney Disease but whose pathogenesis is even less well understood. In fact, metformin is often considered first line therapy for the treatment of Type II DM, due to its relatively small side effect profile. Recent literature suggests that metformin's activation of AMPK may be due to its ability to prevent AMP breakdown, although the exact mechanisms of action of metformin in Polycystic Ovary Syndrome or in Type II DM remain largely unknown. Recent reports also suggest that metformin may exert an anti-neoplastic effect. It has been reported that metformin acts in a dose-dependent manner to inhibit the proliferation of breast cancer cells and that this effect can be blocked in the presence of small interfering RNA directed against AMPK. This inhibition is also associated with a decrease in mTOR activation, suggesting that metformin's anti-proliferative effect is directed through the activation of AMPK, and consequent inhibition of mTOR.

There are numerous therapies for ADPKD in development or in clinical trials, including vasopressin receptor inhibitors, calcium sensing receptor inhibitors, CFTR-inhibitors, cell cycle inhibitors, and rapamycin. Each of these strategies targets one or the other of the key processes (proliferation and secretion) thought to be involved in the pathogenesis of PKD. By acting through AMPK, metformin may offer the significant advantage of blocking both (SI 4). Moreover, metformin is already FDA approved and generally well-tolerated. The most serious, albeit rare, side effect of metformin is lactic acidosis and, since metformin is cleared by the kidney, chronic renal disease has been considered to be a potential predisposing factor for this complication. However, metformin use could ideally be initiated at an early stage in ADPKD progression, prior to the development of substantial cyst burden and compromise of renal function, thus allowing for maximal preventive benefit and minimizing the potential for renal dysfunction to limit the safe use of the drug. Given the relatively late onset and slow progression of ADPKD it is conceivable that, even if metformin were to have only modest effects in delaying or slowing cyst development, it might significantly increase the time to the development of end stage renal disease and perhaps reduce the need for renal replacement therapy.

We find that metformin stimulates AMPK, resulting in inhibition of both CFTR and mTOR, and thereby, both epithelial secretion and proliferation, respectively. Our data suggest the possible utility of metformin as a therapy for ADPKD and that AMPK is a novel potential pharmacological target for ADPKD therapy. The large body of knowledge associated with metformin administration could conceivably facilitate the translation of these findings into clinical trials to test the proposition that metformin is a safe and promising approach that exploits AMPK activity to treat this challenging disease.

References

1.	Torres VE, Harris PC, and Pirson Y. Autosomal dominant polycystic kidney disease. *Lancet.* 2007;369(9569):1287-301.
2.	Davidow CJ, Maser RL, Rome LA, Calvet JP, and Grantham JJ. The cystic fibrosis transmembrane conductance regulator mediates transepithelial fluid secretion by human autosomal dominant polycystic kidney disease epithelium in vitro. *Kidney Int.* 1996;50(1):208-18.
3.	Wahl PR, Serra AL, Le Hir M, Molle KD, Hall MN, and Wuthrich RP. Inhibition of mTOR with sirolimus slows disease progression in Han:SPRD rats with autosomal dominant polycystic kidney disease (ADPKD). *Nephrol Dial Transplant.* 2006;21(3):598-604.
4.	Shibazaki S, Yu Z, Nishio S, Tian X, Thomson R, Mitobe M, Louvi A, Velazquez H, Ishibe S, Cantley L, et al. Cyst formation and activation of the extracellular regulated kinase pathway after kidney specific inactivation of Pkd1. *Hum Mol Genet.* 2008;17(11):1505-16.
5.	Hallows KR, Raghuram V, Kemp BE, Witters LA, and Foskett JK. Inhibition of cystic fibrosis transmembrane conductance regulator by novel interaction with the metabolic sensor AMP-activated protein kinase. *J Clin Invest.* 2000;105(12):1711-21.
6.	King JD, Jr., Fitch AC, Lee JK, McCane JE, Mak DO, Foskett JK, and Hallows KR. AMP-activated protein kinase phosphorylation of the R domain inhibits PKA stimulation of CFTR. *Am J Physiol Cell Physiol.* 2009;297(1):C94-101.
7.	Gwinn DM, Shackelford DB, Egan DF, Mihaylova MM, Mery A, Vasquez DS, Turk BE, and Shaw RJ. AMPK phosphorylation of raptor mediates a metabolic checkpoint. *Mol Cell.* 2008;30(2):214-26.
8.	Inoki K, Zhu T, and Guan KL. TSC2 mediates cellular energy response to control cell growth and survival. *Cell.* 2003;115(5):577-90.
9.	Hardie DG. AMP-activated/SNF1 protein kinases: conserved guardians of cellular energy. *Nat Rev Mol Cell Biol.* 2007.
10.	Zhou G, Myers R, Li Y, Chen Y, Shen X, Fenyk-Melody J, Wu M, Ventre J, Doebber T, Fujii N, et al. Role of AMP-activated protein kinase in mechanism of metformin action. *J Clin Invest.* 2001;108(8):1167-74.
11.	Shaw RJ, Lamia KA, Vasquez D, Koo SH, Bardeesy N, Depinho RA, Montminy M, and Cantley LC. The kinase LKB1 mediates glucose homeostasis in liver and therapeutic effects of metformin. *Science.* 2005;310(5754):1642-6.
12.	Hallows KR, Kobinger GP, Wilson JM, Witters LA, and Foskett JK. Physiological modulation of CFTR activity by AMP-activated protein kinase in polarized T84 cells. *Am J Physiol Cell Physiol.* 2003;284(5):C1297-308.
13.	Hallows KR, McCane JE, Kemp BE, Witters LA, and Foskett JK. Regulation of channel gating by AMP-activated protein kinase modulates cystic fibrosis transmembrane conductance regulator activity in lung submucosal cells. *J Biol Chem.* 2003;278(2):998-1004.
14.	Walker J, Jijon HB, Churchill T, Kulka M, and Madsen KL. Activation of AMP-activated protein kinase reduces cAMP-mediated epithelial chloride secretion. *Am J Physiol Gastrointest Liver Physiol.* 2003;285(5):G850-60.
15.	Magenheimer BS, St John PL, Isom KS, Abrahamson DR, De Lisle RC, Wallace DP, Maser RL, Grantham JJ, and Calvet JP. Early embryonic renal tubules of wild-type and polycystic kidney disease kidneys respond to cAMP stimulation with cystic fibrosis transmembrane

conductance regulator/Na(+),K(+),2Cl(-) Co-transporter-dependent cystic dilation. *J Am Soc Nephrol.* 2006;17(12):3424-37.

16. Yu S, Hackmann K, Gao J, He X, Piontek K, Garcia-Gonzalez MA, Menezes LF, Xu H, Germino GG, Zuo J, et al. Essential role of cleavage of Polycystin-1 at G protein-coupled receptor proteolytic site for kidney tubular structure. *Proc Natl Acad Sci U S A.* 2007;104(47):18688-93.

17. Ma T, Thiagarajah JR, Yang H, Sonawane ND, Folli C, Galietta LJ, and Verkman AS. Thiazolidinone CFTR inhibitor identified by high-throughput screening blocks cholera toxin-induced intestinal fluid secretion. *J Clin Invest.* 2002;110(11):1651-8.

18. Iida S, Miki Y, Ono K, Akahira J, Suzuki T, Ishida K, Watanabe M, and Sasano H. Novel classification based on immunohistochemistry combined with hierarchical clustering analysis in non-functioning neuroendocrine tumor patients. *Cancer Sci.* 2010;101(10):2278-85.

19. Mount PF, Hill RE, Fraser SA, Levidiotis V, Katsis F, Kemp BE, and Power DA. Acute renal ischemia rapidly activates the energy sensor AMPK but does not increase phosphorylation of eNOS-Ser1177. *Am J Physiol Renal Physiol.* 2005;289(5):F1103-15.

20. Fraser S, Mount P, Hill R, Levidiotis V, Katsis F, Stapleton D, Kemp BE, and Power DA. Regulation of the energy sensor AMP-activated protein kinase in the kidney by dietary salt intake and osmolality. *Am J Physiol Renal Physiol.* 2005;288(3):F578-86.

21. Lee MJ, Feliers D, Mariappan MM, Sataranatarajan K, Mahimainathan L, Musi N, Foretz M, Viollet B, Weinberg JM, Choudhury GG, et al. A role for AMP-activated protein kinase in diabetes-induced renal hypertrophy. *Am J Physiol Renal Physiol.* 2007;292(2):F617-27.

22. Solskov L, Lofgren B, Kristiansen SB, Jessen N, Pold R, Nielsen TT, Botker HE, Schmitz O, and Lund S. Metformin induces cardioprotection against ischaemia/reperfusion injury in the rat heart 24 hours after administration. *Basic Clin Pharmacol Toxicol.* 2008;103(1):82-7.

23. Zou MH, Kirkpatrick SS, Davis BJ, Nelson JS, Wiles WGt, Schlattner U, Neumann D, Brownlee M, Freeman MB, and Goldman MH. Activation of the AMP-activated protein kinase by the anti-diabetic drug metformin in vivo. Role of mitochondrial reactive nitrogen species. *J Biol Chem.* 2004;279(42):43940-51.

24. Takiar V, Nishio S, Seo-Mayer P, King JD, Jr., Li H, Zhang L, Karihaloo A, Hallows KR, Somlo S, and Caplan MJ. Activating AMP-activated protein kinase (AMPK) slows renal cystogenesis. *Proc Natl Acad Sci U S A.* 2011;108(6):2462-7.

25. Miller RA, Chu Q, Xie J, Foretz M, Viollet B, and Birnbaum MJ. Biguanides suppress hepatic glucagon signalling by decreasing production of cyclic AMP. *Nature.* 2013;494(7436):256-60.

26. Yamaguchi T, Wallace DP, Magenheimer BS, Hempson SJ, Grantham JJ, and Calvet JP. Calcium restriction allows cAMP activation of the B-Raf/ERK pathway, switching cells to a cAMP-dependent growth-stimulated phenotype. *J Biol Chem.* 2004;279(39):40419-30.

27. Chapin HC, and Caplan MJ. The cell biology of polycystic kidney disease. *J Cell Biol.* 2010;191(4):701-10.

28. Gattone VH, 2nd, Wang X, Harris PC, and Torres VE. Inhibition of renal cystic disease development and progression by a vasopressin V2 receptor antagonist. *Nat Med.* 2003;9(10):1323-6.

29. Torres VE, Chapman AB, Devuyst O, Gansevoort RT, Grantham JJ, Higashihara E, Perrone RD, Krasa HB, Ouyang J, and Czerwiec FS. Tolvaptan in patients with autosomal dominant polycystic kidney disease. *N Engl J Med.* 2012;367(25):2407-18.

30. Rowe I, Chiaravalli M, Mannella V, Ulisse V, Quilici G, Pema M, Song XW, Xu H, Mari S, Qian F, et al. Defective glucose metabolism in polycystic kidney disease identifies a new therapeutic strategy. *Nat Med.* 2013;19(4):488-93.

31. Merrick D, Chapin H, Baggs JE, Yu Z, Somlo S, Sun Z, Hogenesch JB, and Caplan MJ. The gamma-Secretase Cleavage Product of Polycystin-1 Regulates TCF and CHOP-Mediated Transcriptional Activation through a p300-Dependent Mechanism. *Dev Cell.* 2012;22(1):197-210.

32. Vander Heiden MG, Cantley LC, and Thompson CB. Understanding the Warburg effect: the metabolic requirements of cell proliferation. *Science.* 2009;324(5930):1029-33.

33. Patel MS, and Korotchkina LG. Regulation of the pyruvate dehydrogenase complex. *Biochem Soc Trans.* 2006;34(Pt 2):217-22.

34. Cardenas C, Miller RA, Smith I, Bui T, Molgo J, Muller M, Vais H, Cheung KH, Yang J, Parker I, et al. Essential regulation of cell bioenergetics by constitutive InsP3 receptor Ca2+ transfer to mitochondria. *Cell.* 2010;142(2):270-83.

35. Gonzalez-Perrett S, Kim K, Ibarra C, Damiano AE, Zotta E, Batelli M, Harris PC, Reisin IL, Arnaout MA, and Cantiello HF. Polycystin-2, the protein mutated in autosomal dominant polycystic kidney disease (ADPKD), is a Ca2+-permeable nonselective cation channel. *Proc Natl Acad Sci U S A.* 2001;98(3):1182-7.

36. Koulen P, Cai Y, Geng L, Maeda Y, Nishimura S, Witzgall R, Ehrlich BE, and Somlo S. Polycystin-2 is an intracellular calcium release channel. *Nat Cell Biol.* 2002;4(3):191-7.

37. Traykova-Brauch M, Schonig K, Greiner O, Miloud T, Jauch A, Bode M, Felsher DW, Glick AB, Kwiatkowski DJ, Bujard H, et al. An efficient and versatile system for acute and chronic modulation of renal tubular function in transgenic mice. *Nat Med.* 2008;14(9):979-84.

38. Ma M, Tian X, Igarashi P, Pazour GJ, and Somlo S. Loss of cilia suppresses cyst growth in genetic models of autosomal dominant polycystic kidney disease. *Nat Genet.* 2013;45(9):1004-12.

39. Takahashi N, Kuwaki T, Kiyonaka S, Numata T, Kozai D, Mizuno Y, Yamamoto S, Naito S, Knevels E, Carmeliet P, et al. TRPA1 underlies a sensing mechanism for O2. *Nat Chem Biol.* 2011;7(10):701-11.

40. Jaakkola P, Mole DR, Tian YM, Wilson MI, Gielbert J, Gaskell SJ, Kriegsheim A, Hebestreit HF, Mukherji M, Schofield CJ, et al. Targeting of HIF-alpha to the von Hippel-Lindau ubiquitylation complex by O2-regulated prolyl hydroxylation. *Science.* 2001;292(5516):468-72.

41. Schofield CJ, and Ratcliffe PJ. Oxygen sensing by HIF hydroxylases. *Nat Rev Mol Cell Biol.* 2004;5(5):343-54.

42. Mangoo-Karim R, Uchic M, Lechene C, and Grantham JJ. Renal epithelial cyst formation and enlargement in vitro: dependence on cAMP. *Proc Natl Acad Sci U S A.* 1989;86(15):6007-11.

43. Yang B, Sonawane ND, Zhao D, Somlo S, and Verkman AS. Small-molecule CFTR inhibitors slow cyst growth in polycystic kidney disease. *J Am Soc Nephrol.* 2008;19(7):1300-10.

44. Golay A. Metformin and body weight. *Int J Obes (Lond).* 2008;32(1):61-72.

45. Guo C, Yang W, and Lobe CG. A Cre recombinase transgene with mosaic, widespread tamoxifen-inducible action. *Genesis.* 2002;32(1):8-18.

46.   Miyazaki J, Takaki S, Araki K, Tashiro F, Tominaga A, Takatsu K, and Yamamura K. Expression vector system based on the chicken beta-actin promoter directs efficient production of interleukin-5. *Gene.* 1989;79(2):269-77.

47.   Piontek K, Menezes LF, Garcia-Gonzalez MA, Huso DL, and Germino GG. A critical developmental switch defines the kinetics of kidney cyst formation after loss of Pkd1. *Nat Med.* 2007;13(12):1490-5.

48.   Michelakis ED, Webster L, and Mackey JR. Dichloroacetate (DCA) as a potential metabolic-targeting therapy for cancer. *Br J Cancer.* 2008;99(7):989-94.

Appendix

Reprints of:

Takiar, V., S. Nishio, J.D. King Jr., H. Li, L. Zhang, A. Karihaloo, K.R. Hallows, S. Somlo, M.J. Caplan. Activating AMPK slows renal cystogenesis. Proc. Nat. Acad. Sci, 108:2462-2467, 2011.

Merrick, D.M., H.C. Chapin, Z. Yu, S. Somlo, J. Hogenesch, and M.J. Caplan The γ-secretase cleavage product of Polycystin-1 regulates Tcf and CHOP-mediated transcriptional activation through a p300-dependent mechanism. Dev. Cell, 22, 197–210, 2012.

Activating AMP-activated protein kinase (AMPK) slows renal cystogenesis

Vinita Takiar[a], Saori Nishio[b], Patricia Seo-Mayer[a], J. Darwin King, Jr.[c,d], Hui Li[c,d], Li Zhang[a], Anil Karihaloo[b], Kenneth R. Hallows[c,d], Stefan Somlo[b], and Michael J. Caplan[a,1]

[a]Department of Cellular and Molecular Physiology, Yale School of Medicine, New Haven, CT 06520; [b]Section of Nephrology, Department of Medicine, Yale School of Medicine, New Haven, CT 06520; [c]Renal-Electrolyte Division, Department of Medicine and [d]Department of Cell Biology and Physiology, University of Pittsburgh School of Medicine, Pittsburgh, PA 15261

Renal cyst development and expansion in autosomal dominant polycystic kidney disease (ADPKD) involves both fluid secretion and abnormal proliferation of cyst-lining epithelial cells. The chloride channel of the cystic fibrosis transmembrane conductance regulator (CFTR) participates in secretion of cyst fluid, and the mammalian target of rapamycin (mTOR) pathway may drive proliferation of cyst epithelial cells. CFTR and mTOR are both negatively regulated by AMP-activated protein kinase (AMPK). Metformin, a drug in wide clinical use, is a pharmacological activator of AMPK. We find that metformin stimulates AMPK, resulting in inhibition of both CFTR and the mTOR pathways. Metformin induces significant arrest of cystic growth in both in vitro and ex vivo models of renal cystogenesis. In addition, metformin administration produces a significant decrease in the cystic index in two mouse models of ADPKD. Our results suggest a possible role for AMPK activation in slowing renal cystogenesis as well as the potential for therapeutic application of metformin in the context of ADPKD.

Autosomal dominant polycystic kidney disease (ADPKD) is characterized by the slow and continuous development of cysts derived from renal tubular epithelial cells. The cysts profoundly alter renal architecture, compressing normal parenchyma and compromising renal function. Nearly half of ADPKD patients ultimately require renal replacement therapy. ADPKD is a common genetic disorder, affecting at least 1 in 1,000 individuals (1). There currently are no effective specific clinical therapies for ADPKD.

Cystic growth and expansion in ADPKD are thought to result from both fluid secretion into cyst lumens and abnormal proliferation of the cyst-lining epithelium. The rate of fluid secretion into the cyst lumen is directly proportional to the amount of the cystic fibrosis transmembrane regulator (CFTR) chloride channel in the apical membranes of cyst-lining epithelial cells (2). The evidence suggesting that CFTR acts as a significant contributor to cyst growth has inspired preclinical trials of CFTR inhibitors in cell and animal models of renal cystic disease (3, 4).

The cells surrounding the cysts manifest increased proliferation (5, 6). Mammalian target of rapamycin (mTOR) activity is elevated in models of polycystic kidney disease (PKD) and probably is responsible, at least in part, for this hyperproliferative phenotype (5). mTOR is a serine/threonine kinase that regulates cell growth and proliferation as well as transcription and protein synthesis. Rapamycin inhibits mTOR's kinase activity (7, 8). Indeed, treatment with rapamycin has been shown to improve parameters of renal cystic expansion in several animal models of ADPKD (5, 9).

Interestingly, both the CFTR chloride channel and the mTOR signaling pathway are negatively regulated by the "energy-sensing" molecule, AMP-activated protein kinase (AMPK). AMPK phosphorylates and directly inhibits CFTR and indirectly antagonizes mTOR through phosphorylation of tuberous sclerosis protein 2 (TSC2) and Raptor (10–13). Both of these actions are consistent with the role of AMPK as a regulator that decreases energy-consuming processes such as transport, secretion, and growth when cellular ATP levels are low (14). Thus,

a drug that activates AMPK might inhibit both the secretory and the proliferative components of cyst expansion. Metformin, a drug in wide clinical use for both non–insulin-dependent diabetes mellitus (type 2 DM) and polycystic ovary syndrome, stimulates AMPK (15, 16). We therefore examined whether metformin-induced activation of AMPK slows cystogenesis through inhibition of mTOR-mediated cellular proliferation and inhibition of CFTR-mediated fluid secretion.

Results

Metformin Stimulates AMPK and Phosphorylated Acetyl-CoA Carboxylase. We first treated Madin–Darby canine kidney (MDCK) renal epithelial cells with metformin to evaluate AMPK activation. Activated AMPK is phosphorylated at residue Thr^{172} of its α subunit. We performed Western blotting using a phosphospecific antibody to measure the level of the phosphorylated AMPK (pAMPK) (Fig. 1A). We found that incubation with metformin for as little as 2 h significantly increases pAMPK levels (Fig. 1B). To determine whether this effect was correlated with increased phosphorylation of an AMPK target, we evaluated metformin's effect on the AMPK-mediated inhibitory phosphorylation of acetyl-CoA carboxylase (ACC) (Fig. 1C). Incubation of MDCK cells with metformin produced a significant increase in phosphorylated ACC (pACC) levels in 6 h (Fig. 1D). In AMPK-α1 knockdown (AMPK-α1–KD) cells, metformin's effects on pAMPK and pACC levels are substantially blunted (Fig. S1). Treatment of mice with increasing doses of metformin administered daily for 3 d results in increasing levels of pAMPK throughout the nephron (Fig. 1 E and F).

Inhibition of CFTR-Dependent Short-Circuit Current by Metformin in MDCK Cells Is AMPK Dependent. We next examined the effect of metformin treatment on the CFTR chloride channel, which is inhibited by AMPK phosphorylation (17–19). Because the CFTR drives, at least in part, the fluid secretion in PKD cystogenesis, we hypothesized that metformin-stimulated AMPK activity would inhibit CFTR channels in renal epithelial cells and slow the rate of cyst growth (20, 21). To test whether metformin inhibits CFTR via AMPK in a kidney-derived epithelial cell line, CFTR was expressed by adenoviral transduction in three different polarized MDCK type II cell lines stably transfected with an empty vector or with shRNA plasmids directed against two isoforms of the catalytic α subunit of AMPK. MDCK cells endogenously express high concentrations of the α1 isoform of the AMPK catalytic α subunit
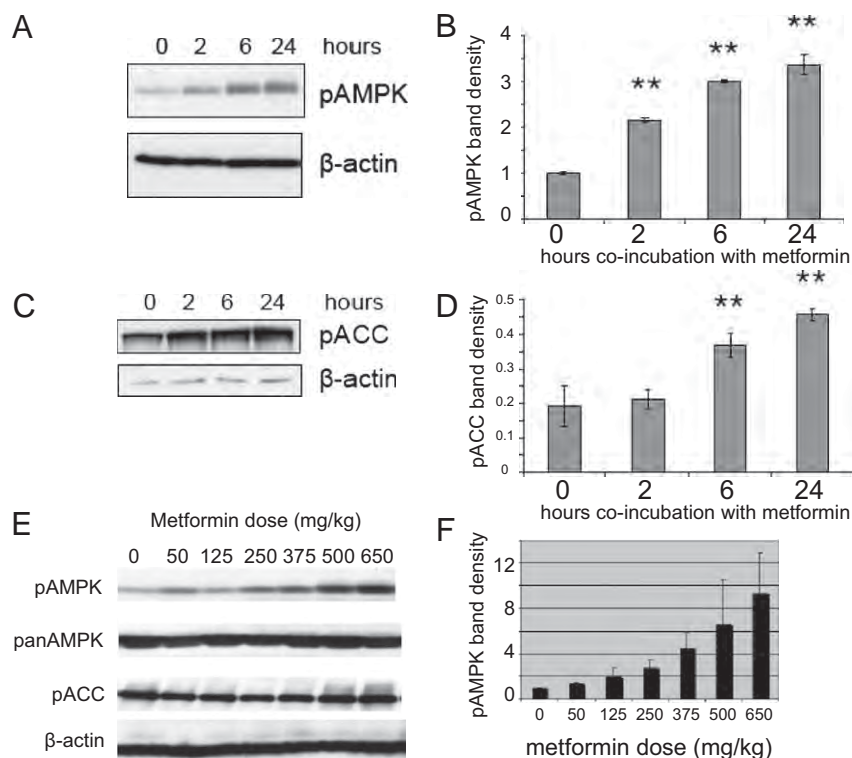
Fig. 1. Metformin activates AMPK in vitro and in vivo. (*A*) MDCK cells were incubated with 1.0 mM metformin for the number of hours stated. Cells lysates were blotted for pAMPK, the activated form of AMPK. (*B*) Quantitation of pAMPK band density normalized to β-actin. Comparisons of the mean (±SEM) are shown for each time point (**$P = 0.00002$ at 2 h, $P = 0.001$ at 6 h, $P = 0.0005$ at 24 h; Tukey's test relative to vehicle-treated control for that set of wells; $n = 3$ wells for each condition). (*C*) MDCK cells were treated as in *A* and blotted for pACC, a downstream target of pAMPK. (*D*) Comparisons of the mean band density relative to β-actin (±SEM) are shown for each time point. There is no significant change in protein expression between 0 and 2 h (**$P = 0.0306$ at 6 h, $P = 0.005$ at 24 h; Tukey's test relative to vehicle-treated control for that set of wells; $n = 3$ for each condition). (*E*) C57BL/6 mice (8 wk old) were treated i.p. with metformin or with vehicle for 3 d. Western blot analysis of kidney homogenates using anti-pAMPK demonstrates increasing activation of AMPK with increasing metformin dosing. (*F*) Quantitation of Western blot of in vivo pAMPK levels by normalized band density to β-actin. Comparisons of the mean (±SEM) are shown for each time point; $n = 3$ mice for each dose.

and very low concentrations of the α2 isoform. Expression of the α1 shRNA construct reduced expression of this protein by ~90%, whereas the α2 shRNA had no effect on α1 protein expression. Knockdown of α1 also reduced the level of total pAMPK by ~90% (Fig. 2*A*). CFTR-dependent short-circuit current (I_{sc}) was measured for cells grown on filters mounted in Ussing chambers for 4 d following adenoviral transduction, with or without exposure to 1 mM metformin for 2–4 h before measurement. To initiate CFTR-mediated secretion, CFTR-expressing and mock-transduced MDCK cells were treated with the cAMP agonists 3-isobutyl-1-methylxanthine (IBMX) and forskolin, and the experiment was concluded by the application of the specific CFTR inhibitor CFTR-Inh$_{172}$ (22). Typical traces of I_{sc} changes are shown in Fig. 2 *B* and *C*. CFTR-expressing cells generally showed an early peak in I_{sc}, within 1–2 min following forskolin/IBMX treatment, followed by a lower plateau current within ~5 min. This remaining current was sensitive to inhibition by CFTR-Inh$_{172}$. Metformin (1 mM) pretreatment of empty vector-transfected and AMPK-α2–KD MDCK cells significantly reduced CFTR-dependent I_{sc} by 60–70% relative to cells pretreated with vehicle (Fig. 2*D*). However, there was no metformin-dependent inhibition of CFTR current in AMPK-α1–KD MDCK cells, suggesting that the metformin-induced inhibition of CFTR occurs specifically via an AMPK-α1–dependent mechanism.

Inhibition of mTOR by Metformin in MDCK Cells Is AMPK Dependent. To determine whether metformin induces AMPK-mediated inhibition of mTOR activity, we tested whether mTOR activity is

diminished in MDCK cells cultured in the presence of metformin by blotting for the phosphorylated form of the mTOR downstream target ribosomal S6 kinase (S6K) p70 subunit (p70 S6K) (Fig. 3*A*) relative to pan-S6K (Fig. 3*B*). This inhibition is time dependent, with increasing exposure to metformin resulting in greater suppression of this pathway. Total S6K levels remain constant. The inhibition takes longer to achieve than inhibition of CFTR or ACC, consistent with the indirect inhibition of mTOR by AMPK via TSC2/1 and Rheb (Ras homolog enriched in brain) (Fig. 3*C*). This effect is markedly less pronounced in AMPK-α1–KD cells (Fig. S1). To evaluate whether these changes in phospho-protein levels translated into changes in proliferation, an Alamar Blue assay was used to quantitate proliferation in wild-type and AMPK-α1–KD MDCK cells. In figure 3*D*, the *y* axis depicts cell number measured at each given concentration of metformin and normalized to the control value, which was obtained for the same cell type at the same time point without metformin treatment. Wild-type MDCK cells exhibited a metformin dose-dependent decrease in proliferation, but this response was diminished significantly in the AMPK-α1–KD MDCK cells (Fig. 3*D*). At the highest concentration of metformin tested (5 mM), substantial growth suppression was detected in AMPK-KD cells, perhaps because of the low level of residual AMPK that is expressed in these KD cells (Fig. 2*A*) or the effects of high doses of metformin on yet to be identified AMPK-independent pathways. A similar suppressive effect of metformin treatment on proliferation was observed in vivo. We performed immunofluorescence analyses on kidneys from metformin-treated and vehicle-treated cystic *Pkd1$^{flox/-}$;Ksp-Cre*
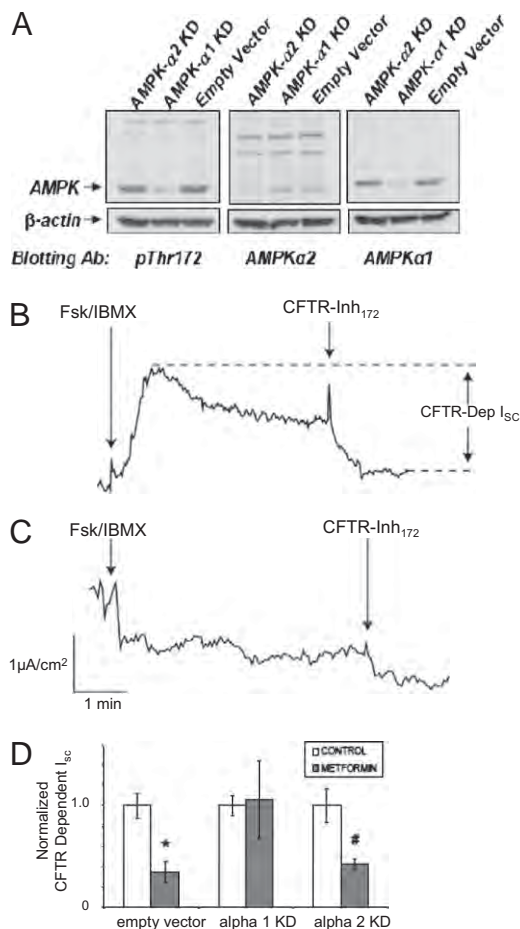
Fig. 2. Metformin inhibits I_{sc} in an AMPK-dependent manner. (*A*) MDCK cells stably expressing empty vector or shRNA plasmids directed against either the catalytic α1 or α2 subunits of AMPK (AMPK-α1–KD and AMPK-α2–KD cells, respectively) were blotted with antibodies against phosphorylated Thr[172] (pThr[172]), AMPKα2, or AMPKα1 to measure the level of AMPK expression. (*B*) A representative I_{sc} trace of cells with or without 1 mM metformin pretreatment. Mock-transduced or NH$_2$-terminally GFP-tagged, CFTR-transduced MDCK empty vector control cells, AMPK-α1–KD cells, or AMPK-α2–KD cells were treated with 1 mM metformin or vehicle for 2–4 h before Ussing chamber measurements of I_{sc}. A representative I_{sc} trace of vehicle-pretreated CFTR-expressing empty vector control MDCK cells treated with IBMX and forskolin (Fsk) and then with CFTR-Inh$_{172}$ at the indicated times is shown. (*C*) A similar representative trace of mock-transduced empty vector control cells shows no response to these cAMP agonists or to CFTR-Inh$_{172}$. There also was no significant change in I_{sc} following addition of 10 μM amiloride, indicating that the epithelial Na$^+$ channel does not contribute significantly to I_{sc} in these MDCK cells. (*D*) Comparisons of the normalized mean (±SEM) CFTR-dependent I_{sc} in empty vector control, AMPK-α1–KD, and AMPK-α2–KD cells with (dark gray bars) or without (white bars) metformin pretreatment (*$P = 0.002$, #$P = 0.022$; unpaired t test relative to vehicle-treated controls for that cell type; $n = 6$–9 filters for each condition).

(Pkd1, polycystic kidney disease-1 gene; Ksp-Cre, kidney specific cadherin promoter-driven Cre recombinase) mice using an antibody directed against Ki67, a marker of actively proliferating cells (Fig. S2). In kidneys from vehicle-treated mice, $19.7 \pm 3.8\%$ of the cells exhibited Ki67 positivity (450 cells were counted from each of six mice) in comparison with $10.6 \pm 3.6\%$ of the cells in metformin-treated mice (450 cells were counted from each of four mice) ($P < 0.0074$). To assess whether the effects of metformin treatment on proliferation correlate with the level of mTOR activity in the cystic kidneys before and after metformin treatment, we performed immunohistochemistry using an antibody directed against the acti-
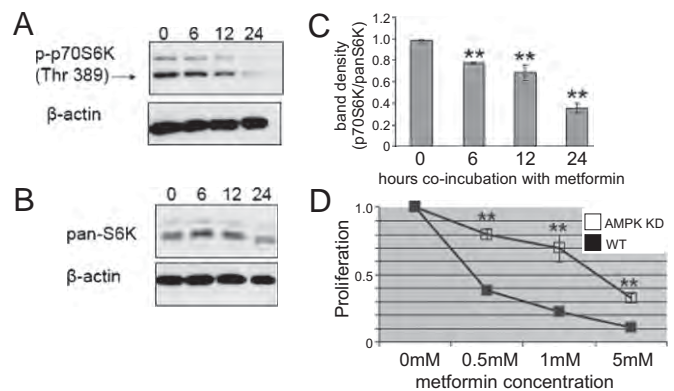

Fig. 3. Metformin inhibits phosphorylation of the mTOR downstream target, p70 S6K, and slows cellular proliferation in an AMPK-dependent manner. A subconfluent monolayer of MDCK cells was incubated with 1.0 mM metformin for the indicated time. Cells lysates were blotted for the downstream marker of mTOR activity. (*A*) p70 S6K. (*B*) Total S6K. (*C*) Quantitation of phospho-S6K Western blot band density normalized to β-actin. Comparisons of the mean (±SEM) are shown for each time point. (**$P = 0.00005$ at 6 h, $P = 0.009$ at 12 h, $P = 0.00009$ at 24 h; one-way ANOVA with Tukey's analysis relative to vehicle-treated control for that set of wells; $n = 3$ wells for each condition). (*D*) Effect of metformin on proliferation of control MDCK cells and MDCK cells stably transfected with shRNA against AMPK, graphed relative to control. The y axis represents cell number at each concentration of metformin, normalized to the control value measured for the same cell type at the same time point without metformin treatment. (**$P = 0.0008$ at 0.5 mM, $P = 0.009$ at 1.0 mM, $P = 0.004$ at 5 mM; unpaired t tests between both cell lines, comparing rates of cell proliferation with $n = 3$ per metformin concentration).

vated form of an mTOR target. As depicted in Fig. S3, we stained tissue from control and metformin-treated cystic mice with an antibody that detects the phosphorylated form of eukaryotic translation initiation factor 4E-binding protein 1 (p4E-BP1), an mTOR target whose level of phosphorylation commonly is used to report levels of mTOR activity (23). We find that the level of p4E-BP1 generally is higher in cyst-lining epithelial cells in control animals than in metformin-treated animals, an observation that is consistent with the interpretation that metformin treatment reduces the level of mTOR activation.

Metformin Treatment Slows Cystogenesis ex Vivo and in Vivo. The 2D culture models do not accurately depict cell growth in the 3D environment in which cysts develop. To evaluate metformin's effects in the context of cystogenesis, we suspended MDCK cells in a 3D collagen matrix and allowed them to form cysts spontaneously in the presence of forskolin and IBMX (24). Cultures coincubated with metformin for the duration of cyst growth produced significantly smaller cysts than those similarly treated with forskolin or IBMX alone ($P = 0.003$, unpaired t test, $n = 3$ gels for each experimental condition) (Fig. 4*A*).

We next tested the effect of metformin on ex vivo cystogenesis. Kidneys were removed from C57/B6 mice at embryonic day 12.5 (E12.5). One embryonic kidney was cultured in the presence of membrane-permeable 8-bromo-cAMP (8-Br-cAMP) to stimulate fluid secretion, and the contralateral kidney was coincubated with 8-Br-cAMP and metformin for 4 d. Culture in the presence of 8-Br-cAMP induces cyst formation in embryonic mouse kidneys (4). Metformin treatment significantly decreased the fractional cyst area ($P = 0.04$, unpaired t test; $n = 4$ for each experimental condition). On day 5, metformin was removed from the treated embryonic kidney, and cyst growth recommenced in the treated kidney, demonstrating that metformin treatment slowed cyst growth without affecting the viability of the tissue (Fig. 4*B*).
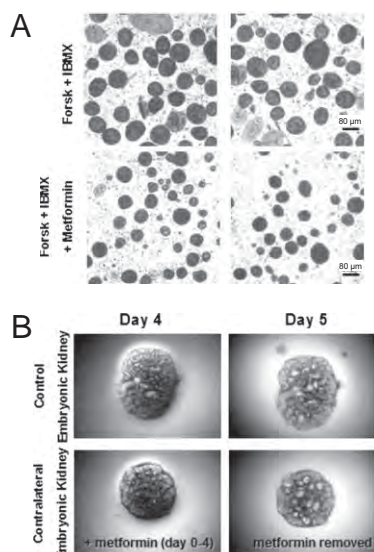
Fig. 4. Metformin reduces cyst size in vitro and ex vivo. (*A*) Representative light micrographs of MDCK cell cysts grown in collagen gels. Cysts were treated with forskolin (Forsk) and IBMX to enhance apical fluid secretion with (*Lower*) or without (*Upper*) 1.0 mM metformin for 20 d. Gels were melted, and the cysts were allowed to precipitate to the bottom for imaging. (*B*) Metformin treatment reduces cyst size in an ex vivo model of renal cystogenesis. Embryonic kidneys were placed in culture at E12 and maintained for 5 d in the continued presence of 100 μM 8-Br-cAMP. Representative light microscopic images from one mouse are shown. Each row shows the same kidney. The contralateral kidney (*Lower*) was treated with metformin for 4 d and then switched to normal medium, illustrating that the embryonic kidney remains viable and capable of cystogenesis.

Metformin Treatment Slows Cystogenesis in the in Vivo models of PKD.

We next tested whether metformin slows cyst growth in a murine model of PKD. Initially, we used the most aggressive viable murine model of PKD (*Pkd1^{flox/-};Ksp-Cre*) in which there is progression of renal cystic disease within the first week of life and death between the second and third weeks of life (6). We treated these mice with daily i.p. injections of metformin (300 mg·kg^{-1}·d^{-1}) dissolved in a 5% (mass/vol) dextrose solution from postnatal day 4 (P4) until P6. This dose is known to activate AMPK (25). Mice then were killed, and kidneys were harvested at P7. The vehicle-treated *Pkd1^{flox/-};Ksp-Cre* kidneys (Fig. 5C) were profoundly cystic and greatly enlarged compared with the *Pkd1^{+/+};Ksp-Cre* kidneys (Fig. 5A). In contrast, cyst burden was significantly reduced in the kidneys from the metformin-treated *Pkd1^{flox/-};Ksp-Cre* mice (Fig. 5B). Because metformin can affect body weight, the kidney weight: body weight ratio was not used as an end point (26). Instead, the effect of metformin on renal morphology was quantitated by evaluating the cystic index, which determines the fraction of a given section that corresponds to luminal area (including both tubule and cyst lumens). Untreated *Pkd1^{flox/-};Ksp-Cre* kidneys had a cystic index of 71.4 ± 4.0%, whereas the cystic index of metformin-treated *Pkd1^{flox/-};Ksp-Cre* kidneys was 51.8 ± 5.2%. (*P* = 0.029; unpaired *t* test; *n* = 4 control mice and *n* = 8 metformin-treated mice). In wild-type kidneys, this evaluation calculates a cystic index of 10% resulting from tubular lumens. Notably, although the metformin-treated kidney is still cystic, it displays significantly more parenchyma than the vector-treated control. Although metformin might prevent further cyst growth, it is unlikely that treatment reduces the size of preexisting cysts.

We established an inducible model for Pkd1 inactivation using a conditional *Pkd1^{flox}* allele in combination with a tamoxifen-inducible Cre recombinase (pCX-CreER) (6, 27, 28). Induction of Cre expression before P13 leads to rapidly progressive cystic disease
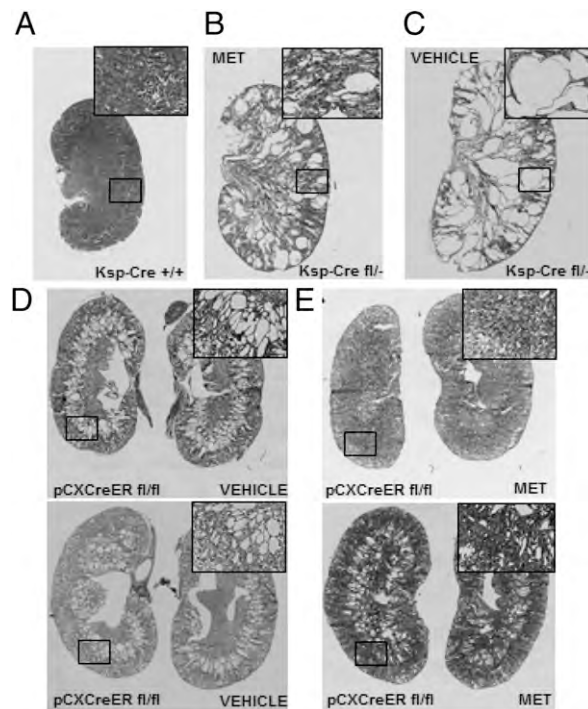

Fig. 5. Metformin treatment reduces the cystic index in two mouse models of ADPKD. (*A–C*) Representative midsagittal sections from the kidneys of (*A*) a *PKD1^{+/+};Ksp-Cre* mouse, (*B*) a metformin-treated *PKD1^{flox/-};Ksp-Cre* mouse, and (*C*) a vehicle-treated P*KD1^{flox/-};Ksp-Cr*e mouse at P7. The metformin- and vehicle-treated mice were given daily weight-adjusted i.p. injections from P4 until P6. (*D* and *E*) Representative images from *PKD^{flox/-};pCX-CreER* mice treated with vehicle (*D*) or metformin (*E*) from P7–P17, with Cre induction at P9 or P10.

in *Pkd1^{flox/flox}* animals (29). In this system, it is possible to initiate metformin treatment before or during cyst development. Thus, this model might replicate more accurately the clinical scenario in which metformin therapy could commence early in the disease process and act to prevent or slow subsequent cyst development. We initiated metformin treatment (300 mg·kg^{-1}·d^{-1}) at P7 and then injected tamoxifen i.p. at P9 or P10 to initiate disease induction. We continued daily metformin injections until P18, when the animal was killed and kidneys were harvested for histology and cystic index evaluation. Once again, metformin treatment resulted in a smaller fractional cyst burden than seen in vehicle-treated controls (31% vs. 43%; *P* = 0.041, unpaired *t* test; *n* = 6 vehicle-treated mice, and *n* = 7 for metformin-treated mice), a decrease of nearly one-third in the cyst burden (Fig. 5 *D* and *E*).

Discussion

AMPK activity can be targeted pharmacologically with metformin to reduce the growth of renal cysts. Metformin acts through AMPK to decrease epithelial fluid secretion by directly inhibiting CFTR and to decrease cellular proliferation by indirectly targeting mTOR. Metformin stimulates AMPK phosphorylation in cultured MDCK renal epithelial cells, and this phosphorylation correlates with increased AMPK activity, as evidenced by an increase in the level of the AMPK-mediated inhibitory phosphorylation of ACC. Metformin's inhibitory action on CFTR-mediated chloride transport is AMPK dependent. Additionally, we show that metformin inhibition of mTOR translates into an AMPK-dependent inhibition of cell proliferation. Using both an in vitro model of MDCK cell cystogenesis and embryonic kidneys ex vivo, we demonstrate that metformin decreases cyst size and fractional cyst area. Finally, we illustrate the potential thera-

MEDICAL SCIENCES

peutic utility of metformin by testing it in two murine models of ADPKD, both of which are attributable to inactivation of the gene encoding polycystin-1.

Metformin is taken by millions of Americans each year. It currently is approved by the Food and Drug Administration for the treatment of type 2 DM and, intriguingly, for polycystic ovary syndrome, a disease that has a name similar to that of polycystic kidney disease but whose pathogenesis is even less well understood. In fact, metformin often is considered first-line therapy for the treatment of type 2 DM because of its relatively small side-effect profile. Recent literature suggests that metformin's activation of AMPK may be the result of its ability to prevent AMP breakdown, although the exact mechanisms of action of metformin in polycystic ovary syndrome or in type 2 DM remain largely unknown (30). Recent reports also suggest that metformin may exert an antineoplastic effect. It has been reported that metformin acts in a dose-dependent manner to inhibit the proliferation of breast cancer cells, and that this effect can be blocked in the presence of siRNA directed against AMPK (31). This inhibition also is associated with a decrease in mTOR activation, suggesting that metformin's antiproliferative effect is directed through the activation of AMPK and consequent inhibition of mTOR.

In transporting epithelial cells, AMPK not only modulates CFTR activity but also inhibits the epithelial sodium channel (ENaC) (32–34). Although in the cystic kidney this effect conceivably could lead to decreased fluid absorption and therefore perhaps to increased accumulation of cyst fluid, the role of ENaC in cyst-lining epithelial cells is uncertain (35). CFTR can inhibit ENaC channel function directly. Thus, inhibition of CFTR by AMPK could reduce such sodium channel inhibition (36, 37). Taken together, the effects of AMPK activation on ENaC function in the context of renal cystic disease are bimodal and complex. The net effect of AMPK modulation in vivo, however, is likely to reduce luminal fluid accumulation (38).

Numerous therapies for ADPKD, including vasopressin receptor inhibitors, calcium-sensing receptor inhibitors, CFTR inhibitors, cell-cycle inhibitors, and rapamycin, are in development or in clinical trials (4, 9, 39, 40). Each of these strategies targets one of the key processes (proliferation and secretion) thought to be involved in the pathogenesis of PKD. By acting through AMPK, metformin may offer the significant advantage of blocking both processes (Fig. S4). Moreover, metformin already is approved by the Food and Drug Administration and generally is well tolerated. The most serious, albeit rare, side effect of metformin is lactic acidosis and, because metformin is cleared by the kidney, chronic renal disease has been considered a potential predisposing factor for this complication. Ideally, however, metformin use could be initiated at an early stage in ADPKD progression, before the development of substantial cyst burden and compromise of renal function, thus allowing maximal preventive benefit and minimizing the potential for renal dysfunction to limit the safe use of the drug (41, 42). Given the relatively late onset and slow progression of ADPKD, it is conceivable that, even if metformin were to have only modest effects in delaying or slowing cyst development, it might increase significantly the time to the development of end-stage renal disease and perhaps reduce the need for renal replacement therapy.

In this study, only one dose known to activate AMPK in vivo was tested. When considered on a simple milligram per kilogram body weight basis, this dose appears considerably higher than the current maximum dose prescribed for patients with diabetes or polycystic ovary syndrome. However, human-equivalent dose extrapolation is calculated more accurately based on body surface area than on weight. When this calculation is performed for a 60-kg adult, the dose used in our mouse studies extrapolates to a daily dose of ~1,500 mg (43), well within the range in which metformin is safely used in humans. We have not tested the efficacy of lower doses or of alternative dosing regimens in these

mouse models. It is likely, however, based on the established pharmacokinetics of metformin, that single daily dosing is suboptimal, and thus we almost certainly did not observe the maximal suppressive effects that metformin potentially could exert on the severity of cyst growth (44). Support for this contention derives from the data presented in Fig. 4C, because in the embryonic kidney model, cyst growth resumes rapidly shortly after removal of metformin from the culture medium. Thus, short-term intermittent exposure to metformin may not be adequate to suppress cyst development optimally. It is quite possible that even lower doses administered more frequently might produce beneficial effects in the setting of polycystic kidney disease. It is important to note that our efforts to assess effects of metformin treatment on renal functional parameters such as serum concentrations of serum urea nitrogen and creatinine were inconclusive, in part because of interindividual variability. Further studies, perhaps using more slowly progressive disease models, will be required to reduce this variance and to assess the extent to which metformin treatment can protect or improve renal function in the setting of PKD. In addition, subsequent development of metformin for this clinical application will require pharmacokinetic and pharmacodynamic studies designed to identify an ideal dosing regimen that achieves maximal activation of renal tubular AMPK.

In conclusion, we find that metformin stimulates AMPK, resulting in inhibition of both CFTR and mTOR and thereby both epithelial secretion and proliferation. Our data suggest the possible utility of metformin as a therapy for ADPKD and that AMPK is a potential pharmacological target for ADPKD therapy. The large body of knowledge associated with metformin administration might facilitate the translation of these findings into clinical trials to test the proposition that metformin is a safe and promising approach that exploits AMPK activity to treat this challenging disease.

Methods

Western Blotting and Proliferation Assay. Cultured MDCK cells were lysed, and protein was extracted for Western blotting using standard protocols. For experiments involving AMPK activation in vivo, kidneys were snap-frozen in situ, and homogenates were prepared according to published protocol before Western blotting (45). Details and antibodies used are given in SI Methods.

Generation of AMPK-KD Cell Lines. AMPK-KD cell lines were established by lentiviral infection. Further details and targeting sequences are given in SI Methods.

CFTR Short-Circuit Current Measurements in MDCK II Cells. MDCK cells expressing either empty vector or shRNA against one of two AMPK isotypes underwent adenoviral transduction to express GFP-tagged CFTR. I_{sc} was assessed by Ussing chamber measurement after stimulation with forskolin and 3-isobutyl-1-methylxanthine and then CFTR-Inh$_{172}$ to determine the CFTR-dependent change in I_{sc}. Cells were pretreated with vector or metformin as noted. Further details are given in SI Methods.

In Vitro Cystogenesis. MDCK cells were suspended in a collagen matrix as previously described by Grantham and coworkers (24). Further details and quantitation method are given in SI Methods.

Ex Vivo Cystogenesis. Embryonic kidneys were microdissected from timed pregnant C57BL/6 mice at E12.5, cultured per standard protocol with the addition of 8-Br-cAMP to promote cyst formation, and treated with either metformin or vector (4, 46). Further details are given in SI Methods.

Mouse Strains, Histology, and Cystic Index. All animal protocols were approved and conducted in accordance with Yale Animal Resources Center and Institutional Animal Care and Use Committee regulations. Pkd1$^{flox/flox}$ and Ksp-Cre lines have been described previously (6, 47, 48). From P4 until P6, experimental mice received either metformin (300 mg/kg body weight) dissolved in 5% (mass/vol) dextrose or 5% (mass/vol) dextrose alone through daily i.p. injections. These mice were killed at P7. The pCX-CreER transgenic line (kindly provided by Corinne Lobe, University of Toronto, Toronto) gives generalized Cre expression based on the pCAGGS chicken β-actin promoter construct. Cre recombinase translocation to the nucleus was induced by

1. Torres VE, Grantham JJ (2008) *Brenner & Rector's The Kidney*, ed Brenner B (Saunders Elsevier, Philadelphia).
2. Davidow CJ, Maser RL, Rome LA, Calvet JP, Grantham JJ (1996) The cystic fibrosis transmembrane conductance regulator mediates transepithelial fluid secretion by human autosomal dominant polycystic kidney disease epithelium in vitro. *Kidney Int* 50:208–218.
3. Li H, Findlay IA, Sheppard DN (2004) The relationship between cell proliferation, Cl-secretion, and renal cyst growth: A study using CFTR inhibitors. *Kidney Int* 66:1926–1938.
4. Yang B, Sonawane ND, Zhao D, Somlo S, Verkman AS (2008) Small-molecule CFTR inhibitors slow cyst growth in polycystic kidney disease. *J Am Soc Nephrol* 19:1300–1310.
5. Wahl PR, et al. (2006) Inhibition of mTOR with sirolimus slows disease progression in Han:SPRD rats with autosomal dominant polycystic kidney disease (ADPKD). *Nephrol Dial Transplant* 21:598–604.
6. Shibazaki S, et al. (2008) Cyst formation and activation of the extracellular regulated kinase pathway after kidney specific inactivation of Pkd1. *Hum Mol Genet* 17:1505–1516.
7. Sabers CJ, et al. (1995) Isolation of a protein target of the FKBP12-rapamycin complex in mammalian cells. *J Biol Chem* 270:815–822.
8. Cardenas ME, Cutler NS, Lorenz MC, Di Como CJ, Heitman J (1999) The TOR signaling cascade regulates gene expression in response to nutrients. *Genes Dev* 13:3271–3279.
9. Shillingford JM, et al. (2006) The mTOR pathway is regulated by polycystin-1, and its inhibition reverses renal cystogenesis in polycystic kidney disease. *Proc Natl Acad Sci USA* 103:5466–5471.
10. Hallows KR, Raghuram V, Kemp BE, Witters LA, Foskett JK (2000) Inhibition of cystic fibrosis transmembrane conductance regulator by novel interaction with the metabolic sensor AMP-activated protein kinase. *J Clin Invest* 105:1711–1721.
11. King JD, Jr, et al. (2009) AMP-activated protein kinase phosphorylation of the R domain inhibits PKA stimulation of CFTR. *Am J Physiol Cell Physiol* 297:C94–C101.
12. Gwinn DM, et al. (2008) AMPK phosphorylation of raptor mediates a metabolic checkpoint. *Mol Cell* 30:214–226.
13. Inoki K, Zhu T, Guan KL (2003) TSC2 mediates cellular energy response to control cell growth and survival. *Cell* 115:577–590.
14. Hardie DG (2007) AMP-activated/SNF1 protein kinases: Conserved guardians of cellular energy. *Nat Rev Mol Cell Biol* 8:774–785.
15. Zhou G, et al. (2001) Role of AMP-activated protein kinase in mechanism of metformin action. *J Clin Invest* 108:1167–1174.
16. Shaw RJ, et al. (2005) The kinase LKB1 mediates glucose homeostasis in liver and therapeutic effects of metformin. *Science* 310:1642–1646.
17. Hallows KR, Kobinger GP, Wilson JM, Witters LA, Foskett JK (2003) Physiological modulation of CFTR activity by AMP-activated protein kinase in polarized T84 cells. *Am J Physiol Cell Physiol* 284:C1297–C1308.
18. Hallows KR, McCane JE, Kemp BE, Witters LA, Foskett JK (2003) Regulation of channel gating by AMP-activated protein kinase modulates cystic fibrosis transmembrane conductance regulator activity in lung submucosal cells. *J Biol Chem* 278:998–1004.
19. Walker J, Jijon HB, Churchill T, Kulka M, Madsen KL (2003) Activation of AMP-activated protein kinase reduces cAMP-mediated epithelial chloride secretion. *Am J Physiol Gastrointest Liver Physiol* 285:G850–G860.
20. Magenheimer BS, et al. (2006) Early embryonic renal tubules of wild-type and polycystic kidney disease kidneys respond to cAMP stimulation with cystic fibrosis transmembrane conductance regulator/Na(+),K(+),2Cl(-) Co-transporter-dependent cystic dilation. *J Am Soc Nephrol* 17:3424–3437.
21. O'Sullivan DA, et al. (1998) Cystic fibrosis and the phenotypic expression of autosomal dominant polycystic kidney disease. *Am J Kidney Dis* 32:976–983.
22. Ma T, et al. (2002) Thiazolidinone CFTR inhibitor identified by high-throughput screening blocks cholera toxin-induced intestinal fluid secretion. *J Clin Invest* 110:1651–1658.
23. Iida S, et al. (2010) Novel classification based on immunohistochemistry combined with hierarchical clustering analysis in non-functioning neuroendocrine tumor patients. *Cancer Sci* 101:2278–2285.
24. Mangoo-Karim R, Uchic M, Lechene C, Grantham JJ (1989) Renal epithelial cyst formation and enlargement in vitro: Dependence on cAMP. *Proc Natl Acad Sci USA* 86:6007–6011.
25. Zou MH, et al. (2004) Activation of the AMP-activated protein kinase by the anti-diabetic drug metformin in vivo. Role of mitochondrial reactive nitrogen species. *J Biol Chem* 279:43940–43951.
26. Golay A (2008) Metformin and body weight. *Int J Obes (Lond)* 32:61–72.
27. Guo C, Yang W, Lobe CG (2002) A Cre recombinase transgene with mosaic, widespread tamoxifen-inducible action. *Genesis* 32:8–18.
28. Miyazaki J, et al. (1989) Expression vector system based on the chicken beta-actin promoter directs efficient production of interleukin-5. *Gene* 79:269–277.
29. Piontek K, Menezes LF, Garcia-Gonzalez MA, Huso DL, Germino GG (2007) A critical developmental switch defines the kinetics of kidney cyst formation after loss of Pkd1. *Nat Med* 13:1490–1495.
30. Ouyang J, Parakhia RA, Ochs RS (2011) Metformin activates AMP-kinase through inhibition of AMP deaminase. *J Biol Chem* 286:1–11.
31. Zakikhani M, Dowling R, Fantus IG, Sonenberg N, Pollak M (2006) Metformin is an AMP kinase-dependent growth inhibitor for breast cancer cells. *Cancer Res* 66:10269–10273.
32. Bhalla V, et al. (2006) AMP-activated kinase inhibits the epithelial Na+ channel through functional regulation of the ubiquitin ligase Nedd4-2. *J Biol Chem* 281:26159–26169.
33. Almaça J, et al. (2009) AMPK controls epithelial Na(+) channels through Nedd4-2 and causes an epithelial phenotype when mutated. *Pflugers Arch* 458:713–721.
34. Carattino MD, et al. (2005) Epithelial sodium channel inhibition by AMP-activated protein kinase in oocytes and polarized renal epithelial cells. *J Biol Chem* 280:17608–17616.
35. Muchatuta MN, Gattone VH, 2nd, Witzmann FA, Blazer-Yost BL (2009) Structural and functional analyses of liver cysts from the BALB/c-cpk mouse model of polycystic kidney disease. *Exp Biol Med (Maywood)* 234:17–27.
36. Konstas AA, Koch JP, Korbmacher C (2003) cAMP-dependent activation of CFTR inhibits the epithelial sodium channel (ENaC) without affecting its surface expression. *Pflugers Arch* 445:513–521.
37. König J, Schreiber R, Voelcker T, Mall M, Kunzelmann K (2001) The cystic fibrosis transmembrane conductance regulator (CFTR) inhibits ENaC through an increase in the intracellular Cl- concentration. *EMBO Rep* 2:1047–1051.
38. Doctor RB, et al. (2007) Regulated ion transport in mouse liver cyst epithelial cells. *Biochim Biophys Acta* 1772:345–354.
39. Gattone VH, 2nd, et al. (2009) Calcimimetic inhibits late-stage cyst growth in ADPKD. *J Am Soc Nephrol* 20:1527–1532.
40. Bukanov NO, Smith LA, Klinger KW, Ledbetter SR, Ibraghimov-Beskrovnaya O (2006) Long-lasting arrest of murine polycystic kidney disease with CDK inhibitor roscovitine. *Nature* 444:949–952.
41. Salpeter S, Greyber E, Pasternak G, Salpeter E (2006) Risk of fatal and nonfatal lactic acidosis with metformin use in type 2 diabetes mellitus. *Cochrane Database Syst Rev* (1):CD002967.
42. Scott KA, Martin JH, Inder WJ (2010) Acidosis in the hospital setting—is metformin a common precipitant? *Intern Med J* 40(5):342–346.
43. Reagan-Shaw S, Nihal M, Ahmad N (2008) Dose translation from animal to human studies revisited. *FASEB J* 22:659–661.
44. Scheen AJ (1996) Clinical pharmacokinetics of metformin. *Clin Pharmacokinet* 30:359–371.
45. Mount PF, et al. (2005) Acute renal ischemia rapidly activates the energy sensor AMPK but does not increase phosphorylation of eNOS-Ser1177. *Am J Physiol Renal Physiol* 289:F1103–F1115.
46. Marlier A, Schmidt-Ott KM, Gallagher AR, Barasch J, Karihaloo A (2009) Vegf as an epithelial cell morphogen modulates branching morphogenesis of embryonic kidney by directly acting on the ureteric bud. *Mech Dev* 126:91–98.
47. Lin F, et al. (2003) Kidney-specific inactivation of the KIF3A subunit of kinesin-II inhibits renal ciliogenesis and produces polycystic kidney disease. *Proc Natl Acad Sci USA* 100:5286–5291.
48. Shao X, Somlo S, Igarashi P (2002) Epithelial-specific Cre/lox recombination in the developing kidney and genitourinary tract. *J Am Soc Nephrol* 13:1837–1846.

MEDICAL SCIENCES

Article

The γ-Secretase Cleavage Product of Polycystin-1 Regulates TCF and CHOP-Mediated Transcriptional Activation through a p300-Dependent Mechanism

David Merrick,[1,2] Hannah Chapin,[1,2] Julie E. Baggs,[5] Zhiheng Yu,[3] Stefan Somlo,[3,4] Zhaoxia Sun,[4] John B. Hogenesch,[5] and Michael J. Caplan[1,2,*]
[1]Department of Cellular and Molecular Physiology
[2]Department of Cell Biology
[3]Department of Medicine, Section of Nephrology
[4]Department of Genetics
Yale University School of Medicine, New Haven, CT 06510, USA
[5]Department of Pharmacology, Institute of Translational Medicine and Therapeutics, Penn Genome Frontiers Institute, University of Pennsylvania School of Medicine, Philadelphia, PA 19104-6145, USA
*Correspondence: michael.caplan@yale.edu
DOI 10.1016/j.devcel.2011.10.028

SUMMARY

Mutations in *Pkd1*, encoding polycystin-1 (PC1), cause autosomal-dominant polycystic kidney disease (ADPKD). We show that the carboxy-terminal tail (CTT) of PC1 is released by γ-secretase-mediated cleavage and regulates the Wnt and CHOP pathways by binding the transcription factors TCF and CHOP, disrupting their interaction with the common transcriptional coactivator p300. Loss of PC1 causes increased proliferation and apoptosis, while reintroducing PC1-CTT into cultured *Pkd1* null cells reestablishes normal growth rate, suppresses apoptosis, and prevents cyst formation. Inhibition of γ-secretase activity impairs the ability of PC1 to suppress growth and apoptosis and leads to cyst formation in cultured renal epithelial cells. Expression of the PC1-CTT is sufficient to rescue the dorsal body curvature phenotype in zebrafish embryos resulting from either γ-secretase inhibition or suppression of *Pkd1* expression. Thus, γ-secretase-dependent release of the PC1-CTT creates a protein fragment whose expression is sufficient to suppress ADPKD-related phenotypes in vitro and in vivo.

INTRODUCTION

Autosomal-dominant polycystic kidney disease (ADPKD), a common genetic disorder, produces fluid-filled renal cysts that disrupt the normal tubular architecture and can ultimately lead to kidney failure (Wilson, 2004). Most cases (85%) result from mutations in the gene encoding polycystin-1 (*Pkd1*), with the remaining 15% resulting from mutations in the gene encoding polycystin-2 (*Pkd2*) (Harris and Torres, 2009; Rossetti et al., 2007). Polycystin-1 (PC1) has a large extracellular domain, 11 transmembrane spans, and a short carboxy-terminal cyto-

plasmic tail (Hughes et al., 1995). The PC1 C-terminal tail (PC1-CTT) has been implicated in the regulation of several signaling pathways, including Wnt (Kim et al., 1999; Lal et al., 2008; Zhang et al., 2007), mTOR (Shillingford et al., 2006), p21/JAK/STAT (Bhunia et al., 2002; Low et al., 2006; Talbot et al., 2011), and activator protein-1 (Arnould et al., 1998; Chauvet et al., 2004; Parnell et al., 2002). Polycystin-2 is a nonselective calcium-permeable cation channel that interacts and forms a complex with PC1 via the coiled-coil domains present in each of these proteins (Qian et al., 1997).

PC1 is subject to several proteolytic cleavages (Chapin and Caplan, 2010; Woodward et al., 2010), including an autocatalytic event that releases the N-terminal extracellular domain, which remains noncovalently associated with the transmembrane domains (Qian et al., 2002). The PC1-CTT is cleaved and translocates to the nucleus (Bertuccio et al., 2009; Chauvet et al., 2004; Low et al., 2006; Talbot et al., 2011). Nuclear PC1-CTT regulates cell-signaling pathways, including activation of STAT6/P100 and STAT3 (Low et al., 2006; Talbot et al., 2011), and inhibition of β-catenin-mediated canonical Wnt signaling (Lal et al., 2008). ADPKD cyst formation is thought to occur, at least in part, as a result of dysregulation of epithelial cell proliferation and of apoptosis (Chapin and Caplan, 2010; Lanoix et al., 1996; Shibazaki et al., 2008; Starremans et al., 2008; Takiar and Caplan, 2011).

We show that the CTT of PC1 is released by a γ-secretase-dependent cleavage and translocates to the nucleus, where it regulates transcriptional pathways involved in proliferation and apoptosis. Expression of the CTT fragment corrects several of the growth and morphogenesis-related phenotypes that characterize *Pkd1* null cells grown in three-dimensional (3D) culture. Furthermore, expression of the PC1-CTT rescues the dorsal body curvature that is produced both by inhibition of PC1 expression and by inhibition of γ-secretase activity in zebrafish. Finally, we provide evidence establishing a common mechanism for PC1-CTT inhibition of proproliferative and proapoptotic signaling pathways through disruption of the relevant transcription factors' interactions with the transcriptional coactivator p300.

RESULTS

Loss of PC1 in Mouse Renal Epithelial Cells Causes Increased Proliferation, Apoptosis, and Cyst Development in 3D Cell Culture

Clonal renal tubular epithelial cell lines derived from $Pkd1^{flox/-}$ mice were transfected with Cre recombinase to generate $Pkd1^{-/-}$ cells (Joly et al., 2006; Shibazaki et al., 2008). These cell lines, which are genetically identical except for the deletion of both copies of the gene encoding PC1 in the $Pkd1^{-/-}$ cells, produced strikingly different multicellular structures when grown in 3D culture. $Pkd1^{flox/-}$ cells grew into extended, tubule-like structures, whereas the $Pkd1^{-/-}$ cells developed into large, spherical cysts with hollow central lumens (Figure 1A). This can be seen graphically in time-lapse videos of $Pkd1^{flox/-}$ and $Pkd1^{-/-}$ cells grown in 3D culture (see Movies S1, S2, and S3 available online). The $Pkd1^{-/-}$ cells acquire a hollow central lumen within the first several days of culture, whereas the $Pkd1^{flox/-}$ cells slowly form linear tubule-like structures.

$Pkd1^{-/-}$ cells displayed higher levels of proliferation as compared to $Pkd1^{flox/-}$ cells, as measured by BrdU incorporation (Figure 1B). Apoptosis, as measured by staining for cleaved caspase-3, was virtually undetectable in the $Pkd1^{flox/-}$ cells, whereas apoptosis was evident in the $Pkd1^{-/-}$ cells, both in cyst-lining cells (Figure 1B, arrowheads) and at the center of cell aggregates that had yet to develop a hollow central lumen (Figure 1B, inset).

To determine the effect of the isolated PC1-CTT on cystogenesis, PC1-CTT was conditionally expressed under the control of doxycycline using a TET-Off inducible expression system in a stably transfected $Pkd1^{-/-}$ cell line. $Pkd1^{-/-}$ cells induced to express PC1-CTT displayed decreased levels of proliferation, as measured by BrdU incorporation. In addition, expression of PC1-CTT in the $Pkd1^{-/-}$ cells resulted in a dramatic change in the morphology of the structures they formed in 3D culture. Instead of large, hollow-lumen, cyst-like structures, the $Pkd1^{-/-}$ cells that express the PC1-CTT developed into branched tubule-like structures lacking a hollow central lumen (Figure 1C). The average sizes of the structures formed by the $Pkd1^{-/-}$ cells that express the PC1-CTT were similar to those measured for the parental $Pkd1^{flox/-}$ cells, and these structures were significantly smaller than the cystic structures formed by the $Pkd1^{-/-}$ cells (Figures 1D and 1E). Immunostaining performed with an antibody directed against the HA epitope appended to the PC1-CTT construct demonstrates that these small cell clusters and tubule-like structures do indeed express the exogenous PC1-CTT protein (shown in red in Figure 1C and in gray scale in the lower right panel of Figure 1D) and that the PC1-CTT protein is concentrated in the nucleus (Figure S1).

The CTT Cleavage of PC1 Is Dependent upon γ-Secretase

C-terminal cleavage of PC1 was detected in HEK cells transfected with a cDNA construct encoding full-length PC1 tagged at the C terminus with the DNA-binding domain of Gal4 (Bertuccio et al., 2009). Cleavage of PC1 allows the released CTT-Gal4 to translocate to the nucleus and to stimulate luciferase production from a cotransfected UAS-Luciferase reporter plasmid. Assays are performed in the presence of clasto-lactacystin, to prevent proteasome degradation of the cleaved PC1-CTT (Bertuccio et al., 2009). The γ-secretase inhibitor DAPT was added to the media after transfection, and the cells were incubated for 24 hr (Shearman et al., 2000). PC1 cleavage, as measured by Gal4-driven luciferase expression, was inhibited in a dose-dependent manner by DAPT, indicating that PC1-CTT cleavage is dependent upon γ-secretase activity (Figure 2A).

Further evidence for γ-secretase-dependent cleavage of PC1 was obtained through DAPT treatment of LLC-PK₁ cells stably expressing a full-length PC1 construct that carries a C-terminal HA tag. Lysates from cells treated with clasto-lactacystin (to prevent proteasome degradation of cleaved PC1 fragments) were fractionated to separate nuclei from cytoplasm, and the resultant fractions were analyzed by immunoblot. Bands corresponding to the cleaved PC1-CTT were detected predominantly in the nuclear fractions, and the intensity of this complex of bands was significantly decreased in cells exposed to DAPT (Figure 2B). We used siRNA to knock down expression in HEK293 cells of Presenilin-1 or Presenilin-2, each of which can serve as the catalytic subunit of the functional γ-secretase complex. Loss of Presenilin-1 did not decrease PC1-CTT cleavage as measured by the PC1-GalVP cleavage assay (Figure 2C, left panels). Presenilin-2 knockdown, however, resulted in a significant decrease in PC1-CTT cleavage (Figure 2C, right panels) and a reduction in the nuclear accumulation of PC1 cleavage products (Figure S2).

We next wished to determine whether γ-secretase-mediated cleavage of PC1 is required for the PC1 protein to exert its effects on epithelial morphogenesis. $Pkd1^{flox/-}$ cells cultured in 3D were treated with either DMSO vehicle or with DAPT for 10 days. DAPT treatment resulted in a significant change in morphology in the $Pkd1^{flox/-}$ cells. Whereas DMSO-treated cells formed linear tubule-like structures, DAPT-treated cells formed spherical cyst-like structures with hollow central lumens (Figure 2D, left panels) reminiscent of the structures formed by the $Pkd1^{-/-}$ cells. DAPT treatment had no significant effect on the morphology of $Pkd1^{-/-}$ cells (Figure 2D, right panels).

Expression of PC1-CTT Results in Reduced Proliferation and Apoptosis in Pkd1⁻/⁻ Cells

To quantify the effects observed in the 3D cell culture system, $Pkd1^{flox/-}$ and $Pkd1^{-/-}$ cells were cultured in two dimensions on glass coverslips, and BrdU incorporation (Figure 3A) and cleaved caspase-3 staining (Figure S3) were assessed as measures of proliferation and apoptosis, respectively. $Pkd1^{-/-}$ cells displayed a significantly higher level of proliferation than $Pkd1^{flox/-}$ controls. However, reintroduction of the isolated PC1-CTT significantly reduced proliferation of the $Pkd1^{-/-}$ cells to levels similar to those observed in $Pkd1^{flox/-}$ cells (Figure 3B). Similarly, $Pkd1^{-/-}$ cells displayed a significantly higher level of apoptosis when compared to $Pkd1^{flox/-}$ controls. When PC1-CTT expression was induced in Pkd1⁻/⁻ cells, the level of apoptosis decreased significantly. Expression of PC1-CTT in the $Pkd1^{-/-}$ cells reduced apoptosis to levels similar to those seen in the $Pkd1^{flox/-}$ cells (Figure 3C; Figure S3).

PC1-CTT Directly Interacts with TCF and Inhibits Canonical Wnt Signaling

Previous data implicate canonical Wnt signaling as a driver of cyst proliferation. Recent studies show activation of Wnt target
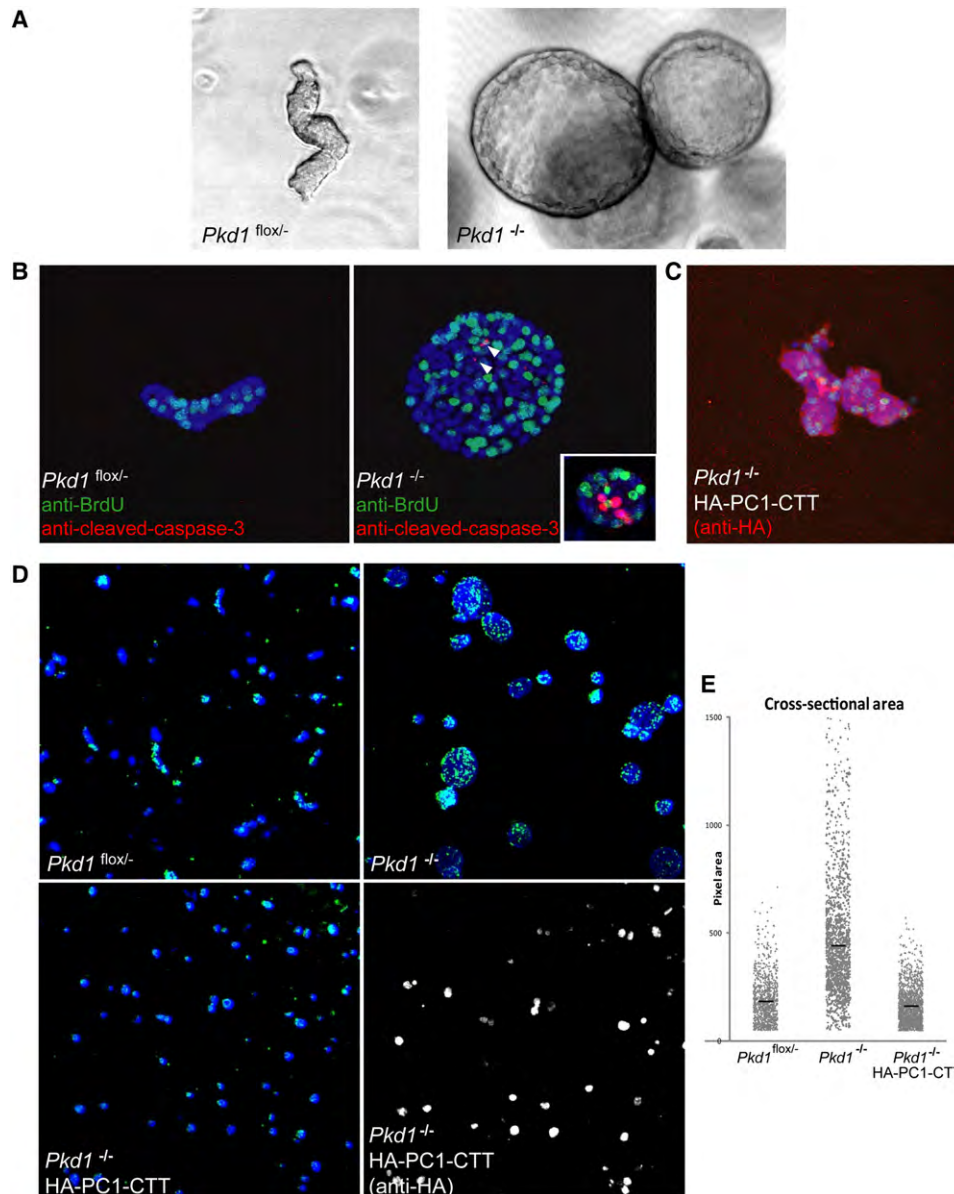
Figure 1. *Pkd1* Knockout Results in Increased Proliferation, Apoptosis, and Cystic Morphology

(A) Phase-contrast imaging of *Pkd1*$^{flox/-}$ and *Pkd1*$^{-/-}$ cells grown in 3D Matrigel matrix for 10 days.

(B) *Pkd1*$^{flox/-}$ and *Pkd1*$^{-/-}$ structures were incubated with BrdU, fixed, and stained with α-BrdU-FITC (green) and α-cleaved caspase-3 (red). Nuclei were counterstained with Hoechst 33342 (blue). The inset depicts a cell aggregate that had yet to develop a hollow central lumen.

(C) *Pkd1*$^{-/-}$ cells stably expressing HA-PC1-CTT were grown in 3D Matrigel matrix for 10 days, exposed to BrdU, fixed, and stained with α-BrdU-FITC (green) and α-HA (red) to detect expression of the HA-PC1-CTT. Nuclei were counterstained with Hoechst 33342 (blue). Cellular structures were imaged on a Leica confocal microscope using a 40× objective.

(D) The top two panels show *Pkd1*$^{flox/-}$ and *Pkd1*$^{-/-}$ cells that were grown in 3D Matrigel matrix for 7 days, incubated with BrdU, and then stained with α-BrdU (green). Nuclei were counterstained with Hoechst 33342 (blue). The bottom two panels show *Pkd1*$^{-/-}$ cells stably expressing HA-PC1-CTT that were grown in 3D Matrigel matrix for 7 days, incubated with BrdU, and then stained with α-BrdU (green). Nuclei were counterstained with Hoechst 33342 (blue, left), and CTT expression was detected with α-HA (gray, right).

(E) Plot of cross-sectional area of cellular structures pictured in (D). Bars indicate mean area in pixels: *Pkd1*$^{flox/-}$ = 185, *Pkd1*$^{-/-}$ = 447, *Pkd1*$^{-/-}$ HA-PC1-CTT = 163, n = 1,000 for each condition.

genes in cells derived from human ADPKD cystic tissue and demonstrate an interaction between the PC1-CTT and components of the Wnt-signaling pathway (Kim et al., 1999; Lal et al., 2008; Zhang et al., 2007). The Wnt pathway regulates the size and activity of the cytosolic pool of β-catenin. At the cell membrane, β-catenin is bound by E-cadherin. In resting polarized epithelial cells, β-catenin is predominantly sequestered at the basolateral plasma membrane, where it participates in the
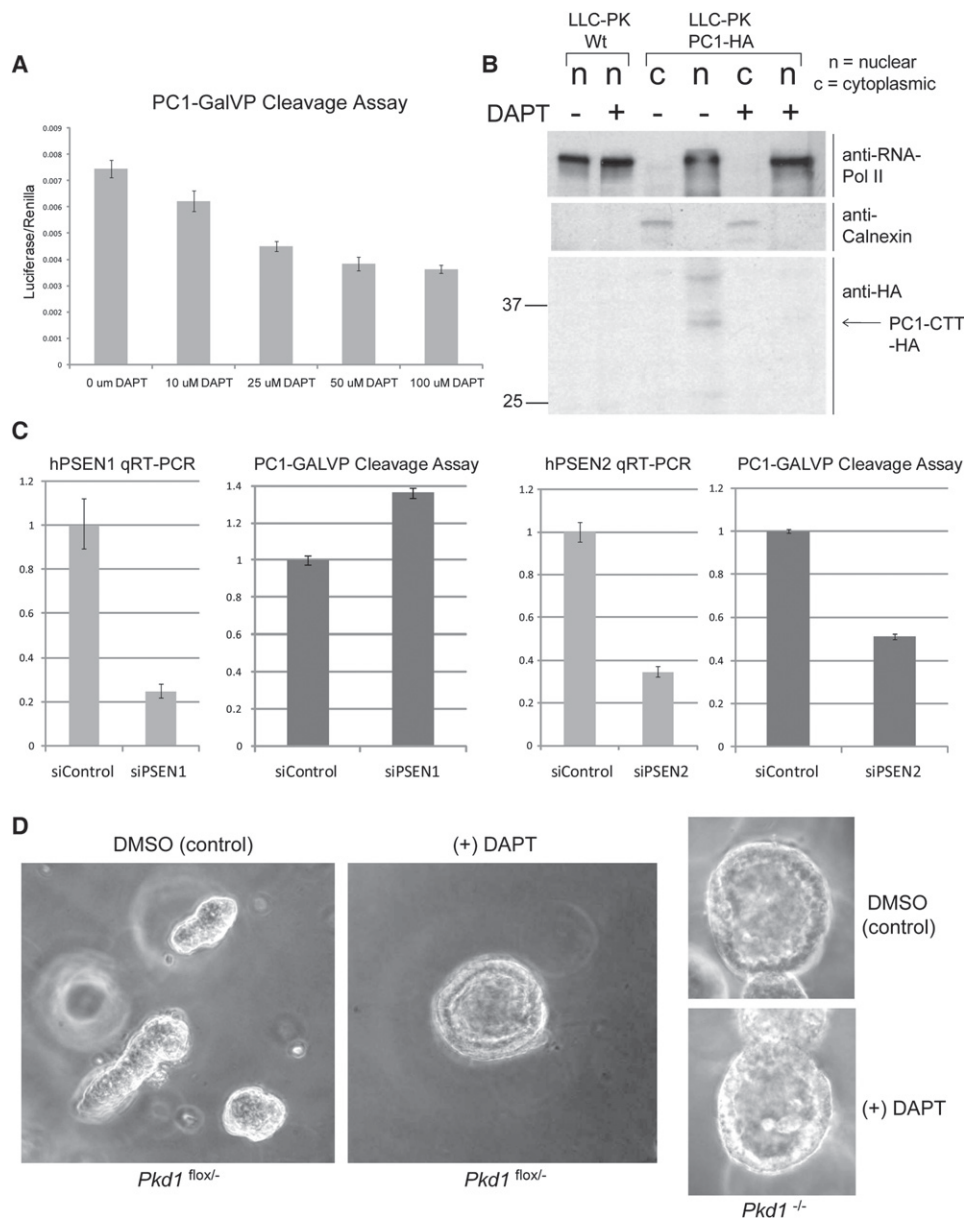
Figure 2. PC1-CTT Cleavage Is Sensitive to the γ-Secretase Inhibitor DAPT

(A) HEK293 cells transfected with PC1-GalVP, UAS-Luciferase, and Renilla were treated with the γ-secretase inhibitor DAPT at the indicated concentrations in the presence of clasto-lactacystin for 24 hr prior to quantification of the luciferase signal.

(B) LLC-PK$_1$ cells stably expressing full-length PC1 with a C-terminal 2× HA tag were exposed to DAPT for 24 hr, in the presence of clasto-lactacystin, before nuclear/cytoplasmic fractionation. Proteins were separated on a 10% SDS-polyacrylamide gel and analyzed by immunoblot. Nuclear purification was assessed using α-RNA-Pol II (nuclear fraction) and α-calnexin (nonnuclear fraction). PC1-CTT cleavage fragments were detected using α-HA.

(C) HEK293 cells were transfected with either siControl (nontargeting RNA) or siRNA directed against human Presenilin-1 or Presenilin-2. qRT-PCR was used to determine knockdown efficiency. PC1-GalVP, UAS-Luciferase, and Renilla were super-transfected into HEK cells after 48 hr of siRNA treatment to report on PC1-CTT cleavage. Data are mean ± SE of four replicates each from two independent experiments. The data in all four panels are normalized to the siControl condition.

(D) Pkd1$^{flox/-}$ and Pkd1$^{-/-}$ cells were cultured in 3D Matrigel matrix for 10 days in media containing either DMSO (vehicle control) or 100 μM DAPT, after which they were fixed and imaged on a phase-contrast microscope.

formation of E-cadherin-dependent adhesive junctions. Free cytoplasmic β-catenin is recognized by a "destruction complex" that mediates its phosphorylation, targeting it for proteosomal degradation. Activation of Wnt signaling prevents the destruction of free cytosolic β-catenin, which enters the nucleus to serve as a coactivator of the TCF transcription factor and thus induces proliferation (Daugherty and Gottardi, 2007). To measure endogenous Wnt-signaling activity, we employed the TopFlash assay, which utilizes a TCF-binding promoter element to drive expression of a luciferase reporter (van de Wetering et al., 1997).
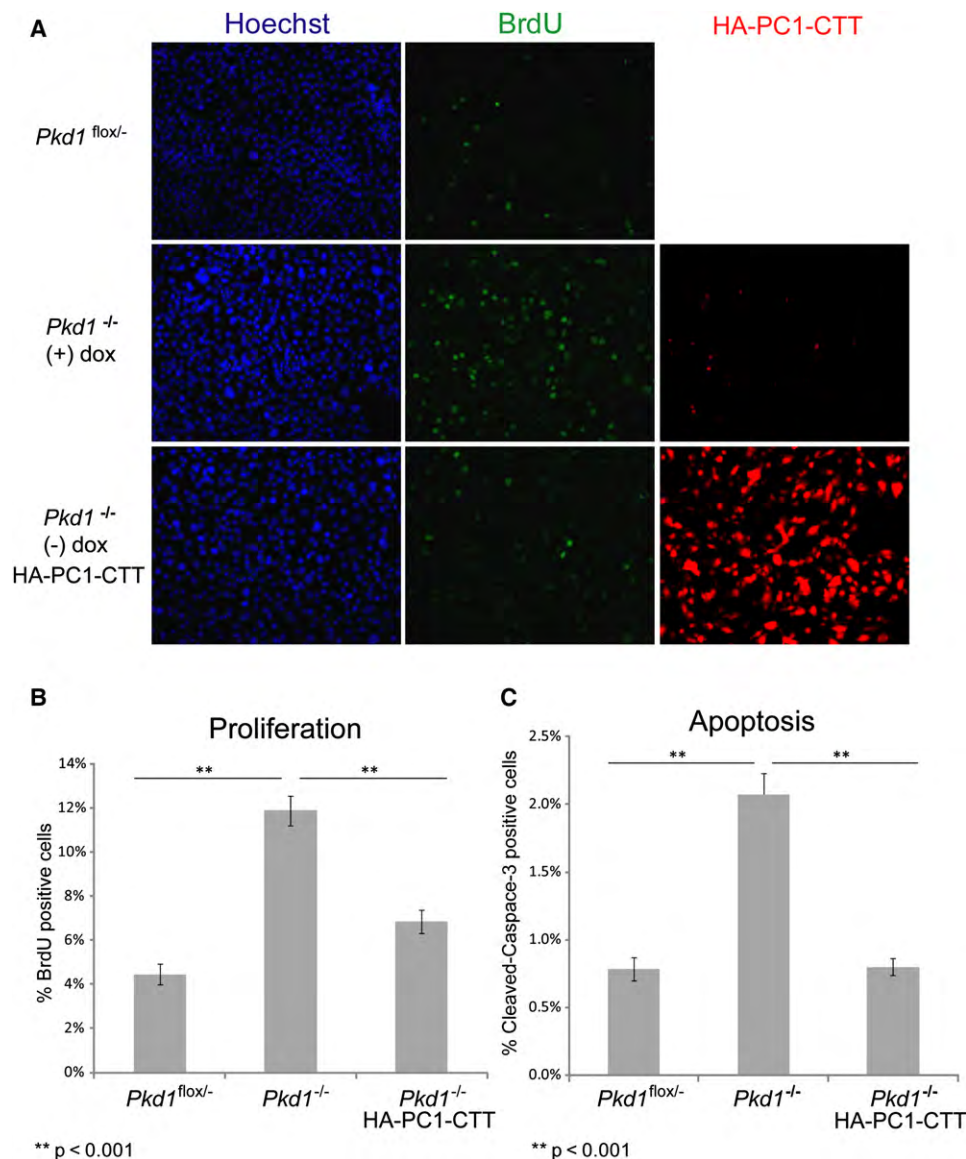
Figure 3. Effects of PC1-CTT Expression on Proliferation and Apoptosis

(A) $Pkd1^{flox/-}$ and $Pkd1^{-/-}$ cells stably expressing HA-PC1-CTT encoded by a TET-Off inducible vector were grown on coverslips. PC1-CTT expression was induced in the $Pkd1^{-/-}$ cell line by withdrawal of doxycycline for 48 hr prior to BrdU exposure and fixation. Proliferating cells were labeled with α-BrdU-FITC (green), PC1-CTT expression was detected with α-HA (red), and nuclei were counterstained with Hoechst 33342 (blue).

(B) Proliferation was quantified using automated cell-counting software. Expression of PC1-CTT in $Pkd1^{-/-}$ cells resulted in a reduction of proliferation to levels approaching those observed in the $Pkd1^{flox/-}$ cells.

(C) Apoptosis was assessed by staining with an antibody directed against cleaved caspase-3 (Figure S3) and quantified using automated cell-counting software. Expression of PC1-CTT in $Pkd1^{-/-}$ cells resulted in a reduction in apoptosis to levels similar to those seen in the $Pkd1^{flox/-}$ cells. Data are mean ± SE of ten fields each from three independent experiments.

$Pkd1^{-/-}$ cells demonstrated significantly higher levels of TCF activity than did the $Pkd1^{flox/-}$ controls. Furthermore, expression of PC1-CTT in the $Pkd1^{-/-}$ cells resulted in a significant reduction in the TopFlash luciferase activity to levels similar to those detected in $Pkd1^{flox/-}$ cells (Figure 4A). This activity is dependent upon the presence of the PC1-CTT nuclear localization sequence (NLS), as evidenced by the fact that a PC1-CTT construct lacking the NLS (PC1-CTT-ΔNLS) (Chauvet et al., 2004) does not exert any inhibitory influence on TopFlash activity

(Lal et al., 2008; Figure 4B). Although the PC1-CTT-ΔNLS construct does not alter TopFlash activity, it is worth noting that this construct is able to produce a significant signal in a reporter assay that measures the activity of the STAT6 pathway (Figure 4C). These data, which are consistent with previous observations indicating that portions of the PC1-CTT can activate STAT6 signaling (Low et al., 2006), demonstrate that loss of the NLS selectively blocks some but not all of the functional activities of the PC1-CTT.
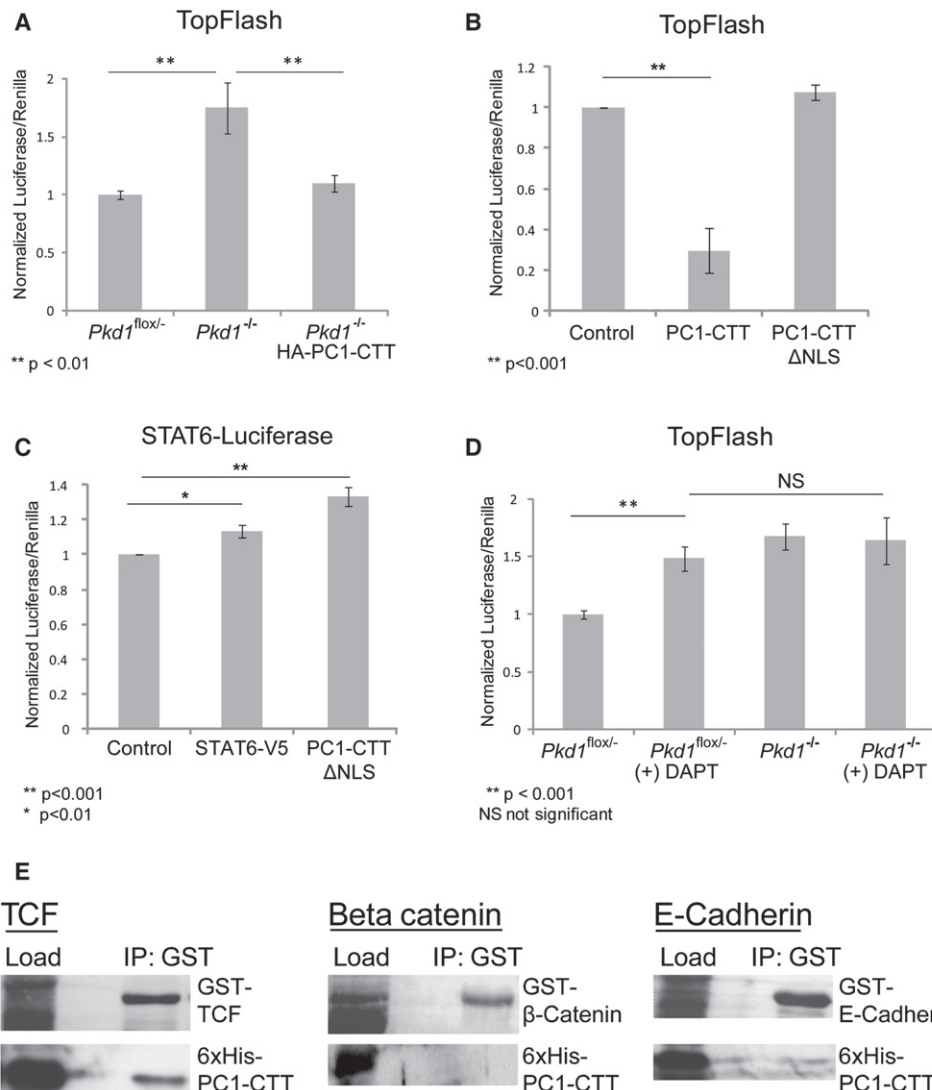
Figure 4. TopFlash Activity Is Elevated in *Pkd1*^{−/−} Cells and Inhibited by PC1-CTT Expression

(A) *Pkd1*^{flox/−} and *Pkd1*^{−/−} cells stably expressing HA-PC1-CTT in a TET-Off inducible vector were transfected with TopFlash and Renilla luciferase reporter constructs in the presence or absence of doxycycline, and luciferase activity was measured 24 hr later.

(B) TopFlash activity is significantly inhibited by expression of the PC1-CTT in HEK293 cells. Expression of the PC1-CTTΔNLS does not inhibit TopFlash activity.

(C) HEK293 cells were transfected with a luciferase reporter construct driven by a STAT6-responsive promoter, as a measure of STAT6 activation. Expression of exogenous STAT6, or PC1-CTTΔNLS results in a significant activation of STAT6 promoter-driven luciferase production.

(D) *Pkd1*^{flox/−} and *Pkd1*^{−/−} cells were transfected with TopFlash and Renilla luciferase reporter constructs and exposed to the γ-secretase inhibitor DAPT for 24 hr prior to quantification of luciferase signal. Data are mean ± SE of four replicates each from three independent experiments.

(E) GST-tagged constructs corresponding to the β-catenin-binding domain of TCF, E-cadherin CTT, and β-catenin were coexpressed with His-tagged PC1-CTT in bacteria. When precipitated with glutathione beads, the PC1-CTT displays a strong direct interaction with TCF, and little direct interaction with E-cadherin or β-catenin.

Treatment of *Pkd1*^{flox/−} cells with DAPT abolished the inhibitory effect of PC1 expression on TopFlash activity, consistent with the hypothesis that PC1-CTT cleavage and nuclear translocation of the released CTT fragment are necessary for its inhibitory effect on TCF. DAPT treatment of *Pkd1*^{−/−} cells did not stimulate any further increase in TopFlash activity, indicating that the increase in Wnt activity obtained through inhibition of γ-secretase is dependent on the presence of PC1 (Figure 4D).

To dissect further the elements of the canonical Wnt-signaling pathway that interact directly with PC1-CTT, a bacterial coexpression system was employed to drive simultaneous expression of a His-tagged PC1-CTT and of GST-tagged polypeptides incorporating the sequences of β-catenin, the E-cadherin cytoplasmic domain, or TCF. When bacterial lysates were subjected to glutathione-Sepharose pull-down and the recovered proteins were blotted with anti-His antibody, PC1-CTT exhibited little direct interaction with β-catenin or with

E-cadherin but showed a strong direct physical interaction with TCF (Figure 4C).

PC1-CTT Interacts with CHOP and Inhibits Its Activity

Data suggesting that the PC1-CTT may regulate apoptosis (Figures 1 and 3; Figure S3) led us to search for novel regulatory targets that could mediate this influence. To identify transcription factors regulated by PC1-CTT, we employed a "coactivator trap" screen, in which over 800 transcription factors are fused to the DNA-binding domain of Gal4 (Amelio et al., 2007). After cotransfection of each transcription factor-Gal4 construct and a Gal4-driven luciferase reporter vector into HEK293 cells, luciferase assays established baseline activities for each transcription factor. PC1-CTT was then cotransfected, and any effect of PC1-CTT on each transcription factor's activity was measured as a change in luciferase production as compared to its baseline level. Several transcription factors were found to be significantly regulated in the presence of PC1-CTT. One of the most profoundly affected was CHOP-10/GADD153, which induces apoptosis in response to ER stress as part of the unfolded protein response (UPR) (Oyadomari and Mori, 2004) (Table S1).

To measure the effects of full-length PC1 expression on CHOP activation, $Pkd1^{flox/-}$ and $Pkd1^{-/-}$ cells were transfected with the CHOP-Gal4 and the Gal4-luciferase reporter constructs. $Pkd1^{-/-}$ cells displayed significantly higher levels of CHOP activity when compared to the $Pkd1^{flox/-}$ cells. Expression of the soluble PC1-CTT in the $Pkd1^{-/-}$ cells resulted in a significant inhibition of CHOP-Gal4 activity (Figure 5A). In addition, treatment of $Pkd1^{flox/-}$ cells with DAPT abolished the inhibitory effect that PC1 expression exerts on CHOP-Gal4 activity. DAPT treatment of $Pkd1^{-/-}$ cells did not stimulate a further elevation in CHOP activity, indicating that the increase in CHOP activity obtained through inhibition of γ-secretase-dependent protein cleavage is dependent on the presence of PC1 (Figure 5B). Thus, the presence of the PC1 protein acts, via its released CTT, to negatively regulate CHOP activity. Once again, this activity is dependent upon the presence of the PC1-CTT NLS because the PC1-CTT-ΔNLS construct does not exert any inhibitory influence on CHOP activity (Figure 5C). To determine whether the increased rate of apoptosis observed in the $Pkd1^{-/-}$ cells is indeed a consequence of CHOP activity, $Pkd1^{-/-}$ and $Pkd1^{flox/-}$ cells were subjected to siRNA-mediated knockdown of CHOP expression. Apoptosis was scored by staining for cleaved caspase-3 (Figure 5D). Consistent with the data shown in Figure 3C, the apoptotic rate manifest by the $Pkd1^{-/-}$ cells transfected with a control siRNA was twice that observed for the similarly treated $Pkd1^{flox/-}$ cells. Whereas knockdown of CHOP expression had no effect on the apoptotic rate observed in the $Pkd1^{flox/-}$ cells, treatment with the CHOP siRNA reduced the apoptotic rate in the $Pkd1^{-/-}$ cells to the level measured in the $Pkd1^{flox/-}$ cells. Taken together, these data demonstrate that PC1 reduces CHOP activity in a cleavage-dependent manner, and that elevated CHOP activity accounts for the increased apoptosis that is measured in cells that lack PC1 expression.

To assess the possibility of a physical interaction between CHOP and the PC1-CTT, HEK cells were transfected with constructs encoding HA-PC1-CTT and a FLAG-tagged CHOP protein. Lysates prepared from these cells were subjected to immunoprecipitation with anti-HA beads. CHOP coprecipitated with the soluble PC1-CTT construct (Figure 5E). This interaction was further validated by immunoprecipitation experiments performed on lysates of nuclear fractions prepared from LLC-PK₁ cells stably expressing a full-length PC1 that carries a C-terminal HA tag (Chapin et al., 2010). The endogenously cleaved PC1-CTT released from the full-length PC1 protein coprecipitated with nuclear CHOP (Figure 5F).

PC1-CTT Inhibits TCF and CHOP Activities by Disrupting Their Interactions with p300

Although TCF and CHOP activate discrete transcriptional pathways, they both utilize and depend upon the common transcriptional coactivator, p300/CBP (Li et al., 2007; Ohoka et al., 2007). To determine the potential importance of p300 in the PC1-CTT-mediated regulation of TCF and CHOP, HEK cells were transfected with PC1-CTT alone, or in the presence of overexpressed p300. As shown previously, PC1-CTT expression inhibits TCF activity (as assessed by TopFlash assay) in the context of native levels of p300 protein expression (Lal et al., 2008). Overexpression of p300 eliminated this inhibitory effect of PC1-CTT, suggesting that this inhibitory effect is achieved through competition between the PC1-CTT and p300 for binding to TCF (Figure 6A).

To test this possibility directly, TCF and CHOP were precipitated from HEK cells transfected with p300 and PC1-CTT (Figures 6B and 6D). As expected, in the absence of PC1-CTT, TCF and CHOP each coprecipitates with p300 (Hecht and Stemmler, 2003; Ohoka et al., 2007). These interactions were significantly disrupted in cells that express PC1-CTT, suggesting that the CTT of PC1 exerts its inhibitory effect on the activities of TCF and CHOP by interfering with their interactions with p300 (Figures 6B–6E).

PC1-CTT Rescues Morphant Phenotypes in Pkd1-Knockdown Zebrafish Embryos

Morpholino-induced knockdown of the two zebrafish $Pkd1$ genes, $Pkd1a$ and $Pkd1b$, produces dorsal body axis curvature, kidney cysts, hydrocephalus, and skeletal abnormalities (Mangos et al., 2010). Of these findings, the dorsal body curvature was considered to be the most reliable marker of Pkd1 knockdown, due to the substantially higher penetrance of this phenotype. Interestingly, treatment of zebrafish embryos with the γ-secretase inhibitor DAPT produces a similar phenotype, characterized by mild and moderate dorsal axis curvature (Arslanova et al., 2010). To determine the capacity of the PC1-CTT to rescue the phenotype associated with impaired $Pkd1$ gene expression in vivo, zebrafish embryos were injected with Pkd1a/b morpholinos alone, or with mRNA encoding the PC1-CTT. Knockdown of $Pkd1a/b$ results in dorsal axis curvature, whereas concurrent injection of the PC1-CTT significantly decreases the severity of the body curvature at 3 dpf (Figures 7A and 7B). Injection of mRNA encoding the PC1-CTT-ΔNLS construct did not rescue the body curvature phenotype (Figures S4A and S4B). A subset of the signaling pathways influenced by the PC1-CTT requires the NLS (Wnt and CHOP), whereas others appear to not require the presence of this motif (e.g., STAT-6) (Figures 4B, 4C, and 5C). Thus, these data suggest that the capacity of the PC1-CTT to ameliorate the severity of the body curvature phenotype involves one or more of the NLS-dependent
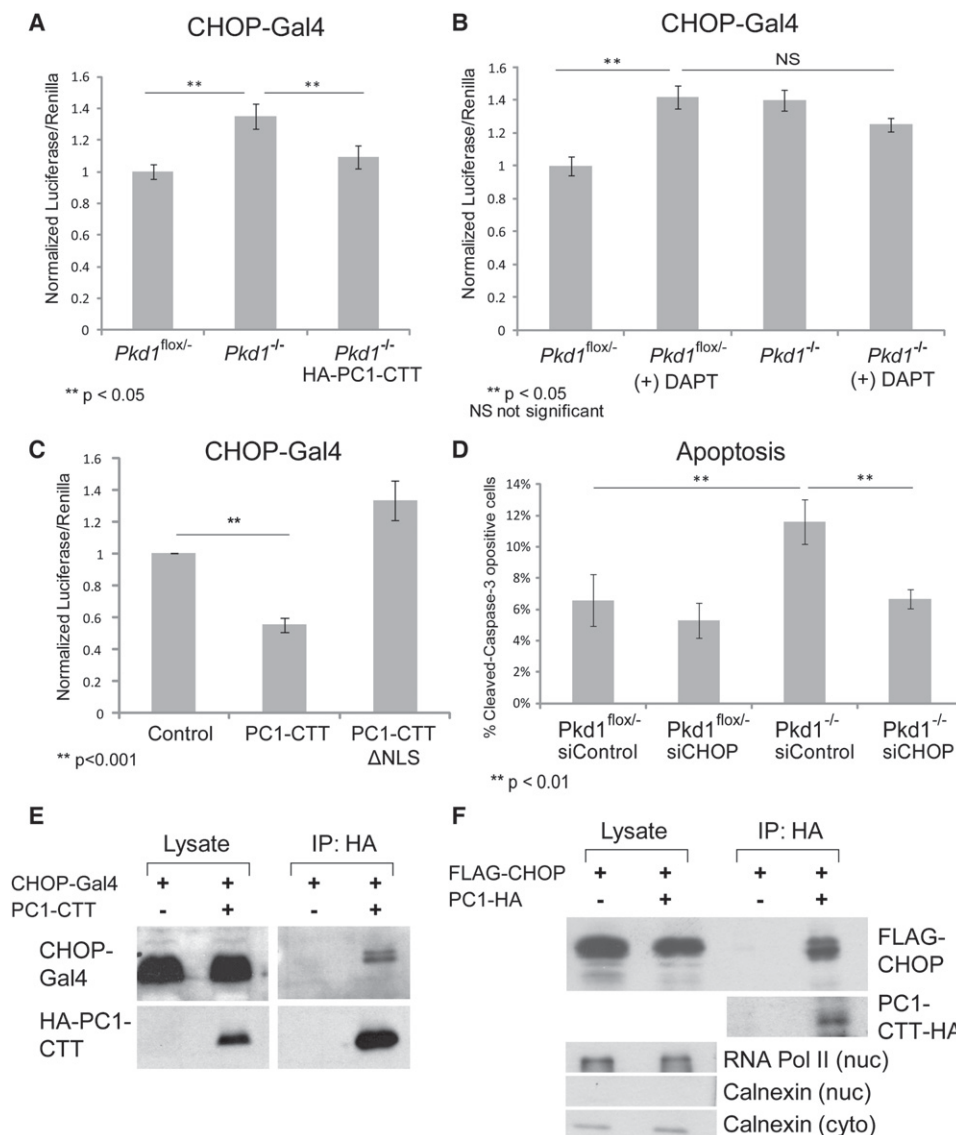
Figure 5. CHOP-Gal4 Activity Is Elevated in Pkd1−/− Cells and Inhibited by PC1-CTT Expression

(A) Pkd1flox/− and Pkd1−/− cells stably expressing HA-PC1-CTT in a TET-Off inducible vector were transfected with CHOP-Gal4, UAS-Luciferase, and Renilla luciferase reporter constructs in the presence or absence of doxycycline, and luciferase activity was measured 24 hr later.

(B) Pkd1flox/− and Pkd1−/− cells were transfected with CHOP-Gal4, UAS-Luciferase, and Renilla luciferase reporter constructs and exposed to the γ-secretase inhibitor DAPT for 24 hr prior to quantification of luciferase signal. Data are mean ± SE of four replicates each from three independent experiments.

(C) CHOP-Gal4 activity is significantly inhibited by expression of the PC1-CTT in HEK293 cells, whereas it is not inhibited in the presence of the PC1-CTTΔNLS.

(D) Pkd1flox/− and Pkd1−/− cells were reverse transfected with either noncoding siRNA (siControl), or siRNA corresponding to CHOP (siCHOP), and apoptosis levels were measured 48 hr later by cleaved caspase-3 staining.

(E) HEK293 cells were cotransfected with CHOP-Gal4 and HA-PC1-CTT. Cell lysates were subjected to immunoprecipitation using α-HA Sepharose, and the immunoprecipitates were then blotted with the indicated antibodies.

(F) LLC-PK1 cells stably expressing full-length PC1 with a C-terminal 2× HA tag were transfected with FLAG-CHOP, and subjected to nuclear/cytoplasmic fractionation. Endogenously cleaved PC1-CTT was immunoprecipitated from the nuclear fraction using α-HA Sepharose, and the resulting complexes were separated on a 10% polyacrylamide gel and blotted with the indicated antibodies.

signaling pathways that are modulated by the PC1-CTT. Finally, injection of mRNA encoding the PC1-CTT, but not mRNA encoding control GFP, partially rescued the body curvature phenotype induced by DAPT treatment, producing a significant increase in the percentage of fish with straight bodies and a decrease in the percentage of moderately curved fish (Figure 7C).

DISCUSSION

Our data confirm the role of PC1 as an inhibitor of renal epithelial cell proliferation and apoptosis, and provide evidence for the mechanism responsible for this regulation, mediated by cleavage and nuclear translocation of the PC1-CTT.
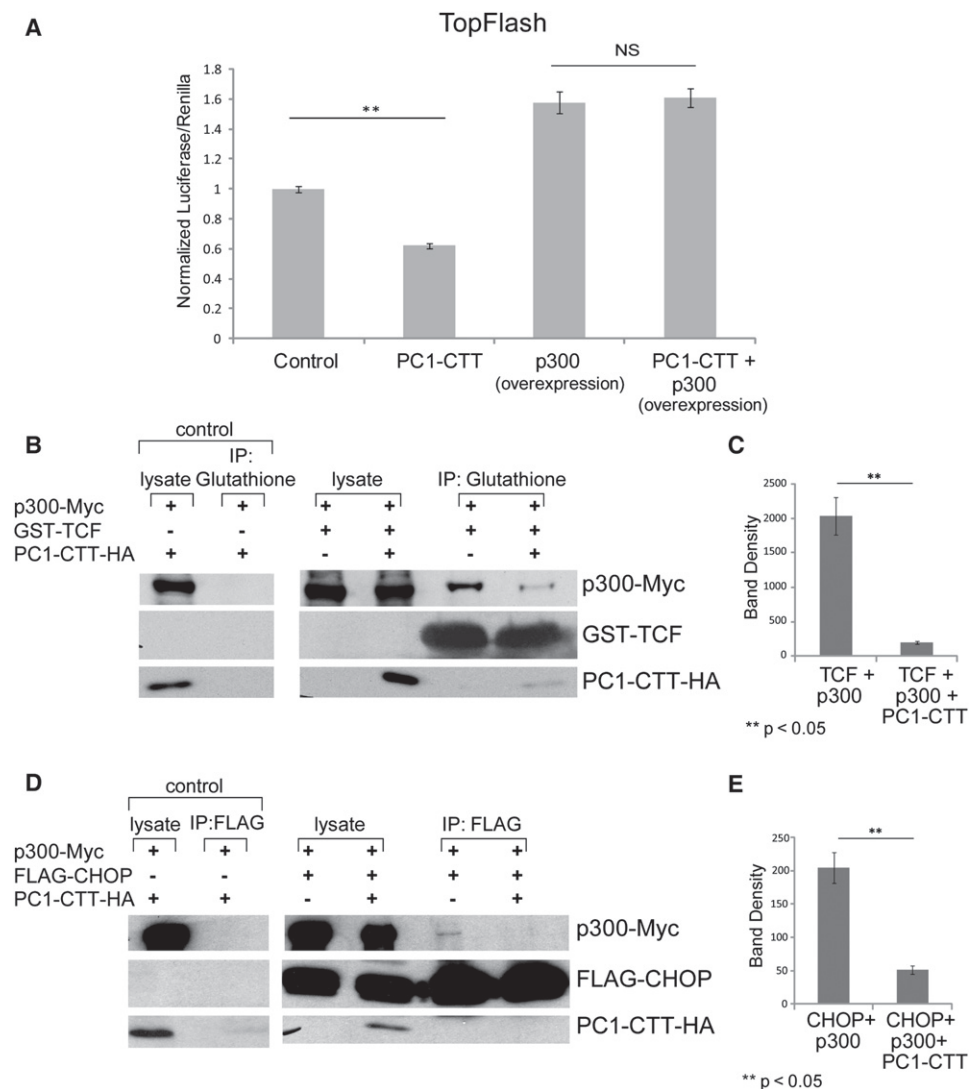
Figure 6. PC1-CTT Competitively Disrupts the Interaction of TCF and CHOP with p300

(A) HEK293 cells were transfected with TopFlash and Renilla luciferase reporter constructs, along with PC1-CTT alone or with PC1-CTT and a construct driving overexpression of full-length p300. NS, not significant.

(B) HEK293 cells were transfected with Myc-p300, and with HA-PC1-CTT where indicated. Cell lysates were incubated with glutathione beads prebound with GST-TCF. Recovered complexes were eluted in SDS-PAGE loading buffer, run on a 10% SDS-polyacrylamide gel, and blotted with the indicated antibodies.

(C and E) Band densitometry was performed using image analysis software to quantitate the data from the coprecipitation experiments shown in (B) and (D). Results are expressed as mean ± SE from four independent experiments.

(D) HEK293 cells were transfected with Myc-p300, FLAG-CHOP, and with HA-PC1-CTT where indicated. Cell lysates were incubated with α-FLAG prebound to agarose beads to precipitate CHOP, and the recovered complexes were eluted in SDS-PAGE loading buffer, run on a 10% SDS- polyacrylamide gel, and blotted with the indicated antibodies.

Reintroduction of the PC1-CTT into *Pkd1* knockout cells is sufficient to normalize their excessive proliferative and apoptotic activities, and the PC1-CTT is sufficient to rescue the dorsal tail curvature phenotype produced by morpholino-mediated disruption of *Pkd1a/b* expression in zebrafish. We show that PC1 cleavage is dependent upon γ-secretase activity, and that the released PC1-CTT inhibits TCF and CHOP, thereby regulating proliferation and apoptosis, respectively. Furthermore, injection of mRNA encoding the PC1-CTT is capable of partially rescuing the dorsal tail curvature phenotype produced by expo-sure of zebrafish embryos to the γ-secretase inhibitor DAPT. The similarity of the phenotypes produced by *Pkd1a/b* disruption and DAPT treatment is intriguing, and the ability of the PC1-CTT to partially rescue both suggests that at least some of the critical biological activities of the PC1 protein are dependent upon its γ-secretase-dependent PC1-CTT cleavage. Finally, we demon-strate that PC1-CTT inhibits TCF and CHOP by disrupting their interaction with the transcriptional coactivator p300, illustrating a common mechanism through which PC1-CTT is capable of regulating two distinct transcriptional pathways.
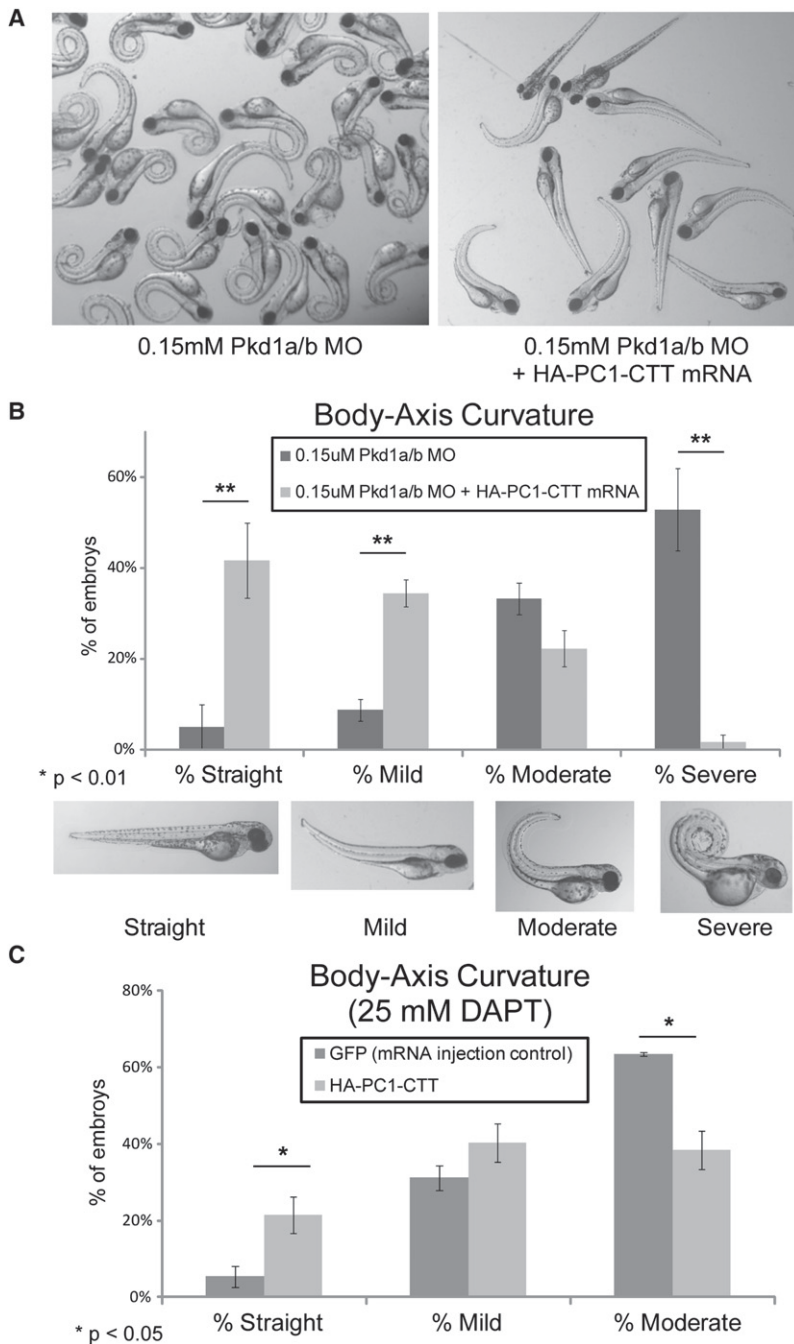
Figure 7. Both Morpholino Knockdown of *Pkd1a/b* and Treatment with DAPT Result in Dorsal Axis Curvature in Zebrafish Embryos, which Can Be Rescued by Expression of the PC1-CTT

(A) Morpholinos corresponding to the zebrafish *Pkd1a* and *Pkd1b* PC1 genes were injected into zebrafish embryos at the one- to two-cell stage to impair expression of the two *Pkd1* genes. The embryos were subsequently injected with 300 nM of mRNA encoding HA-PC1-CTT, where indicated, and imaged at 3 days post fertilization (dpf).

(B) Embryo phenotypes were scored based on the degree of dorsal tail curvature: mild (<90°), moderate (>90°), and severe (tail tip crossing the body axis). The data represent the averages of three separate experiments; error bars represent SEM.

(C) Embryos were injected with 300 nM mRNA encoding either GFP (control) or HA-PC1-CTT at the one- to two-cell stage, then immersed in embryo media containing 25 μM DAPT, imaged at 3 dpf, and scored for the tail curvature phenotype.

Cleavage of the CTT of PC1 has been observed in several studies (Bertuccio et al., 2009; Chauvet et al., 2004; Lal et al., 2008; Low et al., 2006), and its subsequent translocation to the nucleus strongly implies its role in the regulation of transcriptional pathways. Although the cleaved CTT fragment certainly does not recapitulate all of the functions of full-length PC1, our data suggest that the isolated CTT is sufficient to reestablish normal low levels of proliferation and apoptosis, and of TCF and CHOP activity, when expressed in *Pkd1* knockout cells. Furthermore, PC1-CTT is capable of at least partially restoring to *Pkd1* knockout cells the tubular morphology that is obtained with wild-type and *Pkd1* heterozygous cells grown in 3D cell culture. Finally, our data suggest that PC1 cleavage by γ-secretase may be necessary for PC1 to mediate its full complement of physiological functions. Inhibiting γ-secretase activity causes PC1-expressing cells that form tubular structures in 3D culture to recapitulate the cystic morphology normally manifest by *Pkd1* null cells. It is possible, of course, that γ-secretase influences epithelial morphogenesis in this assay via additional pathways that are independent of PC1. Because *Pkd1*^{−/−} cells were unaffected by DAPT treatment in both the morphogenesis and the TCF and CHOP assays, however, we conclude that γ-secretase-mediated cleavage of PC1 plays an obligate role in at least a subset of this protein's physiological functions.

The shedding of the extracellular domain of PC1 and the cleavage and nuclear translocation of its cytoplasmic domain together mark PC1 as a member of a growing collection of plasma membrane proteins that is cleaved by γ-secretase and participates in direct signaling to the nucleus (Lal and Caplan, 2011). This behavior is exemplified by the Notch (Fortini, 2009),

Hyperproliferation and increased apoptosis are characteristic of ADPKD (Lanoix et al., 1996; Starremans et al., 2008). We found that loss of *Pkd1* in otherwise genetically identical cell lines resulted in a significant increase in both proliferation and apoptosis. These experiments were performed in vitro, thus eliminating any potential effects of the cyst microenvironment on the proliferative or apoptotic potential of the cyst-lining cells that might complicate the situation in vivo. Thus, our data establish that the loss of expression of the *Pkd1* gene product is primarily responsible for the proliferative and apoptotic changes seen in ADPKD.

EpCAM (Maetzel et al., 2009), and DCC pathways (Taniguchi et al., 2003). The precise site at which γ-secretase cleaves PC1-CTT has not yet been determined. It is worth noting, however, that γ-secretase appears to exhibit substantial promiscuity in the sequence compositions of its substrate cleavage sites (Beel and Sanders, 2008; Struhl and Adachi, 2000). This promiscuity may account, at least in part, for the number of discrete PC1-CTT cleavage products that can be detected in nuclear fractions (Figure 2B). The precise signals that stimulate γ-secretase-mediated cleavage of PC1 have yet to be discovered.

We report a direct physical interaction between the PC1-CTT and TCF. Lal et al. have suggested that the PC1-CTT inhibits canonical Wnt signaling through an interaction with β-catenin (Lal et al., 2008). Because these experiments assessed the coimmunoprecipitation of epitope-tagged proteins coexpressed in human cell lines, the recovered protein complexes may have contained additional members of the signaling pathway, such as TCF, that were not detected in immunoblots that assessed only the presence of the tagged proteins. Thus, it seems likely that the coprecipitation of the PC1-CCT and β-catenin observed by Lal et al. (Lal et al., 2008) could be attributable to a mutual interaction of both of these proteins with TCF to form an inactive tertiary complex. The bacterial coexpression system utilized in the present study allowed us to further dissect the canonical Wnt pathway and to determine that TCF is a direct binding partner of PC1-CTT. It should be noted that, while activation of the Wnt-signaling pathway is sufficient to produce renal cystic disease (Qian et al., 2005; Saadi-Kheddouci et al., 2001), and markers of Wnt signaling appear to be elevated in the context of human ADPKD (Lal et al., 2008), a recent study found that the cyst-lining cells of mouse models of ADPKD that express a Wnt/TCF reporter did not manifest elevated levels of Wnt activity (Miller et al., 2011). Therefore, it is possible that activation of Tcf-mediated transcription plays an early, transient role in the initiation of cyst formation that is terminated by the time cysts are manifest. It is also possible that pathways other than those associated with Wnt/TCF drive the hyperproliferation that is associated with the cystic epithelial cells in ADPKD. In either case, our data demonstrate that cleavage of the PC1 generates a protein that is both antiproliferative and sufficient to suppress ADPKD-related phenotypes in vitro and in vivo.

The activities of both TCF and CHOP depend upon the common transcriptional coactivator p300 (Li et al., 2007; Ohoka et al., 2007). Our data suggest that PC1-CTT binds directly to the transcription factors TCF and CHOP, and are consistent with the hypothesis that PC1-CTT acts by blocking the p300 binding sites on both TCF and CHOP. Therefore, the p300 protein constitutes a promising convergence point that appears to be utilized by PC1-CTT to regulate two distinct transcription factors. This regulation of TCF and CHOP through interactions with the released PC1-CTT provides a simple and compelling explanation for the dysregulation of proliferation and apoptosis seen in ADPKD.

EXPERIMENTAL PROCEDURES

Antibodies, Plasmids, and Cell Lines
The following antibodies and labeling reagents were used: α-HA antibody, Rat (Roche), FITC α-BrdU Kit (BD Bioscience), α-cleaved caspase-3 (Cell Signaling

Technology), α-RNA Pol II (Santa Cruz Biotechnology), α-calnexin (Stratagene), α-His (QIAGEN), α-GST (Amersham), and α-FLAG and α-cMyc (Sigma-Aldrich). For laser-scanning fluorescence microscopy, dye-coupled Alexa antibodies (Alexa 488, 594; Molecular Probes) were used as secondary reagents.

The sequence encoding the final 200 amino acids of human PC1 (4102–4302), containing a 2× HA tag at the N terminus, was cloned into the pNRTis-21 vector (Tenev et al., 2000). The sequence for human PC1-CTT (residues 4102–4302 of Pkd1) was modified by deleting residues 4134–4154, corresponding to the putative NLS to generate the PC1-CTTΔNLS (Chauvet et al., 2004). Stable cell lines were generated by transfection using Lipofectamine 2000 (Invitrogen) and selection with 350 μg ml^{-1} Zeocin (Invitrogen). Expression was inhibited with 100 ng ml^{-1} doxycycline. Full-length human PC1 was cloned into pcDNA3.1.neo (Invitrogen) with 2× HA tag or Gal4VP16 appended to the C terminus as described (Bertuccio et al., 2009). Stable cell clones were selected with 2 mg ml^{-1} Geneticin (GIBCO). GL4.31[luc2P/GAL4UAS] (Promega, Madison, WI, USA) was used as a Gal4 promoter-driven firefly luciferase reporter construct. The TopFlash plasmid was purchased from Upstate Biotechnology. pRL-TK, a vector constitutively expressing Renilla luciferase, was included as an internal control to normalize for transfection differences. The sequence encoding the PC1-CTT was cloned into the pETDuet vector with an N-terminal 6xHis tag, along with either the GST-E-cadherin cytoplasmic domain, GST-β-catenin, or GST-TCF β-catenin binding region (Gottardi and Gumbiner, 2004). The CHOP-Gal4 construct was provided by Dr. John Hogenesch (Department of Pharmacology, University of Pennsylvania). The sequence encoding full-length CHOP was cloned into the pCMV-3Tag-1A vector (Stratagene) to generate 3xFLAG-CHOP. The sequence encoding human p300 (full-length or amino acid residues 1–664) was cloned into the pCMV-Tag 3B vector (Stratagene) to generate Myc-p300.

HEK293T cells (Chauvet et al., 2004), LLC-PK$_1$ cells, and Pkd1$^{flox/-}$ and Pkd1$^{-/-}$ temperature-sensitive SV40 large T antigen renal proximal tubule cells (Joly et al., 2006; Shibazaki et al., 2008) were maintained as described.

3D Cell Culture, α-BrdU Staining, and Cell Counting
Pkd1$^{flox/-}$, Pkd1$^{-/-}$, and Pkd1$^{-/-}$ stably expressing pNRTis HA-PC1-CTT were trypsinized and mixed with 300 μl liquid Matrigel (BD Biosciences) and allowed to solidify for 30 min at 37°C, after which media were added with or without 100 ng ml^{-1} doxycycline, and the cells were grown for 7–10 days. These cell lines were grown on coverslips in parallel for quantification of proliferation and apoptosis.

BrdU was added to the media for 90 min prior to fixation. Cells grown on coverslips were stained as per BD protocol. Cells grown in Matrigel were fixed for 1.5 hr at 37°C, permeabilized for 30 min at 4°C, refixed for 15 min at RT, treated with DNase for 3 hr at 37°C, incubated with the α-BrdU 1°Ab (1:100) for 5 days at 4°C, followed by three 2 hr washes, and by incubation for 1 day with 2°Ab (1:200); nuclei were stained with Hoechst 33342 (Molecular Probes).

Cells grown on coverslips were imaged using an Olympus BX51 epifluorescent microscope equipped with a 20× objective. The percentages of BrdU or caspase-3-positive cells were quantified using a threshold method in conjunction with the ImageJ software package plug-in "Nucleus Counter."

The cross-sectional areas of the cell structures grown in 3D Matrigel culture were calculated using ImageJ software. Cells were stained with α-BrdU, α-HA, and Hoechst 33342 and imaged using an Olympus BX51 epifluorescent microscope equipped with a 10× objective. Cell structures were thresholded from background, and the cross-sectional area of each cell cluster was calculated using the ImageJ Analyze Particles plug-in, with a minimum size cutoff of 50 pixels to filter out isolated cells and debris.

Cell Fractionation
Preparation of nuclear and cytoplasmic fractions was performed as previously described (Chauvet et al., 2004). Cells grown in 10 cm dishes in the presence of 25 μM clasto-lactacystin were harvested in cold PBS, centrifuged for 5 min at 500 × g, and resuspended in hypotonic buffer (10 mM HEPES, 1.5 mM MgCl$_2$, 10 mM KCl, and protease inhibitors). Cells were homogenized in a tight-fitting Dounce homogenizer, chilled on ice for 10 min, and then rotated for 15 min. Nonidet P-40 was added to a final concentration of 1%,

and the preparations were rotated for an additional 15 min. The lysates were centrifuged at 1,500 × *g* for 5 min. The resulting supernatant formed the nonnuclear fractions. The pellets (nuclear fractions) were washed in hypotonic buffer for 10 min, resuspended in lysis buffer (50 mM HEPES [pH 7.4], 200 mM NaCl, 0.5% NP-40, 1 mM EDTA, and protease inhibitors), and rotated for 10 min. Pelleted nuclei were lysed by sonication in lysis buffer and prepared for immunoblot analysis. The protein concentration of each sample was determined using a Bio-Rad colorimetric protein concentration assay.

Coactivator Trap Screen
The coactivator trap screen was performed as previously described (Amelio et al., 2007). A pcDNA3.1 construct expressing HA-PC1-CTT was cotransfected with each of 837 transcription factor-Gal4 fusion proteins and the GAL4 luciferase and Renilla reporter plasmids into HEK293Tcells in a 384-well plate. Cells were cultured for 24 hr in a humidified incubator at 37°C in 5% CO_2. Bright-Glo (Promega) reagent (35 µl) was added to each well, and luciferase luminescence was measured with an Acquest plate reader (LJL Biosystems).

Transient Transfection and Luciferase Assay
$Pkd1^{flox/-}$ cells, $Pkd1^{-/-}$ cells, and $Pkd1^{-/-}$ cells stably expressing pNRTis HA-PC1-CTT were plated in 24-well tissue culture plates and transfected using Lipofectamine 2000 (Invitrogen) at 80%–100% confluency. Luciferase reporter constructs TopFlash or GL4.31[luc2P/GAL4UAS] (0.2 µg), and CHOP-Gal4 (0.05 µg) and pRL-TK (Renilla), were mixed with 2 µl Lipofectamine. HEK293 cells were transfected with STAT6-Luciferase (kind gift of Dr. S.J. Hacque, Cleveland Clinic Foundation) (Haque et al., 1997) or with TopFlash-luciferase, or with CHOP-Gal4/Gal4-luciferase (0.2 µg), as well as with either control plasmid, STAT6-V5, HA-PC1-CTT or HA-PC1-CTTΔNLS, and with pRL-TK (Renilla). Transfection mixtures were added drop wise to cell culture media (containing 80 µM DAPT [Sigma-Aldrich] when indicated) and incubated at 37°C for 24 hr. The amount of DNA in each well was equalized through the addition of a control plasmid, pcDNA3.1, which was also used for mock transfection. Transfected cells were harvested with PBS and lysed with 100 ml of passive lysis buffer (Promega). Luciferase levels were assayed using the Dual Luciferase Assay Reagent kit (Promega). Luciferase signals were determined in a GloMax 20/20 luminometer (Promega).

siRNA Treatment
HEK293 cells were transfected with 100 nM target-specific siRNA or control siRNA using Lipofectamine 2000. As a control siRNA, we used Silencer Negative Control siRNA#1 (#AM4611; Ambion). To knock down PSEN1 and PSEN2, we used validated siRNAs (for PSEN1, SI02662688 from QIAGEN; for PSEN2, AM51331 from Ambion). Knockdown of CHOP was accomplished according to a published protocol (Ishikawa et al., 2009).

Immunoprecipitation, Immunoblot, and GST Pull-Down
Cells were lysed by sonication in 50 mM HEPES (pH 7.4), 150 mM NaCl, 0.5% NP-40, 1 mM EDTA with protease inhibitors (Roche). Precleared lysates (18,000 × *g*, 30 min) were incubated at 4°C overnight with either monoclonal-anti-HA agarose, anti-FLAG-M2 agarose (Sigma-Aldrich), or glutathione-Sepharose 4B beads (Amersham) prebound with indicated GST fusion protein constructs harvested from BL21 bacteria by standard procedures (Stratagene). Beads were collected by centrifugation, and the pellets were washed in lysis buffer three times for 10 min with rotation at 4°C. Immunoprecipitates were eluted in SDS-PAGE loading buffer (25 mM Tris-HCl [pH 6.7], 10% glycerol, 1% SDS, 50 mM DTT, bromophenol blue).

Proteins were separated on a 10% SDS-polyacrylamide gel and then electrophoretically transferred to a nitrocellulose membrane (Bio-Rad), incubated in blocking buffer (150 mM NaCl, 20 mM Tris, 5% [w/v] powdered milk, 0.1% Tween) for 60 min, and then incubated with one of the following primary antibodies at 4°C overnight: monoclonal α-HA (rat) antibody (1:5,000; Roche); polyclonal α-FLAG (1:5,000; Sigma-Aldrich); polyclonal α-cMyc (1:5,000; Sigma-Aldrich); polyclonal α-GST (goat) (1:10,000; Amersham); and α-His (1:5,000; QIAGEN). Subsequently, primary antibody binding was detected with horseradish peroxidase-conjugated anti-rat, anti-rabbit, or anti-goat secondary antibodies (1:5,000–10:000; Jackson Labs), and proteins were visualized with an enhanced chemiluminescence detection kit (ECL; Amersham Biosciences).

Zebrafish Experiments: Morpholino Antisense Oligonucleotide and mRNA Injections and Drug Treatment
Morpholino-induced knockdown of *Pkd1a* and *Pkd1b* expression was performed as previously reported (Mangos et al., 2010). Wild-type embryos at the one- to two-cell stage were microinjected with 4.6 nl of a 0.15 mM antisense morpholino oligonucleotide solution (Gene Tools LLC) with 0.1% phenol red using a nanoject2000 microinjector (World Precision Instruments). The sequences of the morpholinos targeting *Pkd1a* and *Pkd1b* were identical to those that have been previously described (Mangos et al., 2010); briefly, the splice donor-blocking oligonucleotide sequences were: *Pkd1a* MO ex8, 5′-GATCTGAGGACTCACTGTGTGATTT-3′; and *Pkd1b* MO ex45, 5′-ACATGA TATTTGTACCTCTTTGGTT-3′. Gene Tools standard negative control morpholino was used as an injection control and demonstrated no effect on development. For drug treatment, after mRNA injection at the one- to two-cell stage, embryos were placed in a 10 cm dish with 30 ml embryo media containing 25 µM DAPT dissolved in DMSO and imaged 3 dpf as described (Arslanova et al., 2010).

Statistical Analysis
Results are expressed as means ± SE. Differences between means were evaluated using Student's t test or analysis of variance as appropriate. Values of $p < 0.05$ were considered to be significant.

REFERENCES

Amelio, A.L., Miraglia, L.J., Conkright, J.J., Mercer, B.A., Batalov, S., Cavett, V., Orth, A.P., Busby, J., Hogenesch, J.B., and Conkright, M.D. (2007). A coactivator trap identifies NONO (p54nrb) as a component of the cAMP-signaling pathway. Proc. Natl. Acad. Sci. USA *104*, 20314–20319.

Arnould, T., Kim, E., Tsiokas, L., Jochimsen, F., Grüning, W., Chang, J.D., and Walz, G. (1998). The polycystic kidney disease 1 gene product mediates protein kinase C alpha-dependent and c-Jun N-terminal kinase-dependent activation of the transcription factor AP-1. J. Biol. Chem. *273*, 6013–6018.

Arslanova, D., Yang, T., Xu, X., Wong, S.T., Augelli-Szafran, C.E., and Xia, W. (2010). Phenotypic analysis of images of zebrafish treated with Alzheimer's gamma-secretase inhibitors. BMC Biotechnol. *10*, 24.

Beel, A.J., and Sanders, C.R. (2008). Substrate specificity of gamma-secretase and other intramembrane proteases. Cell. Mol. Life Sci. *65*, 1311–1334.

Bertuccio, C.A., Chapin, H.C., Cai, Y., Mistry, K., Chauvet, V., Somlo, S., and Caplan, M.J. (2009). Polycystin-1 C-terminal cleavage is modulated by polycystin-2 expression. J. Biol. Chem. *284*, 21011–21026.

Bhunia, A.K., Piontek, K., Boletta, A., Liu, L., Qian, F., Xu, P.N., Germino, F.J., and Germino, G.G. (2002). PKD1 induces p21(waf1) and regulation of the cell

cycle via direct activation of the JAK-STAT signaling pathway in a process requiring PKD2. Cell *109*, 157–168.

Chapin, H.C., and Caplan, M.J. (2010). The cell biology of polycystic kidney disease. J. Cell Biol. *191*, 701–710.

Chapin, H.C., Rajendran, V., and Caplan, M.J. (2010). Polycystin-1 surface localization is stimulated by polycystin-2 and cleavage at the G protein-coupled receptor proteolytic site. Mol. Biol. Cell *21*, 4338–4348.

Chauvet, V., Tian, X., Husson, H., Grimm, D.H., Wang, T., Hiesberger, T., Igarashi, P., Bennett, A.M., Ibraghimov-Beskrovnaya, O., Somlo, S., and Caplan, M.J. (2004). Mechanical stimuli induce cleavage and nuclear translocation of the polycystin-1 C terminus. J. Clin. Invest. *114*, 1433–1443.

Daugherty, R.L., and Gottardi, C.J. (2007). Phospho-regulation of Beta-catenin adhesion and signaling functions. Physiology (Bethesda) *22*, 303–309.

Fortini, M.E. (2009). Notch signaling: the core pathway and its posttranslational regulation. Dev. Cell *16*, 633–647.

Gottardi, C.J., and Gumbiner, B.M. (2004). Distinct molecular forms of beta-catenin are targeted to adhesive or transcriptional complexes. J. Cell Biol. *167*, 339–349.

Haque, S.J., Wu, Q., Kammer, W., Friedrich, K., Smith, J.M., Kerr, I.M., Stark, G.R., and Williams, B.R. (1997). Receptor-associated constitutive protein tyrosine phosphatase activity controls the kinase function of JAK1. Proc. Natl. Acad. Sci. USA *94*, 8563–8568.

Harris, P.C., and Torres, V.E. (2009). Polycystic kidney disease. Annu. Rev. Med. *60*, 321–337.

Hecht, A., and Stemmler, M.P. (2003). Identification of a promoter-specific transcriptional activation domain at the C terminus of the Wnt effector protein T-cell factor 4. J. Biol. Chem. *278*, 3776–3785.

Hughes, J., Ward, C.J., Peral, B., Aspinwall, R., Clark, K., San Millán, J.L., Gamble, V., and Harris, P.C. (1995). The polycystic kidney disease 1 (PKD1) gene encodes a novel protein with multiple cell recognition domains. Nat. Genet. *10*, 151–160.

Ishikawa, F., Akimoto, T., Yamamoto, H., Araki, Y., Yoshie, T., Mori, K., Hayashi, H., Nose, K., and Shibanuma, M. (2009). Gene expression profiling identifies a role for CHOP during inhibition of the mitochondrial respiratory chain. J. Biochem. *146*, 123–132.

Joly, D., Ishibe, S., Nickel, C., Yu, Z., Somlo, S., and Cantley, L.G. (2006). The polycystin 1-C-terminal fragment stimulates ERK-dependent spreading of renal epithelial cells. J. Biol. Chem. *281*, 26329–26339.

Kim, E., Arnould, T., Sellin, L.K., Benzing, T., Fan, M.J., Grüning, W., Sokol, S.Y., Drummond, I., and Walz, G. (1999). The polycystic kidney disease 1 gene product modulates Wnt signaling. J. Biol. Chem. *274*, 4947–4953.

Lal, M., and Caplan, M. (2011). Regulated intramembrane proteolysis: signaling pathways and biological functions. Physiology (Bethesda) *26*, 34–44.

Lal, M., Song, X., Pluznick, J.L., Di Giovanni, V., Merrick, D.M., Rosenblum, N.D., Chauvet, V., Gottardi, C.J., Pei, Y., and Caplan, M.J. (2008). Polycystin-1 C-terminal tail associates with beta-catenin and inhibits canonical Wnt signaling. Hum. Mol. Genet. *17*, 3105–3117.

Lanoix, J., D'Agati, V., Szabolcs, M., and Trudel, M. (1996). Dysregulation of cellular proliferation and apoptosis mediates human autosomal dominant polycystic kidney disease (ADPKD). Oncogene *13*, 1153–1160.

Li, J., Sutter, C., Parker, D.S., Blauwkamp, T., Fang, M., and Cadigan, K.M. (2007). CBP/p300 are bimodal regulators of Wnt signaling. EMBO J. *26*, 2284–2294.

Low, S.H., Vasanth, S., Larson, C.H., Mukherjee, S., Sharma, N., Kinter, M.T., Kane, M.E., Obara, T., and Weimbs, T. (2006). Polycystin-1, STAT6, and P100 function in a pathway that transduces ciliary mechanosensation and is activated in polycystic kidney disease. Dev. Cell *10*, 57–69.

Maetzel, D., Denzel, S., Mack, B., Canis, M., Went, P., Benk, M., Kieu, C., Papior, P., Baeuerle, P.A., Munz, M., and Gires, O. (2009). Nuclear signalling by tumour-associated antigen EpCAM. Nat. Cell Biol. *11*, 162–171.

Mangos, S., Lam, P.Y., Zhao, A., Liu, Y., Mudumana, S., Vasilyev, A., Liu, A., and Drummond, I.A. (2010). The ADPKD genes pkd1a/b and pkd2 regulate extracellular matrix formation. Dis. Model. Mech. *3*, 354–365.

Miller, M.M., Iglesias, D.M., Zhang, Z., Corsini, R., Chu, L., Murawski, I., Gupta, I., Somlo, S., Germino, G.G., and Goodyer, P.R. (2011). T-cell factor/β-catenin activity is suppressed in two different models of autosomal dominant polycystic kidney disease. Kidney Int. *80*, 146–153.

Ohoka, N., Hattori, T., Kitagawa, M., Onozaki, K., and Hayashi, H. (2007). Critical and functional regulation of CHOP (C/EBP homologous protein) through the N-terminal portion. J. Biol. Chem. *282*, 35687–35694.

Oyadomari, S., and Mori, M. (2004). Roles of CHOP/GADD153 in endoplasmic reticulum stress. Cell Death Differ. *11*, 381–389.

Parnell, S.C., Magenheimer, B.S., Maser, R.L., Zien, C.A., Frischauf, A.M., and Calvet, J.P. (2002). Polycystin-1 activation of c-Jun N-terminal kinase and AP-1 is mediated by heterotrimeric G proteins. J. Biol. Chem. *277*, 19566–19572.

Qian, F., Germino, F.J., Cai, Y., Zhang, X., Somlo, S., and Germino, G.G. (1997). PKD1 interacts with PKD2 through a probable coiled-coil domain. Nat. Genet. *16*, 179–183.

Qian, F., Boletta, A., Bhunia, A.K., Xu, H., Liu, L., Ahrabi, A.K., Watnick, T.J., Zhou, F., and Germino, G.G. (2002). Cleavage of polycystin-1 requires the receptor for egg jelly domain and is disrupted by human autosomal-dominant polycystic kidney disease 1-associated mutations. Proc. Natl. Acad. Sci. USA *99*, 16981–16986.

Qian, C.N., Knol, J., Igarashi, P., Lin, F., Zylstra, U., Teh, B.T., and Williams, B.O. (2005). Cystic renal neoplasia following conditional inactivation of apc in mouse renal tubular epithelium. J. Biol. Chem. *280*, 3938–3945.

Rossetti, S., Consugar, M.B., Chapman, A.B., Torres, V.E., Guay-Woodford, L.M., Grantham, J.J., Bennett, W.M., Meyers, C.M., Walker, D.L., Bae, K., et al; CRISP Consortium. (2007). Comprehensive molecular diagnostics in autosomal dominant polycystic kidney disease. J. Am. Soc. Nephrol. *18*, 2143–2160.

Saadi-Kheddouci, S., Berrebi, D., Romagnolo, B., Cluzeaud, F., Peuchmaur, M., Kahn, A., Vandewalle, A., and Perret, C. (2001). Early development of polycystic kidney disease in transgenic mice expressing an activated mutant of the beta-catenin gene. Oncogene *20*, 5972–5981.

Shearman, M.S., Beher, D., Clarke, E.E., Lewis, H.D., Harrison, T., Hunt, P., Nadin, A., Smith, A.L., Stevenson, G., and Castro, J.L. (2000). L-685,458, an aspartyl protease transition state mimic, is a potent inhibitor of amyloid beta-protein precursor gamma-secretase activity. Biochemistry *39*, 8698–8704.

Shibazaki, S., Yu, Z., Nishio, S., Tian, X., Thomson, R.B., Mitobe, M., Louvi, A., Velazquez, H., Ishibe, S., Cantley, L.G., et al. (2008). Cyst formation and activation of the extracellular regulated kinase pathway after kidney specific inactivation of Pkd1. Hum. Mol. Genet. *17*, 1505–1516.

Shillingford, J.M., Murcia, N.S., Larson, C.H., Low, S.H., Hedgepeth, R., Brown, N., Flask, C.A., Novick, A.C., Goldfarb, D.A., Kramer-Zucker, A., et al. (2006). The mTOR pathway is regulated by polycystin-1, and its inhibition reverses renal cystogenesis in polycystic kidney disease. Proc. Natl. Acad. Sci. USA *103*, 5466–5471.

Starremans, P.G., Li, X., Finnerty, P.E., Guo, L., Takakura, A., Neilson, E.G., and Zhou, J. (2008). A mouse model for polycystic kidney disease through a somatic in-frame deletion in the 5′ end of Pkd1. Kidney Int. *73*, 1394–1405.

Struhl, G., and Adachi, A. (2000). Requirements for presenilin-dependent cleavage of notch and other transmembrane proteins. Mol. Cell *6*, 625–636.

Takiar, V., and Caplan, M.J. (2011). Polycystic kidney disease: pathogenesis and potential therapies. Biochim. Biophys. Acta *1812*, 1337–1343. Published online December 10, 2010. 10.1016/j.bbadis.2010.11.014.

Talbot, J.J., Shillingford, J.M., Vasanth, S., Doerr, N., Mukherjee, S., Kinter, M.T., Watnick, T., and Weimbs, T. (2011). Polycystin-1 regulates STAT activity by a dual mechanism. Proc. Natl. Acad. Sci. USA *108*, 7985–7990.

Taniguchi, Y., Kim, S.H., and Sisodia, S.S. (2003). Presenilin-dependent "gamma-secretase" processing of deleted in colorectal cancer (DCC). J. Biol. Chem. *278*, 30425–30428.

Tenev, T., Böhmer, S.A., Kaufmann, R., Frese, S., Bittorf, T., Beckers, T., and Böhmer, F.D. (2000). Perinuclear localization of the protein-tyrosine

phosphatase SHP-1 and inhibition of epidermal growth factor-stimulated STAT1/3 activation in A431 cells. Eur. J. Cell Biol. *79*, 261–271.

van de Wetering, M., Cavallo, R., Dooijes, D., van Beest, M., van Es, J., Loureiro, J., Ypma, A., Hursh, D., Jones, T., Bejsovec, A., et al. (1997). Armadillo coactivates transcription driven by the product of the Drosophila segment polarity gene dTCF. Cell *88*, 789–799.

Wilson, P.D. (2004). Polycystic kidney disease. N. Engl. J. Med. *350*, 151–164.

Woodward, O.M., Li, Y., Yu, S., Greenwell, P., Wodarczyk, C., Boletta, A., Guggino, W.B., and Qian, F. (2010). Identification of a polycystin-1 cleavage product, P100, that regulates store operated Ca entry through interactions with STIM1. PLoS One *5*, e12305.

Zhang, K., Ye, C., Zhou, Q., Zheng, R., Lv, X., Chen, Y., Hu, Z., Guo, H., Zhang, Z., Wang, Y., et al. (2007). PKD1 inhibits cancer cells migration and invasion via Wnt signaling pathway in vitro. Cell Biochem. Funct. *25*, 767–774.